Physical Activity and Genetics as Determinants of Limb Bone Structure

A Dissertation Presented

by

Ian Jacob Wallace

to

The Graduate School

in Partial Fulfillment of the

Requirements

for the Degree of

Doctor of Philosophy

in

Anthropological Sciences

Stony Brook University

December 2013

Stony Brook University

The Graduate School

Ian Jacob Wallace

We, the dissertation committee for the above candidate for the

Doctor of Philosophy degree, hereby recommend

acceptance of this dissertation.

Brigitte Demes, Ph.D. – Dissertation Advisor
Professor, Department of Anatomical Sciences

William L. Jungers, Ph.D. – Chairperson of Defense
Distinguished Teaching Professor and Chair, Department of Anatomical Sciences

Jack Stern, Jr., Ph.D. – Member
Distinguished Teaching Professor, Department of Anatomical Sciences

Stefan Judex, Ph.D. – External Member
Professor, Department of Biomedical Engineering
Stony Brook University

This dissertation is accepted by the Graduate School

Charles Taber
Dean of the Graduate School

Abstract of the Dissertation

Physical Activity and Genetics as Determinants of Limb Bone Structure

by

Ian Jacob Wallace

Doctor of Philosophy

in

Anthropological Sciences

Stony Brook University

2013

The skeleton has the capacity to adjust its structure and strength throughout life in response to loads borne during physical activity. Typically, loading promotes bone formation, retards bone loss, and ultimately enhances structure and strength. Based on this observation, many anthropologists consider it possible to deduce the physical activity levels of ancient human populations by analyzing their skeletal remains. Populations with thick, strong bones are inferred to have been very physically active, while populations with slender, fragile bones are inferred to have been more sedentary.

Although the responsiveness of bone to applied loads is well documented, non-mechanical factors, particularly genetic background, also affect skeletal structure and strength, which may undermine the accuracy of anthropological inferences about the physical activity of past human populations. The goals of this dissertation were to clarify (1) the relative importance of genetics and physical activity in determining variation in limb bone morphology among populations and (2) the degree to which bone's response to loading varies among populations. To this end, an experimental approach was adopted using mice as a model organism.

The research consisted of three experiments. In the first experiment, mice were employed from a long-term artificial selection experiment for high levels of voluntary wheel running. Growing males from four replicate high runner (HR) lines and four replicate non-selected control (C) lines were either allowed or denied wheel access for 2 months. Using μCT, femoral

morphology was assessed at two cortical sites (mid-diaphysis, distal metaphysis) and one trabecular site (distal metaphysis). It was found that genetic differences between the linetypes (HR vs. C), between the replicate lines within linetype, and between individuals with and without the so-called 'mini-muscle' phenotype (caused by a Mendelian recessive gene that halves limb muscle mass) gave rise to significant variation in nearly all morphological indices examined. Wheel access also influenced femoral morphology, although the functional response did not generally result in enhanced structure. Exercise caused moderate periosteal enlargement, but relatively greater endocortical expansion, resulting in significantly thinner cortices and reduced bone quantity in the metaphysis. The magnitude of the response was independent of distance run. Mid-diaphyseal bone quantity and area moments, as well as trabecular morphology, were unaffected by exercise. These results underscore the strong influence of genetics on bone structure and the complexity by which mechanical stimuli may cause alterations in it.

In the second experiment, mice were used from two commercially available outbred stocks (Hsd:ICR, Crl:CD1) that have been reproductively isolated for >120 generations and that large-scale genetic analyses have shown to possess genetic architecture (variation) that is comparable to that of living human populations. Beginning shortly after weaning, females from each stock were either treated with a treadmill-running regimen for 1 month or served as sedentary controls. Home-cage activity of all animals was monitored during the experiment. Limb forces were recorded to verify that they were similar in the two stocks. At the end of the experiment, μCT was used to quantify cortical structure in femoral and tibial mid-diaphyses and trabecular structure in the distal femoral metaphysis and proximal tibial metaphysis. Mechanical testing was used to determine femoral and tibial diaphyseal strength. Among the Hsd:ICR mice, treadmill running led to significant improvements in femoral and tibial diaphyseal bone quantity, structural geometry, and mechanical strength, as well as enhanced trabecular bone morphology in the distal femur. In contrast, among the Crl:CD1 mice, the same running regimen had little effect on limb bone cortical and trabecular morphology, and led to significant reductions in femoral diaphyseal strength. Importantly, in neither stock was body mass, muscle mass, or cage activity level significantly different between runners and sedentary controls. Given that most environmental variables were controlled in this study, the differential effects of exercise on the limb bones of Hsd:ICR and Crl:CD1 mice can reasonably be attributed to genetic differences between the stocks. These results suggest that the magnitude of the functional response can vary

in the limb bones of individuals from different populations despite similar physical activity levels during life.

The third experiment investigated the possibility that genetic variation underlying limb bone structure is influenced by the physical activity levels of ancestral populations and might therefore have functional significance in an evolutionary context. In this experiment, 1-week-old mice were employed from the artificial selection experiment for high voluntary wheel running. Differences in limb bone structure at 1 week can be assumed to primarily reflect the effects of selective breeding rather than direct mechanical stimuli, given that the onset of locomotion in mice is shortly after day 7. It was hypothesized that if genetically influenced limb bone diaphyseal structure reflects the physical activity levels of members of a lineage, then selected animals would have enhanced femoral diaphyseal structure (measured using μCT) at 1 week of age compared to non-selected controls. The results provide strong support for this hypothesis and suggest that limb bone structure may not always only reflect the physical activity levels of particular fossil individuals, but may also convey an evolutionary signal providing information about human physical activity in the past.

In sum, the results of the research presented in this dissertation indicate that genetic background plays a significant role in determining variation in limb bone structure among populations and in the responsiveness of bone to loading. Ultimately, the results suggest that much prudence is necessary when using skeletal remains to gain information about the physical activity levels of human populations living in the past.

Dedicated to my brother, Simon, for never leaving my side.

"...bone shape may be caused only by the stresses acting on the element...the assumption of genetical determination of morphological characters seems to be unnecessary, at least in regard to details of the postcranial skeletons."

H. Preuschoft, 1973, p. 35

"The form of the traditional question in comparative anatomy or physical anthropology is: describe with words and measurement, compare and draw conclusions...The modified form is: choose what is to be compared on the basis of some clearly defined important problem; compare; speculate; then devise experiments to determine the probability of the speculations. The main research effort should be in the experimental analysis."

S.L. Washburn, 1983, p. 7

Table of Contents

List of Tables

Chapter 4

Appendix

List of Figures

Chapter 4

Chapter 1

Introduction: The Responsiveness of Bone to Mechanical Signals

The human skeleton is able to alter its structure and strength throughout life in response to the loads it sustains during the physical activities to which we subject our bodies. Typically, skeletal loading shifts the balance in bone turnover toward net formation, which can lead to bigger, stronger bones, whereas decreased loading causes net resorption, which can result in more slender, fragile bones. This phenomenon, commonly referred to as 'bone functional adaptation' (Ruff et al., 2006), has fascinated biologists and clinicians for well over a century (Roux, 1881; Wolff, 1892), for it is an exquisite example of the capacity of organisms to adjust to their environments (West-Eberhard, 2003), and harnessing the sensitivity of our skeletons to mechanical signals provides opportunities for promoting bone health and treating skeletal injuries and degenerative diseases such as osteoporosis (Rubin et al., 2001a; Ozcivici et al., 2010). The responsiveness of bone to loading is an ancient and widespread evolutionary trait among vertebrates, observable in animals as distantly related to humans as birds and reptiles (Carter and Beaupré, 2001; Currey, 2002).

Biological anthropologists have long been interested in bone's responsiveness to loading, because if our bones are shaped by our physical activity patterns, then it might be possible to infer the lifestyles of ancient human populations by analyzing their skeletal remains (Lieberman, 1997; Ruff, 2005). Populations characterized by thick, strong bones would be interpreted as having been highly active, whereas populations with slender, gracile bones would be interpreted as having been more sedentary. Over the last few decades, this paradigm has been the foundation for numerous reconstructions of past human behavior (e.g., Ruff et al., 1984, 1993; Bridges, 1989; Trinkaus et al., 1991, 1998, 1999; Trinkaus, 1997; Holt, 2003; Marchi et al., 2006, 2011; Sládek et al., 2006; Shackelford, 2007; Maggiano et al., 2008; Stock et al., 2010, 2011; Lambert et al., 2013; Shaw and Stock, 2013). Strong empirical support for this paradigm has been provided by controlled experiments—many conducted by anthropologists—involving animal models such as sheep, pigs, rodents, and fowl that have demonstrated the potential for skeletal

loading activities (e.g., running) to promote bone formation, retard bone loss, and, ultimately, enhance structure and strength (e.g., Woo et al., 1981; Newhall et al., 1991; Biewener and Bertram, 1994; Lieberman, 1996; Judex et al., 1997; Lieberman and Pearson, 2001; Lieberman et al., 2001, 2003; Joo et al., 2003; Hamrick et al., 2006; Devlin and Lieberman, 2007; Leppänen et al, 2008; Plochocki et al., 2008; Barak et al., 2011). In addition, compelling evidence for a relationship between skeletal morphology and physical activity patterns in living humans is provided by controlled exercise intervention studies and cross-sectional studies of athletes documenting enhanced bone structure among individuals who frequently engage in activities involving skeletal loading (Pearson and Lieberman, 2004; Daly, 2007; Hind and Burrows, 2007; Macdonald et al., 2009; Shaw and Stock, 2009; Nikander et al., 2010; Behringer et al., 2013).

A growing number of anthropologists, however, argue that, although mechanical signals engendered by physical activity affect skeletal structure and strength, this does not necessarily mean that patterns of physical activity can be accurately inferred from the skeletal remains of human populations living in the past (Demes et al., 1998, 2001; Pearson, 2000; Lieberman et al., 2004; Pearson and Lieberman, 2004; Demes, 2007; Devlin and Lieberman, 2007; Schmitt et al., 2010; Jurmain et al., 2012; Wallace et al., 2013). Several issues have been raised, including the weak correspondence between bone structure and its *in vivo* loading environment (Demes et al., 1998, 2001; Lieberman et al., 2004; Demes, 2007; Schmitt et al., 2010), the age dependency of bone mechanoresponsiveness (Bertram and Swartz, 1991; Lovejoy et al., 2003; Pearson and Lieberman, 2004), and the mechanical inefficiency of bone's functional response (Bertram and Swartz, 1991; Ohman and Lovejoy, 2003; Demes, 2007). This dissertation addresses another potentially critical issue, namely, the degree to which genetic background influences bone morphology and its responsiveness to mechanical signals. The purpose of this chapter is to provide an overview of mechanical regulation of bone turnover, as well as an introduction to the research presented in this dissertation.

Mechanical Regulation of Bone Turnover

The complexity of bone's response to loading, from organ to molecules

2

Bone's response to mechanical loading is extremely complex, from the organ level, to the tissue level, to the cellular and molecular levels. At the organ level, bones are subjected to multiple modes of loading, including axial compression, axial tension, bending, and torsion. Not surprisingly, the magnitude of stresses endured by a bone during any given functional activity varies greatly according to the structural role of that bone in the activity (Hillam, 1996; Lieberman, 1996) and the intensity of the activity (Rubin and Lanyon, 1982; Biewener and Taylor, 1986; Burr et al., 1996). Under natural conditions, bones rarely experience a single type of loading, but instead sustain various combinations of loading modes. During striding legged locomotion, for example, limb bones experience a superimposition of bending and axial compression (Rubin and Lanyon, 1982; Biewener and Taylor, 1986; Demes et al., 1998, 2001; Lieberman et al., 2004), and probably torsion as well (Gross et al., 1992; Demes et al., 1998). As a result of this superimposition, dramatically non-uniform gradients of stress develop along limb bone longitudinal axes (Biewener et al., 1986; Biewener and Bertram, 1993) and throughout their transverse cross sections (Gross et al., 1992; Rubin et al., 2013).

Whole-bone loading exposes bone tissue to barrage of biophysical signals including strain (deformation), pressure developed in intramedullary canals and within cortices with transient pressure waves, fluid flow through the network of lacunae and canaliculi within the bone matrix, dynamic electric fields, and oscillatory accelerations. Numerous studies have shown that many of these factors are independently able to modulate bone turnover (Rubin et al., 2006; Jacobs et al., 2010; Thompson et al., 2012). These signals, however, are not mutually exclusive. All are produced simultaneously during skeletal loading. This cacophony of mechanical signals is further complicated by the fact that components of individual signals also influence bone turnover. For example, the effects of mechanical strain on bone tissue are known to be threshold-driven, such that certain degrees of strain must be achieved to stimulate a cellular response (Lanyon, 1987); however, a response can be triggered by alterations in several parameters of the strain signal, including the temporal variation of strain (Lanyon and Rubin, 1984), the number of strain cycles (Rubin and Lanyon, 1984a), as well as strain magnitude (Rubin and Lanyon, 1985; Sugiyama et al., 2012), rate (O'Connor et al., 1982), distribution (Judex et al., 1997; Gross et al., 1997), and frequency (Qin et al., 1998; Rubin et al., 2001b). The cellular response to loading also depends on the timing of sequential loading events, where brief refractory periods between events can enhance the anabolic potential of loading (Srinivasan et al., 2007).

Bone cells are tightly coupled to the extracellular tissue matrix, and therefore biophysical signals induced at the cellular level depend on tissue-level behavior (Jacobs et al., 2010), as well as the precise location of the cells within the tissue matrix (Rubin et al., 2013). Most tissue-level mechanical signals result in deformation at the cellular level, although it is unclear if deformation *per se* is what triggers the cellular response (Jacobs et al., 2010). At least four types of cells are involved in bone's response to loading: bone-destroying osteoclasts derived from hematopietic stem cells, bone-forming osteoblasts derived from mesenchymal stem cells, matrix-embedded osteocytes derived from osteoblasts, and osteoprogenitor cells (i.e., preosteoblasts and preosteoclasts). Many researchers envision a clear division of labor among these cells such that osteocytes are the primary sensory cells and osteoblasts and osteoclasts are effector cells (e.g., Lanyon, 1993; Turner and Pavalko, 1998; Burger and Klein-Nulend, 1999; Bonewald, 2006; Jacobs et al., 2010). However, all four cell types have been demonstrated to be sensitive to mechanical signals, so isolating the critical sensory cell is difficult (Rubin et al., 2006). Nevertheless, osteocytes are particularly well situated to perceive load-generated signals and orchestrate a coordinated response among cells. Osteocytes are distributed throughout the bone matrix in lacunae and network with other osteocytes, osteoblasts, and bone-lining cells by long cytoplasmic processes that occupy canaliculi containing interstitial fluid, enabling intercellular communication through gap junctions between processes, as well as extracellular communication by fluid flow (Riddle and Donahue, 2009). Furthermore, the microarchitecture of both osteocyte processes and lacunae have been suggested to promote the amplification of relatively small tissue-level mechanical signals to ranges that can be sensed by cell bodies (Han et al., 2004; Nicolella et al., 2006).

Several mechanisms by which bone cells may perceive mechanical signals have been proposed, most of which involve force-induced changes in protein configuration (Jacobs et al., 2010; Thompson et al., 2012). Mechanical loads that cause cell deformation will inevitably disrupt the structure of the intracellular cytoskeleton, making cytoskeletal proteins logical candidate mechanosensors (Wang et al., 1993). Membrane-spanning integrins and integrin-associated proteins are also possible mechanosensors, as they link the cytoskeleton to the extracellular matrix and regulate signaling pathways (Wang et al., 2007; Litzenberger et al., 2010). Other transmembrane proteins are altered by mechanical stimulation, including ion channels and connexin hemichannels, which may also represent incipient molecular

4

mechanotransduction events (Duncan, 1998; Batra and Jiang, 2012). Plasma membrane dynamics provide another possible mechanosensory mechanism through the organization of lipid raft microdomains with the ability to coordinate interactions between regulatory molecules that result in signaling cascades (Simons and Toomre, 2000; Rubin et al., 2007). Much recent work has been devoted to understanding the mechanosensory role of primary cilia, antenna-like structures that extend from cell surfaces (Hoey et al., 2012). Deflections or perturbations of cilia result in increased membrane tension, which may open mechanosensitive membrane channels (Kwon et al., 2011). In all likelihood, the response of bone cells to mechanical signals is defined by multiple mechanoreceptors acting in concert.

Mechanical signals perceived by mechanosensors must be translated into biochemical signals to induce expression of genes that encode proteins involved in bone cell differentiation, proliferation, and survival (Runx2, COX-2, osteonectin, osteocalcin, osterix, sclerostin, c-fos, RANK-L, etc.). Numerous mechanically mediated intracellular signaling cascades have been implicated in bone mechanotransduction (Rubin et al., 2006; Thompson et al., 2012). Some of the better characterized of these include activation of β-catenin (Case and Rubin, 2010), protein kinase signaling (e.g., D. Liu et al., 2008), calcium signaling (e.g., Hung et al., 1995), and signaling mediated by G-proteins (e.g., Arnsdorf et al., 2009). A coordinated response among cells also requires intercellular signaling. Several cell-cell pathways have been proposed that either are activated by, or mediate, mechanical signals (Jacobs et al., 2010). Gap junctions formed between neighboring osteocytes and osteoblasts by alignment of transmembrane connexons provide a critical avenue through which cells can communicate (Yellowley et al., 2000). Two particularly well-studied intermediaries for intercellular communication are nitric oxide and the eicosinoids, prostaglandin and prostacyclin, release of both of which has been shown to be stimulated by mechanical signals (Rawlinson et al., 1991, 1995; Klein-Nulend et al., 1995) and affect the osteogenic potential of loading (Forwood, 1996; Turner et al., 1996).

Non-mechanical influences on bone mechanoresponsiveness

Many human exercise intervention studies have shown that the effects of mechanical loading on the skeleton vary from person to person (Dalsky et al., 1988; Snow-Harter et al., 1992; Hind and Burrows, 2007; Macdonald et al., 2009; Nikander et al., 2010; Behringer et al.,

2013). The degree of bone loss associated with skeletal unloading (bed rest, spaceflight) has also frequently been observed to vary among individuals (LeBlanc et al., 1990; Laugier et al., 2000; Vico et al., 2000; Lang et al., 2004). These studies underscore the fact that the responsiveness of an individual's bone to mechanical signals depends on a number of non-mechanical factors, particularly genetics, as well as age, sex, and others (Goodship and Cunningham, 2001; Ozcivici et al., 2010).

Over the last two decades, numerous genetic polymorphisms have been identified that affect human skeletal structure and strength (Ralston, 2010; Richards et al., 2012). One way in which alleles may exert their influence on the skeleton is by regulating the responsiveness of bone to mechanical signals. Currently, however, our knowledge of the identity of polymorphisms affecting bone mechanotransduction in humans is very limited (Bonjour et al., 2007), although some candidate alleles have been proposed (e.g., Tajima et al., 2000; Dhamrait et al., 2003; Suuriniemi et al., 2004, 2007; Y.-Z. Liu et al., 2008; Mencej-Bedrač et al., 2011; Saxon et al., 2011; Wesselius et al., 2011; Gartland et al., 2012). Instead, at this time, the most compelling evidence for the influence of genetic variations on bone mechanoresponsiveness comes from research involving inbred mice. Animal models are critical for experimentally defining the genetic regulation of bone mechanotransduction, and inbred mice have become the gold standard for such research because they offer large numbers of genetically homogenous animals whose mechanical environments can be strictly controlled (e.g., Akhter et al., 1998, 2002; Kodama et al., 1999, 2000; Judex et al., 2002, 2004a, 2013; Robling and Turner, 2002; Amblard et al., 2003; Robling et al., 2003, 2007; Squire et al., 2004; Kesavan et al., 2005, 2006; Zhong et al., 2005; Lau et al., 2006; Preston, 2009). Furthermore, the genes and molecular pathways affecting the skeleton are highly conserved in mice and humans (Karsenty, 2003) and the skeletal response to altered mechanical signals is often observed to be similar in the two species (Luu et al., 2009).

Two inbred strains have been especially common in bone mechanotransduction research, and, indeed, in biomedical research in general, namely, C3H/HeJ (C3H) and C57BL/6J (B6). To examine bone mechanoresponsiveness in C3H and B6 mice, Robling and Turner (2002) applied exogenous mechanical loads (axial compression) to ulnae of animals from the two strains. The responsiveness of C3H ulnae was found to be lower in two independent parameters. First, C3H mice required relatively more mechanical strain in their ulnar diaphyses before bone formation was triggered. Second, once the bone-formation threshold was surpassed in C3H ulnae, the

increase in bone formation per unit increase of mechanical strain was significantly less than that in B6 mice, and therefore equal changes in suprathreshold strain did not result in equal changes in bone formation between C3H and B6 mice. Findings consistent with these were obtained by Akhter and colleagues (1998, 2002) who subjected tibiae of C3H and B6 mice to four-point bending and found that load-induced bone formation was significantly higher in B6 mice than in C3H mice. Similarly, in a study by Kodama et al. (2000), C3H and B6 mice were treated with 4 weeks of jumping exercise, which significantly increased cortical area and periosteal bone formation in B6 tibiae (relative to unexercised controls), but no effects of exercise were detected in C3H tibiae. In addition, Judex et al. (2002) found that trabecular bone quantity and quality in proximal tibiae of B6 mice, but not C3H mice, were significantly enhanced by low-level mechanical vibration. Together, these studies demonstrate well the importance of an individual's particular allelic complement in defining bone mechanoresponsiveness.

Subsequent investigations have been aimed at identifying specific regions of the mouse genome harboring polymorphisms responsible for regulating bone mechanotransduction. Kesavan and colleagues (2006) used tibial four-point bending to stimulate bone formation in an F2 population derived from the intercross of C3H and B6 strains. Quantitative trait loci (QTLs) for bone mechanoresponsiveness were then identified by interval mapping on six different chromosomes. Robling et al. (2003, 2007) applied exogenous ulnar loads to strains of congenic mice to examine the contribution of four QTLs to regulating bone mechanotransduction. Four congenic strains were created by moving the particular QTLs from C3H onto a B6 background by repeated backcrossing. They found that the responsiveness of each of these strains was significantly different from B6 controls, with some strains exhibiting reduced sensitivity and others enhanced sensitivity. Differences in responsiveness were manifest as changes in minimum level of strain required to initiate osteogenesis and/or the ability to form bone per unit of mechanical strain. Together, these results show that bone mechanotransduction is mediated by several gene polymorphisms, which theoretically increases the potential for interindividual variability in bone mechanoresponsiveness.

Age appears to have a strong effect in humans on bone's responsiveness to mechanical signals, such that the anabolic potential of mechanical loading peaks during the growing years and diminishes thereafter (Pearson and Lieberman, 2004). This phenomenon is evident in numerous human trials where exercise interventions that augment young skeletons typically fail

to do the same in mature and elderly skeletons (Hind and Burrows, 2007; Nikander et al., 2010; Srinivasan et al., 2012). Underlying this age-related degradation in bone mechanoresponsiveness are alterations in bone cell numbers (i.e., declining density of osteocytes and osteoblasts), as well as alterations in cellular function, including attenuated mechanical stimulation of bone cells and changes in load-activated signaling pathways (Srinivasan et al., 2012). Aging is associated with a decrease in bone mineral surface to volume ratio and an increase in interstitial fluid viscosity, which could reduce the velocity of load-induced fluid flow and likewise the magnitude biophysical signals directed at bone cells (Rubin et al., 1992). In terms of signaling pathways, age-related alterations have been documented in load-induced activation of second messengers such as calcium (Donahue et al., 2001), activation of kinases downstream of second messengers (Pahlavani and Vargas, 2000), and, even further downstream, activation and DNA binding of transcription factors such as Wnt/β-catenin (Manolagas and Almeida, 2007). In addition, ontogenetic changes in bone's responsiveness to loading may be affected by age-related alterations in levels of circulating hormones such as estrogen that affect bone mechanotransduction (Devlin, 2011).

Age-related degradation in bone's responsiveness to loading has also been demonstrated in several experiments involving animal models (Rubin et al., 1992; Turner et al., 1995; Lieberman et al., 2001, 2003; Srinivasan et al., 2003, 2010; Willie et al., 2013). For example, Srinivasan and colleagues (2003) observed that diaphyseal cortical bone formation stimulated by exogenous tibial bending was 2.5-fold less in aged B6 mice than young B6 mice, despite the fact that loading engendered similar strains in the diaphyses of the two groups. Interestingly, however, other experiments with animal models have found bone mechanoresponsiveness to be either unaffected by age (Buhl et al., 2001; Brodt and Silva, 2010) or even enhanced by aging (Leppänen et al., 2008). For example, Leppänen and colleagues (2008) subjected mature and senescent rats to treadmill running and found that hind limb bone structure and strength were significantly enhanced by exercise in senescent animals but not mature animals. However, the bones of senescent animals were structurally weaker at the beginning of the exercise treatment, so running presumably engendered greater strains in their bones compared to mature animals, which may explain their greater bony response to loading. In other words, the distinct responses observed between the two groups may not have been due to age-related differences in bone tissue mechanosensitivity *per se*. To circumvent this potentially confounding issue, Brodt and

8

Silva (2010) applied exogenous axial compressive loads to tibiae of mature and aged BALB/c inbred mice, which produced similar levels of strain in their diaphyses, and found that loading had a similar anabolic effect in the two groups. The difference in the results obtained by Srinivasan et al. (2003) using B6 mice and by Brodt and Silva (2010) using BALB/c mice is intriguing and may indicate that the effects of aging on bone mechanoresponsiveness vary according to an individual's particular allelic complement.

Sex seemingly also influences bone's responsiveness to loading, as suggested by studies of both humans (Macdonald et al., 2007; Kriemler et al., 2008; Weeks et al., 2008; Cardadeiro et al., 2012) and animal models (Yingling et al., 2001; Robling et al., 2007; Wallace et al., 2007; Vicente et al., 2013; see also Squire et al., 2004). For example, Macdonald and colleagues (2007) examined the effects of a jumping exercise intervention program on tibial structure in prepubertal children and found that loading enhanced distal shaft geometry in boys but not girls. Similarly, in a study by Wallace and coworkers (2007) of the effects of treadmill running on hind limb bone structure and strength in growing C57BL6/129 inbred mice, tibial diaphyses of males were significantly augmented by exercise, but similar benefits were not observed in females. The influence of sex on bone mechanoresponsiveness is typically attributed to hormonal differences (but see Mosley and Lanyon, 2002); however, currently, the precise mechanisms involved are elusive.

Does body size influence bone's response to loading?

Although small animals such as mice and rats are widely considered appropriate models for addressing questions about bone mechanobiology (Forwood, 2008; Middleton et al., 2008b), some researchers have argued that extrapolating results from small rodents to humans requires caution due to potential effects of body size on bone's response to loading (Barak et al., 2011; Skedros, 2012). Skeletal allometry dictates that limb bones of smaller animals are not subject to the same constraints on functional capacity as those of larger animals (Biewener, 1990). Therefore, they would not necessarily be expected to react in the same way to altered mechanical signals. Since limb bone diaphyseal dimensions scale roughly geometrically with body size (Alexander et al., 1979), and bone tissue material properties are similar over a wide range of body size (Currey, 2002), the same proportional forces associated with locomotion should

engender greater bone strain in larger animals than smaller animals. Since strain is an important physical signal regulating bone's response to loading (Lanyon, 1987), and the 'optimal strain environment' for limb bones is generally independent of body size (Rubin and Lanyon, 1984b), then relatively greater increases in bone stress should be required to stimulate osteogenesis in smaller animals compared with larger animals (Biewener, 1982). However, numerous studies have found moderate increases in locomotor activity—limb loading at magnitudes well within the normal physiological range—to be anabolic to small rodent limb bones (e.g., Kodama et al., 2000; Wu et al., 2001, 2004; Umemura et al., 2002; Joo et al., 2003, Mori et al., 2003; Hamrick et al., 2006; Leppänen et al., 2008; Plochocki et al., 2008; Preston, 2009; see also Chapter 3), similar to what is often observed in studies of larger animals (e.g., Woo et al., 1981; Lieberman, 1996; Lieberman and Pearson, 2001; Lieberman et al., 2001, 2003; Devlin and Lieberman, 2007; Barak et al., 2011). Furthermore, external application of extremely low-magnitude, high-frequency loads has been shown to enhance limb cortical bone in both growing mice (Xie et al., 2006) and growing humans (Wren et al., 2010). Therefore, while there are sound theoretical reasons to expect body size to influence bone's response to loading, a clear allometric relationship is not supported by existing data.

Is the goal of bone mechanotransduction to optimize skeletal structure?

All functional activities engender mechanical signals in bone, whether running across a landscape in pursuit of a next meal (Carrier, 1984) or crouching beside a campfire roasting that meal (Wrangham, 2009). Throughout the daily course of functional activities, vigorous skeletal loading events generating peak mechanical signals are rare, while 'other than peak' mechanical signals are produced constantly, such as those stemming from muscle contractions required to maintain posture (Fritton et al., 2000; Ozcivici et al., 2010). However, because peak loading events pose the greatest challenge to the structural integrity of the skeleton, it is commonly assumed that the purpose of bone's response to loading is to optimize skeletal structure to withstand peak loads with a minimum of construction material (Roux, 1881; Kummer, 1959, 1972; Pauwels, 1965; Amtmann, 1971; Lanyon, 1981; Lieberman and Crompton, 1998; Martin et al., 1998), in which case vigorous activities would be expected to have the greatest influence

on bone turnover (Carter, 1984; Frost, 2003). However, this view of bone's response to loading can be questioned for at least three reasons.

First, although the osteogenic potential of physical activities producing peak mechanical signals is well documented (e.g., Biewener and Bertram, 1994; Lieberman, 1996; Judex et al., 1997; Judex and Zernicke, 2000a; Lieberman et al., 2003), it is not the case that vigorous skeletal loading *always* augments bone structure and strength, even during the growing years. This has been shown in studies of both animal models and humans where particular vigorous limb-loading exercise regimens (e.g., running) had little effect on bone turnover (MacDougall et al., 1992; Judex and Zernicke, 2000b; Notomi et al., 2000; Middleton et al., 2008a, 2010; see also Chapter 2) and in some cases even diminished skeletal structure and strength (Matsuda et al., 1986; Li et al., 1991; Hetland et al., 1993; Bourrin et al., 1994; Burrows et al., 2003; Ma et al., 2010, 2011). For example, in a study by Judex and Zernicke (2000b) of the skeletal effects of high-speed treadmill running in growing roosters, exercise was shown to significantly increase tarsometatarsal strain magnitude, strain rate, and circumferential and radial strain gradients, yet at the end of the experimental period, no significant differences were found between runners and sedentary controls in tarsometatarsal structure or strength. In a related study by Matsuda and colleagues (1986), growing roosters were subjected to a somewhat different high-speed treadmill running regimen that was found to cause significant reductions tarsometatarsal diaphyseal cortical bone area and second moments of area, as well as whole-bone stiffness.

Second, experiments with animal models involving both exogenous loading and exercise have shown that bone formation stimulated by loading does not always occur in areas of the bone surface where mechanical integrity is most challenged (Judex et al., 1997; Gross et al., 1997; Judex and Zernicke, 2000a; Devlin and Lieberman, 2007; Main, 2007; see also Demes et al., 1998, 2001). For example, in a study by Gross and coworkers (1997) in which turkey radii were functionally isolated and subjected to exogenous loading and diaphyseal strains engendered by loading were calculated using finite element methods, it was observed that locations on the periosteal surface where load-induced bone formation was initiated did not significantly correspond to areas that experienced maximal strain magnitudes. Furthermore, functional load-driven bone formation does not always take place in areas of the bone surface where additional bone tissue might provide the greatest benefits for whole-bone strength (Woo et al., 1981; Judex and Zernicke, 2000a; Ohman and Lovejoy, 2003; Plochocki et al., 2008). For example, Woo and

colleagues (1981) found that treating pigs with running exercise significantly increased femoral diaphyseal cortical area, but this was brought about primarily by a decrease in endocortical area rather than an increase in periosteal area. Adding bone to the endosteal surface would theoretically increase whole-bone compressive strength. However, bending is the primary mode of loading in the limb bones of most legged vertebrates (presumably including pigs) (Bertram and Biewener, 1988), and whole-bone bending strength would be enhanced far more by the addition of bone to the periosteal surface than the endosteal surface because bone bending strength is proportional to the fourth power of its distance from the plane of bending.

Third, as shown by Qin et al. (1998), the response of bone to mechanical signals is non-linear such that it can be affected not only by rare high-magnitude loading events, but also by numerous low-magnitude loading events. There seems to be no 'adapted state' in which bone becomes unresponsive to mechanical signals (Sugiyama et al., 2012). In fact, several studies have demonstrated in both humans and animal models that even extremely low-magnitude signals, orders of magnitude below those generated by vigorous exercise, can augment bone structure if sustained at high enough frequencies (Rubin et al., 2001b,c,d, 2004; Judex et al., 2002, 2007; Ward et al., 2004; Xie et al., 2006; Wren et al., 2010). In these studies, loads were applied exogenously as subjects stood on a vibrating plate, yet the loads generated by the plate closely mimic the spectral content of muscle contractibility (Ozcivici et al., 2010), suggesting that all functional activities, including those such as maintaining posture that do not threaten the skeleton's structural integrity, have the potential to influence bone morphology and strength.

Therefore, rather than considering bone's response to mechanical signals as a process aimed at optimization of skeletal structure to withstand peak loads with a minimum of material, it is perhaps more prudent (and less teleological) to view it as simply bone cells reacting to particular 'biologically relevant' parameters of the bone tissue's overall mechanical loading history (Ozcivici et al., 2010). In my opinion, the phrase 'bone functional adaptation' (Ruff et al., 2006) is somewhat misleading.

Issues Addressed in this Dissertation

The foregoing overview of bone's response to mechanical loading highlights the complexity of the process, its unpredictable nature, and its tendency to vary among individuals

according to non-mechanical factors. These aspects of this biological phenomenon would seemingly undermine the accuracy of anthropological inferences about the physical activity of past humans based on skeletal remains. One especially critical concern is the influence of genetic background on bone morphology and its responsiveness to loading (Brothwell, 1975; Kennedy, 1985; Smith et al., 1989; Lieberman, 2000; Lovejoy et al., 2002, 2003; O'Neill and Dobson, 2008; Cowgill, 2010; Devlin, 2011; Morimoto et al., 2011).

As noted, variation in human skeletal structure is affected by numerous genetic polymorphisms (Ralston, 2010; Richards et al., 2012). The fact that heritability estimates for most bone structural traits in humans tend to be high suggests that the influence of genetic factors in shaping interindividual variation in skeletal morphology is relatively large compared to physical activity and other environmental factors. For limb bone shaft size—a trait of interest in many investigations of past human activity—genetic factors have been estimated to account for 25% to over 75% of the morphological disparity within living human populations (e.g., Demissie et al., 2007; Havill et al., 2007; Wagner et al., 2013). Thus, although physical activity certainly plays a role in shaping variation in skeletal structure, genetic factors clearly also have an important role, which may weaken our ability to accurately assign morphological patterns detected in the skeletal remains of past humans to either environmental or genetic factors. Moreover, again, as discussed above, one pathway through which allelic differences determine interindividual morphological variation is by affecting the responsiveness of bone to mechanical signals (e.g., Judex et al., 2002; Robling and Turner, 2002), which means that the 'functional signal' in the skeletal remains of particular individuals could vary depending on their genetic background despite very similar physical activity patterns during life.

From an anthropological perspective, however, the contribution of genetics to shaping interindividual variation in bone structure and its responsiveness to loading is perhaps of limited relevance since attempts to reconstruct the physical activity of particular individuals are relatively rare (e.g., Trinkaus et al., 1998, 1999), while it is far more common to use samples of skeletal remains to gain insight into behavioral differences between populations (e.g., Ruff et al., 1984, 1993; Bridges, 1989; Trinkaus et al., 1991; Trinkaus, 1997; Holt, 2003; Marchi et al., 2006, 2011; Sládek et al., 2006; Shackelford, 2007; Maggiano et al., 2008; Stock et al., 2010, 2011; Lambert et al., 2013; Shaw and Stock, 2013). Therefore, what is most relevant is the importance of genetics in determining *populational* variation in bone structure and

mechanoresponsiveness. Because the vast majority of genetic diversity among humans (>80%) is accounted for by within-population variation (Li et al., 2008), and there is currently limited evidence that alleles affecting bone morphology and mechanoresponsiveness are biased toward the small fraction of genetic diversity that is explained by between-population variation (Styrkarsdottir et al., 2010; Estrada et al., 2012), it is not unreasonable to expect that genetic differences play a greatly reduced role in affecting skeletal variation between populations than within populations (Leslie, 2012). In which case, anthropological analyses that statistically test for populational differences in skeletal morphology relative to within-population variation might be fairly immune to the potentially confounding effects of genetic background on bone structure and mechanoresponsiveness, assuming that sample sizes are sufficiently large.

Nevertheless, genetic differences between populations probably have *some* effect on skeletal variation. Consider, for example, the observation that African-Americans tend to have enhanced bone structure compared to Americans of European ancestry (Danielson et al., 2013), even during early childhood (Wetzsteon et al., 2011). Most researchers assume that structural differences between these two 'ethnic' groups relate, at least in part, to genetic differences between Africans and Europeans. In that case, one would expect that skeletal enhancement in African Americans would be negatively proportional to their degree of genetic admixture with European populations. To test this hypothesis, Chen and colleagues (2011) used ancestry informative single-nucleotide polymorphisms to quantify degree of African admixture in a large sample of African-American women and found that, indeed, individuals with the greatest percentage of African admixture had the most structurally enhanced femoral diaphyses, and individuals with the lowest degree of African admixture generally had more gracile femora. However, the precise genetic mechanisms underlying bone structural differences between African Americans and Americans of European decent, as well as between other 'ethnic' groups, remain unclear.

The goals of this dissertation are to clarify (1) the relative importance of genetics and physical activity in determining populational variation in limb bone morphology and (2) the degree to which bone's functional response varies among populations. To this end, an experimental approach is adopted using mice as a model organism. The research consists of three experiments. In the first experiment (Chapter 2), mice are employed from a long-term artificial selection experiment for high levels of voluntary wheel running (Swallow et al., 1998; Garland,

2003). In the second experiment (Chapter 3), mice are used from two commercially available outbred stocks that large-scale genetic analyses have shown to possess genetic architecture that is comparable to that of living human populations (Aldinger et al., 2009; Yalcin et al., 2010). In both of these experiments, half of the animals from the various genetically distinct populations are treated with moderately intense running exercise—voluntary wheel running in the first experiment and forced treadmill running in the second experiment—and half of the animals serve as sedentary controls. This provides the opportunity to simultaneously test for differences in limb bone structure between the different populations (i.e., genetic effects), between animals given or denied running exercise (i.e., physical activity effects), and interactions between these two factors such that the effects of physical activity on limb bone structure depend on genetic background. The third experiment investigates the possibility that genetic variation underlying limb bone structure is influenced by the physical activity levels of ancestral populations and might therefore have functional significance in an evolutionary context (Chapter 4). In this experiment, perinatal mice are again employed from the artificial selection experiment for high voluntary wheel running. As discussed in the final chapter of this dissertation (Chapter 5), a major conclusion of the research described herein is that, contrary to what might be expected, genetic background plays a significant role in determining populational variation in limb bone structure and its responsiveness to loading. Ultimately, this dissertation contributes to the growing voice within anthropology suggesting that much prudence is necessary when using skeletal remains to gain information about the physical activity patterns of humans living in the past (Bertram and Swartz, 1991; Demes et al., 1998, 2001; Pearson, 2000; Lovejoy et al., 2003; Lieberman et al., 2004; Pearson and Lieberman, 2004; Demes, 2007; Devlin and Lieberman, 2007; Schmitt et al., 2010; Morimoto et al., 2011; Jurmain et al., 2012; Wallace et al., 2013).

Chapter 2

Physical Activity and Genetics as Determinants of Limb Bone Structure:
An Experimental Evolution Approach[*]

Darwin (1859) envisioned evolution by natural selection as a slow process, far too slow to be observable in a human lifetime. However, he was somewhat mistaken. Evolution can indeed be a slow and elusive process, but it can also proceed rapidly on time scales of years and decades in organisms with short generation intervals (Thompson, 2013). Rapid evolution is not only observable and measureable, but it can be experimentally induced by the implementation of a selection regime. Controlled experiments designed to give rise to rapid evolution fall under the heading of 'experimental evolution' (Garland and Rose, 2009). This chapter examines the influence of functional loading and genetic background on variation in limb bone morphology by adopting an experimental evolution approach.

Mice were employed from a long-term selective breeding experiment for high levels of voluntary wheel running (Swallow et al., 1998; Garland, 2003). The selection protocol (described below) began with a base population of genetically heterogeneous mice from which 8 closed lines were established, 4 replicate selected High Runner (HR) lines and 4 non-selected control (C) lines. By generation 16, selection resulted in a ~2.7-fold increase in daily running distance by the mice in the HR lines as compared with the C line mice. Mice from these lines are the subject of an extensive body of research (reviewed in Garland, 2003; Rhodes et al., 2005; Swallow et al., 2009), including several studies of limb bone structure and mechanics (Garland and Freeman, 2005; Kelly et al., 2006; Middleton et al., 2008a,b, 2010; Young et al., 2009; Farber et al., 2011; Wallace et al., 2011; Copes, 2012). For the present study, to examine the effects of increased functional loading on limb bone morphology, HR and C mice from generation 21 were either allowed or denied wheel access for two months, beginning shortly after weaning. Possible dose relationships between distance run and bone response were assessed using the wheel-access mice. To examine the effects of genetic changes due to selective

---

[*] Portions of this research were published in the *American Journal of Physical Anthropology* (Wallace et al., 2012).

breeding, comparisons were made between mice from the two linetypes (HR vs. C). Significant linetype effects were presumed to reflect the existence of pleiotropic gene action (i.e., genes that affect both running behavior and bone development). Differences among the replicate lines within the linetypes were also tested to examine the effects of chance genetic events such as random drift, founder effects, and mutations unique to particular lines. To examine the degree to which genetic background affected the response of bone to mechanical loading, statistical interactions between linetype and wheel access were tested, as well as interactions between replicate line and wheel access. Finally, the effects of a naturally occurring Mendelian recessive allele named 'mini-muscle' (MM) were tested. This allele, which causes an approximately 50% reduction in hind limb muscle mass (Garland et al., 2002; Houle-Leroy et al., 2003), occurs at a high frequency in two of the HR lines.

Two general questions were asked. First, do genetic differences among populations (i.e., the linetypes and replicate lines) or among individuals (i.e., MM vs. non-MM) play a major role in determining limb bone morphology and bone's responsiveness to loading? Second, does limb bone morphology reflect functional loading history, such that bone geometric properties are enhanced in the mice who engaged in voluntary running exercise compared to the sedentary mice and positively correlated with distance run at the level of individual variation for the wheel-access mice? If exercise loading has a positive, dose-dependent effect on bone structure, and genetic variations among groups have little effect, then the results would support the belief held by many anthropologists that physical activity patterns can be accurately inferred from variation in limb bone morphology. However, if bone structure and mechanoresponsiveness are strongly influenced by genetic background, and/or the effects of exercise loading are negligible or negative, then the results would suggest that prudence is necessary when using limb bone remains to glean information about the physical activity levels of past humans.

Materials and Methods

The selection experiment

The selection experiment for high voluntary wheel running in mice is ongoing and led by Theodore Garland, Jr. (University of California, Riverside). The complete design of the selection

experiment has been described elsewhere (Swallow et al., 1998; Garland, 2003), and only a summary is provided here. The 8 lines involved in the experiment are descended from a base population of outbred (genetically heterogeneous) mice of the Hsd:ICR stock (Harlan Sprague Dawley, Indianapolis, IN). Each line is maintained with 10 or more breeding pairs per generation. In each successive generation, when the offspring of the pairs are ~6-8 weeks of age, they are housed individually with access to a running wheel for 6 days. Wheel running is monitored with a computer-automated system. The selection criterion is the total number of revolutions on the last 2 days of the 6-day trial. In the 4 HR lines, the highest-running male and female from each family are chosen as breeders to propagate the next generation. In the 4 non-selected C lines, breeders are randomly chosen from each family. Within the lines, chosen breeders are randomly paired, except that sibling mating is not allowed.

The dramatic increase in daily wheel running in the HR lines has been associated with numerous correlated responses to selection (Garland et al., 2011b), including changes in limb bone morphology. Relative to controls, HR mice have larger femoral heads (Garland and Freeman, 2005; Kelly et al., 2006; Middleton et al., 2008a), wider distal femoral condyles (Middleton et al., 2008a), reduced directional asymmetry in hind limb lengths (Garland and Freeman, 2005), and mediolaterally wider femoral and tibial mid-diaphyses (Kelly et al., 2006). Additional changes include increased home-cage activity (Malisch et al., 2008, 2009), decreased body mass and fat content (Swallow et al., 1999, 2001; Morgan et al., 2003; Nehrenberg et al., 2009), decreased levels of circulating leptin (especially or possibly only in females; Girard et al., 2007; Vaanholt et al., 2007, 2008), and altered signaling in the cannabinoid receptor CB1 pathway (Keeney et al., 2008, 2012), all of which potentially influence skeletal physiology.

The MM allele, which halves hind limb muscle mass, was originally present at low frequency in the base population, and subsequently increased in frequency in two of the HR lines (Garland et al., 2002). The MM allele has been mapped to a 2.6-Mb region of mouse chromosome 11 (Hartmann et al., 2008). Pleiotropic effects include altered muscle contractile physiology (Houle-Leroy et al., 2003; Syme et al., 2005; Guderley et al., 2006, 2008) and reduced hind limb bone diaphyseal diameters (Kelly et al., 2006). Significant effects of the MM allele on limb bone morphology are expected, given that muscle mass and bone structure are strongly correlated throughout development, although the mechanisms responsible for this association remain unresolved (Judex and Carlson, 2009; DiGirolamo et al., 2013).

18

The animals used in this study were from generation 21 (second litters), as described in Kelly et al. (2006). The pups were weaned at 21 days and toe-clipped for identification. At 25-28 days, two males from each of five families in each line (n=80) were housed individually for 8-9 weeks in standard cages, half with and half without access to a running wheel (1.12-m circumference, 10-cm-wide running surface of 10-mm wire mesh; Lafayette Instruments, Lafayette, IN). Thus, four groups were established: HR with wheels, HR without wheels, C with wheels, and C without wheels (n=20 per group) (Figure 2.1). Families were dispersed evenly across the four groups. Mice were maintained on a 12:12-hr light-dark cycle with access to food (Rodent Diet [W] 8604, Harlan Tekland, Madison, WI) and water *ad libitum*. A computerized counting system recorded daily wheel revolutions. By the end of the first month of wheel access, HR and C mice were voluntarily running, on average, more than 13 and 5 km/day, respectively (see Kelly et al., 2006, for analyses of wheel-running data). During the second month, average daily running distance declined slightly in HR mice to 11 km, but increased in C mice to 6 km (Figure 2.2). After the 8-9 week experimental period, mice were sacrificed via CO_2 inhalation and body mass was measured. Mean age at sacrifice was 86 days (range=80-91). Triceps surae muscles were dissected and weighed to identify the MM mice (laboratory designation line 3 [HR]: n=3, 2 with wheels; line 6 [HR]: n=6, 3 with wheels), as described in Garland et al. (2002). Carcasses were skinned and eviscerated, air-dried, and placed in a colony of dermestid beetles. Defleshed limb bones were disarticulated manually as necessary.

Microcomputed tomography

Cortical and trabecular bone morphology was assessed in the left femur by microcomputed tomography (μCT 40, Scanco Medical AG, Brüttisellen, Switzerland). A 600-μm-long region of the diaphysis and a 1500-μm-long region of the distal metaphysis were scanned at an isometric voxel size of 12 μm (55 kVp, 145 μA, 300-ms integration time). The diaphyseal volume of interest was centered at midspan between the growth plates and encompassed only cortical bone. The metaphyseal volume of interest started 600 μm proximal of

the eiphyseal-metaphyseal boundary and encompassed both cortical and trabecular bone (Figure 2.3). These regions were chosen for analysis because they are the most commonly assessed sites in studies of limb bone structure in rodents using μCT (Bouxsein et al., 2010). Micro-CT images were calibrated using hydroxyapatite phantoms (Scanco Medical AG). Volumes were segmented using a constrained 3D Gaussian filter to reduce noise (support=1, sigma=0.1 [diaphysis] and 0.5 [metaphysis]) and thresholded to extract the bone phase. The threshold values chosen for cortical and trabecular bone (922.9 and 634.4 mg HA/cm^3, respectively) were determined empirically to achieve maximal concordance between the raw and thresholded images. Repeatability of this thresholding method is high (Judex et al., 2004b). In the metaphysis, cortical and trabecular bone were separated and analyzed using an automated algorithm that has been shown to facilitate accurate, precise, and rapid evaluation of bone structure (Lublinsky et al., 2007).

Bone properties were computed using the internal imaging code supplied by the scanner manufacturer and defined according to Bouxsein et al. (2010). Cortical bone morphometric traits included cortical bone area (Ct.Ar; mm^2) and average thickness (Ct.Th; mm), periosteal (Ps.Ar; mm^2) and endocortical areas (Ec.Ar; mm^2), and polar moment of area (J; mm^4). Trabecular bone traits included bone volume fraction (BV/TV; %), and trabecular number (Tb.N; 1/mm), thickness (Tb.Th; μm), and separation (Tb.Sp; μm). Of the morphometric properties measured, the most relevant in terms of the mechanical performance of the bone shaft are cortical bone area and polar moment of area. Cortical bone area approximates a cross section's rigidity in pure axial loading, and polar moment of area approximates average bending and torsional rigidity, assuming that the material strength of the bone tissue is invariable (Ruff et al., 1993).[†] In the metaphysis, trabecular bone contributes to shaft strength, but its mechanical function is likely limited (Glatt et al., 2007). Although the focus of this study is bone morphology and not tissue composition, tissue mineral density (TMD; mg HA/cm^3)—the primary determinant of tissue

---

[†] Mechanically testing bone tissue is not possible using palaeontological and archaeological skeletal remains. Therefore, biomechanical analyses of skeletal remains focus entirely on gross structural variation and assume that tissue strength is invariable. Variation in human diaphyseal tissue strength is relatively small compared to tissue strength differences between bones with radically different functions (e.g., tympanic bullae vs. antlers; Currey, 1979). However, it is not the case that tissue strength is invariable in human diaphyses. Significant differences have been documented between individuals (Tommasini et al., 2008), between different bones of a single individual (Yamada, 1970), and throughout ontogeny (Currey and Butler, 1975). Thus, although the words 'structure' and 'strength' are often used interchangeably in biomechanical analyses of skeletal remains, they mean different things. If tissue strength is ignored, substantial variation in whole-bone strength is inevitably obscured.

strength (Currey, 1984, 2002)—was also quantified at each site analyzed by comparing bone radiodensity with hydroxyapatite phantoms.

Statistical analyses

Analysis of covariance (ANCOVA) models with Type III tests of fixed effects were applied using SAS procedure mixed (version 9.2; SAS Institute, Cary, NC) with scripts provided by Prof. Garland. Traits were first analyzed by cross-nested, two-way ANCOVA with linetype (HR vs. C) and activity (wheel vs. no wheel) as the primary grouping factors. Line was nested within linetype, and family was nested within line. Linetype and activity were considered fixed effects, while line and family were considered random effects. The effect of linetype was tested over the effect of line, and the effects of activity and the linetype X activity interaction were tested over the line X activity interaction. Presence of the MM allele was also included as a main effect and was tested relative to the residual variance. Body mass was included as a covariate because it may be associated with cortical bone morphology (e.g., Middleton et al., 2008a, 2010) and because a previous study of this sample found that HR and wheel-access mice were significantly lighter than C and sedentary mice, respectively, throughout much of the experimental period (Kelly et al., 2006) (Figure 2.4). The effect of body mass was also tested relative to the residual variance.

Variability among the lines was analyzed by two-way ANCOVA with line and activity as the fixed factors and body mass included as a covariate; lines from the two linetypes were analyzed separately (Garland et al., 2011a). For these tests, it was not considered necessary to distinguish between the variance attributable to line and family; therefore, family was not included in the model as a nested variable. Consequently, each effect was tested relative to the residual variance.

To test for dose relationships between distance run and bone response, nested, one-way ANCOVA was used. These analyses involved only the 40 mice given wheel access, none of which were siblings. Linetype was the fixed effect and line was nested within linetype as a random effect. Covariates used in the model included body mass and mean daily running distance during the last 6 days of wheel access. The effect of quantitative wheel running was tested relative to the residual variance.

Statistical significance was judged using a 95% criterion (P<0.05), and all tests were two-tailed. Raw (unadjusted) means and standard deviations for bone traits are provided in the Appendix.

Results

Diaphyseal cortical bone

Body mass was a significant positive predictor of most diaphyseal cortical bone traits (Tables 2.1 and 2.2). After controlling statistically for the effects of body mass, bone geometric properties were found to be significantly affected by genetic background. Analyses of the effects of genetic selection history (linetype) on diaphyseal morphology (Tables 2.1 and 2.3) showed that, on average, HR mice have larger periosteal areas (P<0.02), endocortical areas (P<0.02), and polar moments of area (P<0.05). However, this is not true of HR mice harboring the MM allele (Tables 2.1 and 2.3), which were observed to have significantly reduced polar moments of area (P<0.05) and almost significantly smaller periosteal areas (P=0.07) and cortical areas (P=0.06). Analyses of replicate line variation within the linetypes (Tables 2.2, 2.4, 2.5) detected among-line differences in endocortical area (HR: P<0.02, C: P<0.001), cortical area (HR: P<0.0001, C: P=0.051), and cortical thickness (HR and C: P<0.001). High Runner lines, but not C lines, also exhibited significant variation in periosteal area (P<0.001) and polar moment of area (P<0.001).

Two months of voluntary wheel running failed to significantly alter bone quantity (Ct.Ar) but had a significant effect on diaphyseal shape after controlling for body mass effects (Figure 2.5). The most salient response to exercise loading was a significant increase in endocortical expansion, resulting in significantly decreased cortical thickness. This pattern was detected when HR and C mice were analyzed together (Ec.Ar: P<0.01, Ct.Th: P<0.03, Tables 2.1 and 2.3) and separately (Ec.Ar: P<0.03 [HR] and 0.0001 [C], Ct.Th: P<0.02 [HR and C], Tables 2.2, 2.4, 2.5). Running exercise also had a significant positive effect on periosteal area in C mice (P < 0.02, Tables 2.2 and 2.5) but not in HR mice (Tables 2.2 and 2.4), and a nearly significant effect across the entire sample (P=0.06, Tables 2.1 and 2.3). For no diaphyseal trait was the interaction between linetype and activity significant (Table 2.1). However, among C lines (Tables 2.2 and 2.5), cortical thickness showed a significant line X activity interaction (P<0.04). Average daily

running distance was never a significant (or nearly significant) covariate in the ANCOVA models used to test for possible dose responses of exercise loading on diaphyseal morphology (P>0.5 for all traits; Table 2.6).

Metaphyseal cortical bone

Similar to the diaphysis, most metaphyseal cortical bone traits showed a significant positive correlation with body mass (Tables 2.1 and 2.2). Once body mass effects were controlled statistically, genetic background was again found to have a significant effect on cortical bone geometric properties, although the pattern was different from that in the diaphysis. In linetype comparisons (Tables 2.1 and 2.3), HR mice had, on average, significantly larger endocortical areas (P<0.05), significantly thinner cortices (P<0.03), and almost significantly greater periosteal areas (P=0.06). Presence of the MM allele in certain HR mice had a significant negative effect on cortical area (P<0.03, Tables 2.1 and 2.3) and a nearly significant negative effect on cortical thickness (P=0.052) and polar moment of area (P=0.054). Within both linetypes (Tables 2.2, 2.4, 2.5), cortical area varied significantly among the replicate lines (HR: P<0.01, C: P=0.02). All other traits varied significantly among the HR lines (Ps.Ar and Ec.Ar: P<0.0001, Ct.Th and J: P<0.01), except tissue mineral density (P=0.07), but not among the C lines.

Voluntary running exercise caused significant changes in metaphyseal cortical bone quantity and shape after controlling for body mass effects (Figure 2.5). Across the entire sample (Tables 2.1 and 2.3), wheel running was associated with significant periosteal expansion (P<0.05), but even greater endocortical expansion (P<0.01), and, ultimately, reduced cortical area (P<0.02) and cortical thickness (P<0.001). When linetypes were analyzed separately, this pattern held for C mice, but less so for HR mice (Tables 2.2, 2.4, 2.5). Mice from non-selected lines given wheel access had significantly greater endocortical area (P<0.01), reduced cortical area (P<0.01), and thinner cortices (P<0.001) as well as lower tissue mineral density (P<0.05). In HR mice, the only significant effect of running exercise was decreased cortical thickness (P<0.01). Despite the differences between HR and C mice, no significant linetype X activity interactions were observed (Table 2.1), nor were the line X activity interactions significant (Table 2.2). Cortical thickness showed a significant negative correlation with daily running

23

distance (P=0.018; Table 2.6; Figure 2.6). All other metaphyseal cortical traits exhibited no such dose response (P>0.5).

Metaphyseal trabecular bone

In contrast to cortical bone structure, body mass was not a statistically significant predictor of metaphyseal trabecular bone traits (Tables 2.1 and 2.2), except trabecular thickness in HR mice (P<0.01). Nevertheless, the variance attributable to body mass was accounted for in all analyses. Genetic differences between linetypes did not lead to significant differences in trabecular bone morphology (Tables 2.1 and 2.3). Analyses of the effects of the MM allele (Tables 2.1 and 2.3) showed that MM mice have significantly thinner trabeculae (P<0.02) as well as lower tissue mineral density (P<0.02). Genetic variation among replicate lines had a strong influence on multiple traits (Tables 2.2, 2.4, 2.5). Both linetypes exhibited significant among-line differences in trabecular number (HR: P=0.001, C: P<0.0001) and trabecular separation (HR: P<0.001, C: P<0.0001). Bone volume fraction varied significantly among C lines (P<0.0001) and almost significantly among HR lines (P=0.07). Trabecular thickness also varied among C lines, but not significantly so (P=0.08).

Metaphyseal trabecular bone was generally unresponsive to exercise-induced loads. Only one comparison between mice allowed and denied wheel access showed a statistically significant effect of exercise: among C mice (Tables 2.2 and 2.5), wheel running led to thinner trabeculae (P<0.05). No significant linetype X activity interactions were observed (Table 2.1). However, among C lines (Table 2.2), a significant line X activity interaction was found for trabecular separation (P<0.04), and a nearly significant interaction was found for trabecular number (P=0.06). Trabecular number was the only trait that showed a significant positive correlation with daily running distance (P=0.039; Table 2.6; Figure 2.6). Bone volume fraction had an almost significant positive association with distance run (P=0.075). Trabecular separation and tissue mineral density exhibited nearly significant negative correlations with running distance (P=0.057 and 0.074, respectively). There was no effect of mean daily running distance during the last 6 days of wheel access on trabecular thickness (P=0.37).

MM mice and HR line variation

To examine the degree to which the observed variation among the HR replicate lines (Table 2.2) was influenced by the MM mice, additional HR line comparisons were performed with these animals excluded (Table 2.7). Significant among-line differences remained detectable in most cortical bone traits of the diaphysis (Ct.Ar, Ct.Th, J) and metaphysis (Ps.Ar, Ec.Ar, Ct.Th, J). No trabecular bone morphological difference detected in analyses including MM mice was detected when MM mice were excluded. (However, among-line differences in trabecular thickness became significant when MM mice were excluded [P=0.04].) Therefore, the MM mice are responsible for a relatively small fraction of the HR line variation in cortical structure, but for most of the variation in trabecular morphology.

Discussion

The simultaneous effects of genetic background and functional loading on limb bone morphology were investigated using a model system in which mice, half from lines selectively bred for high voluntary wheel running (HR) and half from non-selected control (C) lines, were either allowed or denied wheel access for two months, beginning shortly after weaning. At the end of the experiment, femoral morphology was quantified at two cortical sites (mid-diaphysis, distal metaphysis) and one trabecular site (distal metaphysis). Genetic background was found to have a strong influence on all morphological indices analyzed. Selectively bred HR mice, on average, had femora with enlarged shafts, expanded marrow areas, and mid-diaphyseal shapes suggesting increased mechanical strength (i.e., higher J values). However, in some HR mice, presence of the MM (mini-muscle) phenotype (expressed by homozygotes for the recessive MM allele) had a negative effect on cortical bone area, shaft shape, and trabecular thickness. Within the HR and C linetypes, the replicate lines exhibited substantial variation in bone quantity and shape, with the particular traits affected differing between linetypes and regions. Wheel running also influenced femoral morphology, although the exercise-stimulated response did not generally result in enhanced structure. Exercise loading caused moderate periosteal enlargement, but relatively greater endosteal enlargement (Figure 2.5). The imbalance between periosteal and endocortical expansion ultimately led to significantly thinner cortices, as well as reduced cortical bone area in the metaphysis. Among individual mice within the wheel-access group, the

magnitude of the response was broadly independent of loading dose (distance run) and genetic background (linetype or line). In the mid-diaphysis, where the forces associated with wheel running were likely highest, the two most mechanically important morphometric properties (Ct.Ar, J) were unaffected by exercise. Increased limb loading also failed to alter trabecular bone. Extrapolating these results from mice to humans requires caution, but if such extrapolation is warranted, then this study suggests that patterns of limb bone morphological variation among paleontological and archaeological human samples probably reflect, to some extent, genetic differences among populations. Furthermore, this study highlights the fact that the effects of mechanical loading on limb bone structure can be unpredictable (i.e., not always anabolic), which limits our ability to infer loading history from the morphology of skeletal remains.

The data also do not indicate an enhancement of bone material properties in response to selective breeding or exercise. Tissue mineral density, a variable of considerable importance for bone tissue strength, showed no significant effect of linetype or activity in most cases, and the one significant difference in tissue mineral density of the metaphyseal cortex between active and sedentary C mice favored the sedentary mice. Previous studies of mice as well as humans have demonstrated trade-offs between geometric properties and material properties, with slender bones having greater tissue mineral density (Jepsen et al., 2007; Tommasini et al., 2008). The coupling of tissue mineral density reduction with periosteal expansion in the metaphyseal cortices of the active C mice supports the existence of such a trade-off.

Differences in femoral structure between HR and C mice are presumably pleiotropic effects of genes that regulate both physical activity and bone development, whereas differences among replicate lines are attributable to stochastic genetic events such as random drift, founder effects, mutations in particular lines, and interactions between these factors and selection (Garland, 2003; Swallow et al., 2009; Garland et al., 2011a,b). Molecular links between skeletal physiology and determinants of locomotor activity (e.g., motivation, energy metabolism) are well documented (Bab, 2007; Bab and Zimmer, 2008; Lee and Karsenty, 2008; Confavreux et al., 2009; Idris and Ralston, 2012; Karsenty and Ferron, 2012), but have not yet been rigorously investigated in these lines of mice (but see Farber et al., 2011). The genetic mechanisms underlying the among-line differences are also not well understood. However, it has been shown that the high frequency of the MM allele in two of the HR lines, which is clearly responsible for some of the observed variation within that linetype, resulted from chance events during line

establishment, followed by random genetic drift and positive selection (Garland et al., 2002). What remains uncertain about the MM mice is the precise etiological pathway for their limb bone phenotype. Reduced muscle mass and bone structure could represent direct pleiotropic effects of the MM allele if the gene is expressed early in development in related cell populations. Alternatively, the gene might act intrinsically only on the muscle cells and not the bone cells, and the MM bone phenotype could arise via mechanical interactions between bone and the reduced limb musculature. Another possibility is that the MM allele influences a circulating hormone or growth factor that regulates both muscle and bone development.

The variation in femoral morphology observed among the HR mice is interesting because it suggests that limb bone structure might be of relatively little adaptive significance when selection favors high levels of locomotor activity. The bones need only be rigid enough to sustain normal physiological loads. The relatively gracile bones of the MM mice evidently meet this requirement, given that they did not spontaneously fracture during the experiment or during several similar studies with these lines during later generations (e.g., Meek et al., 2010). In fact, light and slender bones are conceivably advantageous for animals that devote much of their total energy budget to locomotion because such a configuration might save energy by decreasing the moment of inertia of the limbs (Currey and Alexander, 1985; Carrano, 1999; Kemp et al., 2005). Roughly 25% of the energy used by the limbs during locomotion is for moving the limbs in swing phase (Marsh et al., 2004), and the metabolic cost of moving the limbs should increase relative to limb mass (Wickler et al., 2004). Because the density of bone tissue is twice that of other tissues in limbs, the metabolic cost of transporting bone is high relative to other tissues (Martin et al., 1998). Therefore, highly physically active animals might be expected to benefit from genetic variants such as the MM allele that minimize rather than maximize limb bone mass. However, Dlugosz and colleagues (2009) recently measured the energetic cost of running in MM and non-MM HR mice and found that the cost of transport—the energy associated with movement *per se*—does not differ between the two groups. Moreover, the 'postural costs' of running (i.e., resting metabolic rate) were significantly higher in MM mice (and maximal sprint running speeds were significantly lower). Thus, neither the structurally augmented bones of the non-MM HR mice nor the gracile MM bones provide obvious benefits for locomotor performance.

The fact that exercise influenced femoral morphology is not surprising considering that (1) the distances run by the mice in this study well exceeded those completed in many forced-exercise studies with mice in which running was found to significantly affect bone structure (Wu et al., 2001, 2004; Hamrick et al., 2006; see also Chapter 3), and (2) the experiment encompassed a period of rapid bone growth in mice (Ferguson et al., 2003; Glatt et al., 2007), and growing bone is generally more responsive to mechanical signals than mature bone (see Chapter 1). What is perhaps surprising is that the functional response did not lead to gains in bone quantity or major improvements in geometry. In a previous analysis of the sample used in this study, Kelly and coworkers (2006) showed that running had a positive effect on certain external linear dimensions of the femoral shaft. The results presented here are consistent with those of Kelly et al. (2006) as this study, too, detected positive effects on shaft perimeter (Ps.Ar). However, external dimensions are inexact estimates of bone quantity and mechanical rigidity. By using μCT to accurately quantify internal and external contours, this study was able to derive mechanically more relevant morphometric properties (Ct.Ar, J) and demonstrate that the structural consequences of exercise overall were not very 'beneficial' (e.g., no change in J or midshaft Ct.Ar), and were, in fact, somewhat 'detrimental' (e.g., decreased metaphyseal Ct.Ar). Recently, Middleton and colleagues (2010) examined the effects of ~3.5 months of wheel-running exercise on the femora of young female mice from a later generation of the selection experiment. Their results accord with the results reported here in that mid-diaphyseal cortical area and area moments were found to be unaffected by exercise. Also consistent with the findings of the current study, Ma and coworkers (2010, 2011) observed that, in young male B6 mice, ~5 months of wheel running did not significantly affect femoral mid-diaphyseal cortical area or area moments, but led to significantly thinner cortices and reduced cortical bone quantity in the metaphysis. In contrast, Plochocki and colleagues (2008) found that growing female B6 mice given one month of voluntary wheel access displayed enhanced periosteal and endosteal bone formation at the femoral midshaft, which resulted in increased cortical area and area moments. The disparity between the results of Plochocki et al. (2008) and other researchers is not easy to explain, but may relate to sex or genetic differences between the animals employed, as well as methodological differences between the studies (e.g., Plochocki et al. [2008] did not control for statistically significant effects of body mass).

The agreement between the results of this study and those of Ma and coworkers (2010, 2011) is important because it implies that the bone functional response observed in the mice employed in this study was not related to their unique breeding history, nor is it unusual for mice in general. The fact that the somewhat unexpected effects of wheel running (e.g., cortical thinning and decreased metaphyseal bone quantity) were found in the C lines—which have not undergone selective breeding—further suggests that this study's findings concerning the effects of running on bone cannot be explained as a phenomenon related solely to artificial selection.

By using a voluntary running model, this study was able to investigate possible dose effects of exercise loading on bone's functional response. Little evidence was found for strong relationships between daily running distance and femoral morphological indices, suggesting that only a small amount of exercise was required to initiate the observed structural changes. Previously, Newhall and colleagues (1991) examined the dose effects of voluntary wheel running on limb bone structure in growing rats. Like this study, they found that the bone response was generally independent of loading dose. (Unlike this study, however, they observed that the response led to increased diaphyseal area and area moments.) The lack of significant dose effects in this study and that of Newhall et al. (1991) is plausibly explained by the fact that over the course of the experiments, wheel running engendered surplus loading environments, which may have allowed the bone cells to become accustomed to the habitual loads and less responsive to the routine mechanical signals (Middleton et al., 2008b).

The lack of statistically significant interactions between genetic background and running exercise could be due to the fact that 21 generations of genetic separation did not lead to frequency differences between the linetypes and replicate lines in alleles influencing bone's responsiveness to loading. However, there are alternative explanations, one of which, of course, is that variation in bone mechanoresponsiveness is difficult to detect when the mechanical stimulus has a relatively small effect, as it did in this study. In addition, the dose of running was variable among the wheel-access mice due to the voluntary nature of the exercise treatment; therefore, differences in running behavior among the linetypes and lines (Garland et al., 2011a) may have obscured variation in bone's functional response. Furthermore, analysis of variance models have relatively low power to detect interactions (Middleton et al., 2008b), and it is possible that by relying on this statistical approach, important linetype and replicate line

differences in bone mechanoresponsiveness were missed. This seems especially likely for the replicate line tests, where sample sizes were particularly small (Chia et al., 2005).

It is important to note that throughout the experiment, mice were allowed to load their limbs during normal cage activities, thus introducing the possibility that the variation in femoral morphology detected among linetypes, lines, and individuals was caused, in part, by differences in cage activity and not only alleles directly influencing bone development (Malisch et al., 2008, 2009). Unfortunately, it was not technically possible to monitor home-cage activity when the experiment was being conducted. Nevertheless, although it is conceivable that variation in cage activity contributed to the observed morphological variation, its contribution is likely to have been small relative to genetic factors, given that structural differences similar to those reported here have been documented in perinatal mice before the onset of locomotion (Wallace et al., 2010, 2011). For example, at 1 week of age, HR males have femoral mid-diaphyses with expanded periosteal areas and greater polar moments of area (Wallace et al., 2010; see also Chapter 4). Replicate line differences in diaphyseal areas and area moments are also evident at 1 week postnatal (Wallace et al., 2011).

The greatest limitation of this study is perhaps that the genetic architecture of the mouse populations examined (i.e., the linetypes and replicate lines) is unlikely to resemble that of human populations. Genetic variation within the mouse groups is almost certainly reduced compared to human populations due to genetic bottlenecks during line formation, low effective population sizes, artificial selection, and other factors (Brotherstone and Goddard, 2005; Yalcin et al., 2010). In the next chapter, an experiment is presented that accounts for this potentially confounding issue by employing mice from outbred stocks that large-scale genetic analyses have shown to display genetic architectures comparable to those of human populations. Other limitations of the present study (e.g., unmonitored cage activity, uncontrolled exercise, and small sample sizes) are also accounted for in the next experiment. Importantly, however, the primary conclusions of the present chapter—i.e., that genetic background can have a relatively large influence on bone morphology, and that the skeletal effects of mechanical loading can be unpredictable—are upheld by the next chapter, which reinforces the utility of experimental evolution approaches like that adopted here as a tool for gaining insight into the factors affecting bone structure (Middleton et al., 2008b).

Table 2.1. Comparison of bone traits across the entire sample. Significance levels are for mixed-model ANCOVAs with body mass as a covariate and linetype, activity, and the linetype X activity interaction, as well as the mini-muscle (MM) phenotype, as fixed factors. Line was a random effect nested within linetype. Statistically significant differences are indicated in bold print.

Trait	Linetype		Activity		Linteype X Activity	MM		Body Mass
DF	1,6		1,6		1,6	1,29		1,29
Diaphyseal cortical								
Ps.Ar	**0.0191**	**HR>C**	0.0590	A>S	0.3606	0.0723	N>MM	**0.0001**
Ec.Ar	**0.0145**	**HR>C**	**0.0017**	**A>S**	0.6729	0.7361	N>MM	**0.0374**
Ct.Ar	0.7855	C>HR	0.2207	S>A	0.4933	0.0557	N>MM	**0.0002**
Ct.Th	0.2503	C>HR	**0.0298**	**S>A**	0.7678	0.1800	N>MM	**0.0416**
J	**0.0477**	**HR>C**	0.5654	A>S	0.2922	**0.0406**	**N>MM**	**<.0001**
TMD	0.1258	C>HR	0.1942	S>A	0.8588	0.8212	N>MM	0.9226
Metaphyseal cortical								
Ps.Ar	0.0640	HR>C	**0.0498**	**A>S**	0.4537	0.9398	MM=N	**0.0002**
Ec.Ar	**0.0445**	**HR>C**	**0.0088**	**A>S**	0.2253	0.5373	MM>N	**0.001**
Ct.Ar	0.4544	C>HR	**0.0152**	**S>A**	0.2135	**0.0237**	**N>MM**	**0.0001**
Ct.Th	**0.0265**	**C>HR**	**0.0007**	**S>A**	0.2029	0.0519	N>MM	0.4687
J	0.3618	HR>C	0.5660	S>A	0.8502	0.0541	N>MM	**<.0001**
TMD	0.1085	C>HR	0.0834	S>A	0.3656	0.1037	N>MM	0.9664
Metaphyseal trabecular								
BV/TV	0.5651	HR>C	0.6259	A>S	0.0841	0.1774	N>MM	0.1252
Tb.N	0.6211	HR>C	0.9213	S=A	0.2953	0.6364	N>MM	0.3394
Tb.Th	0.3169	C>HR	0.3742	S>A	0.0660	**0.0159**	**N>MM**	0.1043
Tb.Sp	0.6498	C>HR	0.9944	A=S	0.4323	0.4319	MM>N	0.3349
TMD	0.1915	C>HR	0.3557	A>S	0.9687	**0.0106**	**N>MM**	0.7639

DF = degrees of freedom; HR = mice from lines selected for high wheel running; C = mice from control lines; A = active mice with wheel access; S = sedentary mice without wheel access; MM = MM mice; N = non-MM mice; Ps.Ar = periosteal area; Ec.Ar = endocortical area; Ct.Ar = cortical area; Ct.Th = cortical thickness; J = polar moment of area; TMD = tissue mineral density; BV/TV = bone volume fraction; Tb.N = trabecular number; Tb.Th = trabecular thickness; Tb.Sp = trabecular separation.

Table 2.2. Comparison of bone traits within the two linetypes. Significance levels are for ANCOVAs with body mass as a covariate, and line, activity, and the line X activity interaction as fixed factors. Significant differences are indicated in bold print.

	High Runner linetype					Control linetype				
Trait	Line	Activity		Line X Activity	Body Mass	Line	Activity		Line X Activity	Body Mass
DF	3,31	1,31		3,31	1,31	3,31	1,31		3,31	1,31
Diaphyseal cortical										
Ps.Ar	**0.0004**	0.3094	A>S	0.6119	**0.0006**	0.4221	**0.0166**	A>S	0.3653	**0.0001**
Ec.Ar	**0.0194**	**0.0263**	**A>S**	0.9925	0.1014	**0.0003**	**<.0001**	**A>S**	0.1738	**0.0091**
Ct.Ar	**<.0001**	0.0874	S>A	0.1977	**0.0004**	0.0513	0.6559	S>A	0.0794	**0.0015**
Ct.Th	**0.0003**	**0.0147**	**S>A**	0.3877	0.0506	**0.0008**	**0.0130**	**S>A**	**0.0374**	0.1276
J	**0.0002**	0.8761	S>A	0.3560	**0.0003**	0.5366	0.1110	A>S	0.2884	**<.0001**
TMD	0.8767	0.4383	S>A	0.9914	0.7842	0.7869	0.3375	S>A	0.4759	0.2433
Metaphyseal cortical										
Ps.Ar	**<.0001**	0.2845	A>S	0.5966	**0.002**	0.7982	0.0916	A>S	0.9735	**0.0176**
Ec.Ar	**<.0001**	0.1107	A>S	0.7592	**0.01**	0.3614	**0.0078**	**A>S**	0.9516	**0.0442**
Ct.Ar	**0.0072**	0.1144	S>A	0.2924	**0.0002**	**0.0201**	**0.0052**	**S>A**	0.4166	**0.0143**
Ct.Th	**0.0017**	**0.0029**	**S>A**	0.8814	0.1166	0.1007	**0.0003**	**S>A**	0.5938	0.8118
J	**0.0012**	0.7587	S>A	0.3477	**<.0001**	0.4874	0.6505	S>A	0.8619	**0.0094**
TMD	0.0675	0.4822	S>A	0.7749	0.6093	0.2491	**0.0410**	**S>A**	0.1327	0.5949
Metaphyseal trabecular										
BV/TV	0.0669	0.0972	A>S	0.4111	0.1334	**<.0001**	0.3173	S>A	0.348	0.1396
Tb.N	**0.001**	0.3731	A>S	0.3513	0.3543	**<.0001**	0.2647	S>A	0.0612	0.2479
Tb.Th	0.1703	0.2840	A>S	0.2268	**0.0083**	0.0809	**0.0424**	**S>A**	0.7651	0.9897
Tb.Sp	**0.0006**	0.4230	S>A	0.6771	0.1511	**<.0001**	0.4219	A>S	**0.0394**	0.4169
TMD	0.3322	0.4022	A>S	0.7561	0.3632	0.5376	0.4924	A>S	0.4520	0.9500

DF = degrees of freedom; A = active mice with wheel access; S = sedentary mice without wheel access; Ps.Ar = periosteal area; Ec.Ar = endocortical area; Ct.Ar = cortical area; Ct.Th = cortical thickness; J = polar moment of area; TMD = tissue mineral density; BV/TV = bone volume fraction; Tb.N = trabecular number; Tb.Th = trabecular thickness; Tb.Sp = trabecular separation.

Table 2.3. Least-squares means and standard errors from SAS procedure mixed, corresponding to tests presented in Table 2.1.

| | Control lines | | | | High-Runner lines | | | | Mini-Muscle | | | |
| | Sedentary | | Active | | Sedentary | | Active | | Normal | | Mini | |
Trait	Mean	SE	Mean	SE	Mean	SE	Mean	SE	Mean	SE	Mean	SE
Diaphyseal cortical												
Ps.Ar	1.71	0.06	1.80	0.06	1.97	0.05	2.01	0.06	1.94	0.03	1.81	0.07
Ec.Ar	0.66	0.05	0.77	0.05	0.88	0.05	0.98	0.05	0.83	0.03	0.81	0.06
Ct.Ar	1.06	0.05	1.04	0.05	1.09	0.04	1.03	0.05	1.10	0.03	1.01	0.05
Ct.Th	0.290	0.014	0.270	0.014	0.271	0.013	0.246	0.013	0.278	0.008	0.260	0.014
J	0.406	0.030	0.434	0.029	0.510	0.027	0.502	0.028	0.499	0.015	0.428	0.033
TMD	1127	8	1122	7	1113	6	1106	7	1118	3	1116	9
Metaphyseal cortical												
Ps.Ar	2.51	0.10	2.65	0.10	2.83	0.09	2.91	0.10	2.73	0.06	2.72	0.11
Ec.Ar	1.58	0.10	1.78	0.09	1.93	0.09	2.04	0.09	1.80	0.06	1.86	0.10
Ct.Ar	0.93	0.02	0.87	0.02	0.90	0.02	0.87	0.02	0.93	0.01	0.86	0.03
Ct.Th	0.143	0.005	0.127	0.004	0.124	0.004	0.114	0.004	0.132	0.003	0.122	0.005
J	0.681	0.033	0.667	0.031	0.715	0.029	0.707	0.031	0.735	0.015	0.650	0.040
TMD	1042	9	1026	8	1018	8	1012	8	1033	4	1017	10
Metaphyseal trabecular												
BV/TV	8.9	1.6	7.8	1.5	8.6	1.5	10.4	1.5	10.0	0.9	7.9	1.6
Tb.N	4.2	0.4	4.0	0.4	4.3	0.4	4.5	0.4	4.3	0.2	4.2	0.4
Tb.Th	43.5	1.0	41.7	1.0	40.9	0.9	41.6	1.0	43.5	0.5	40.4	1.2
Tb.Sp	252	26	261	26	245	25	236	26	240	16	257	25
TMD	843	6	847	6	832	6	837	6	851	3	829	7

Ps.Ar = periosteal area (mm^2); Ec.Ar = endocortical area (mm^2); Ct.Ar = cortical area (mm^2); Ct.Th = cortical thickness (mm); J = polar moment of area (mm^4); TMD = tissue mineral density (mg HA/cm^3); BV/TV = bone volume fraction (%); Tb.N = trabecular number (1/mm); Tb.Th = trabecular thickness (μm); Tb.Sp = trabecular separation (μm).

Table 2.4. Least-squares means and standard errors from two-way ANCOVAs with body mass as a covariate, and line, activity, and the line X activity interaction as fixed factors, corresponding to tests presented in Table 2.2 for High Runner lines.

| | Line 3 | | | | Line 6 | | | | Line 7 | | | | Line 8 | | | |
| | Sedentary | | Active | | Sedentary | | Active | | Sedentary | | Active | | Sedentary | | Active | |
Trait	Mean	SE	Mean	SE	Mean	SE	Mean	SE	Mean	SE	Mean	SE	Mean	SE	Mean	SE
Diaphyseal cortical																
Ps.Ar	1.74	0.08	1.75	0.07	1.84	0.07	2.00	0.07	2.10	0.07	2.09	0.07	1.96	0.07	2.01	0.07
Ec.Ar	0.72	0.06	0.83	0.06	0.92	0.06	1.03	0.06	0.87	0.06	0.96	0.06	0.89	0.06	0.98	0.06
Ct.Ar	1.03	0.04	0.92	0.04	0.92	0.04	0.96	0.04	1.24	0.04	1.13	0.04	1.08	0.04	1.04	0.04
Ct.Th	0.270	0.014	0.233	0.013	0.226	0.013	0.229	0.013	0.307	0.013	0.275	0.013	0.273	0.013	0.244	0.013
J	0.425	0.035	0.389	0.032	0.419	0.032	0.478	0.033	0.596	0.032	0.550	0.034	0.497	0.033	0.505	0.032
TMD	1117	11	1110	10	1109	10	1106	10	1116	10	1112	10	1113	10	1104	10
Metaphyseal cortical																
Ps.Ar	2.55	0.10	2.50	0.10	2.61	0.10	2.75	0.10	2.70	0.10	2.73	0.10	2.95	0.10	3.14	0.10
Ec.Ar	1.66	0.09	1.68	0.09	1.78	0.09	1.92	0.09	1.79	0.09	1.86	0.09	2.05	0.09	2.24	0.09
Ct.Ar	0.89	0.02	0.82	0.02	0.83	0.02	0.83	0.02	0.91	0.02	0.87	0.02	0.90	0.02	0.90	0.02
Ct.Th	0.134	0.004	0.122	0.004	0.122	0.004	0.110	0.004	0.129	0.004	0.122	0.004	0.117	0.004	0.109	0.004
J	0.663	0.038	0.589	0.036	0.609	0.036	0.628	0.037	0.704	0.036	0.677	0.037	0.736	0.037	0.785	0.036
TMD	1015	11	1005	10	1031	10	1032	10	1028	10	1031	11	1013	10	999	10
Metaphyseal trabecular																
BV/TV	6.7	1.6	7.4	1.5	8.4	1.5	13.0	1.5	11.3	1.5	11.2	1.5	7.8	1.5	10.0	1.5
Tb.N	3.4	0.3	3.7	0.3	4.5	0.3	5.3	0.3	5.1	0.3	4.7	0.3	3.8	0.3	4.1	0.3
Tb.Th	43.7	1.1	41.8	1.1	39.7	1.1	41.4	1.1	41.3	1.1	42.7	1.1	39.8	1.1	42.0	1.1
Tb.Sp	304	23	292	22	220	22	183	22	192	22	208	23	275	22	256	22
TMD	833	10	837	9	835	9	852	9	851	9	853	10	836	9	835	9

Ps.Ar = periosteal area (mm^2); Ec.Ar = endocortical area (mm^2); Ct.Ar = cortical area (mm^2); Ct.Th = cortical thickness (mm); J = polar moment of area (mm^4); TMD = tissue mineral density (mg HA/cm^3); BV/TV = bone volume fraction (%); Tb.N = trabecular number (1/mm); Tb.Th = trabecular thickness (μm); Tb.Sp = trabecular separation (μm).

Table 2.5. Least-squares means and standard errors from two-way ANCOVAs with body mass as a covariate, and line, activity, and the line X activity interaction as fixed factors, corresponding to tests presented in Table 2.2 for control lines.

	Line 1				Line 2				Line 4				Line 5			
	Sedentary		Active		Sedentary		Active		Sedentary		Active		Sedentary		Active	
Trait	Mean	SE	Mean	SE	Mean	SE	Mean	SE	Mean	SE	Mean	SE	Mean	SE	Mean	SE
Diaphyseal cortical																
Ps.Ar	1.89	0.05	1.88	0.05	1.90	0.05	2.01	0.05	1.79	0.05	1.97	0.05	1.81	0.05	1.93	0.06
Ec.Ar	0.73	0.03	0.84	0.03	0.81	0.03	0.85	0.03	0.61	0.03	0.73	0.03	0.64	0.03	0.83	0.03
Ct.Ar	1.16	0.04	1.05	0.04	1.09	0.04	1.16	0.04	1.19	0.04	1.25	0.04	1.17	0.04	1.10	0.04
Ct.Th	0.305	0.010	0.262	0.010	0.276	0.011	0.285	0.011	0.327	0.011	0.322	0.010	0.316	0.010	0.273	0.011
J	0.497	0.029	0.469	0.029	0.488	0.029	0.541	0.029	0.473	0.029	0.554	0.029	0.467	0.029	0.500	0.030
TMD	1132	12	1123	12	1123	12	1121	12	1129	12	1135	12	1135	12	1106	12
Metaphyseal cortical																
Ps.Ar	2.63	0.11	2.81	0.11	2.72	0.11	2.82	0.11	2.59	0.11	2.76	0.11	2.62	0.11	2.73	0.11
Ec.Ar	1.67	0.09	1.93	0.09	1.73	0.10	1.89	0.10	1.58	0.10	1.75	0.09	1.60	0.09	1.80	0.10
Ct.Ar	0.96	0.03	0.88	0.03	0.99	0.03	0.93	0.03	1.01	0.03	1.00	0.03	1.02	0.03	0.93	0.03
Ct.Th	0.148	0.005	0.123	0.005	0.149	0.005	0.136	0.005	0.155	0.005	0.143	0.005	0.146	0.005	0.130	0.006
J	0.757	0.047	0.724	0.047	0.811	0.048	0.779	0.048	0.791	0.048	0.825	0.047	0.778	0.047	0.745	0.049
TMD	1065	9	1029	9	1046	9	1048	9	1045	9	1045	9	1042	9	1019	9
Metaphyseal trabecular																
BV/TV	9.8	1.3	7.1	1.3	5.9	1.3	7.2	1.3	13.3	1.3	13.3	1.3	12.9	1.3	10.5	1.3
Tb.N	4.5	0.2	3.7	0.2	3.2	0.3	3.6	0.3	4.8	0.3	4.9	0.3	5.0	0.2	4.5	0.3
Tb.Th	42.7	1.4	42.3	1.4	47.0	1.4	44.1	1.4	46.8	1.4	44.7	1.4	46.5	1.4	43.4	1.4
Tb.Sp	218	16	277	16	319	16	282	16	208	17	204	16	204	16	227	17
TMD	863	9	859	9	842	10	862	10	854	10	863	9	851	9	845	10

Ps.Ar = periosteal area (mm^2); Ec.Ar = endocortical area (mm^2); Ct.Ar = cortical area (mm^2); Ct.Th = cortical thickness (mm); J = polar moment of area (mm^4); TMD = tissue mineral density ($mg\ HA/cm^3$); BV/TV = bone volume fraction (%); Tb.N = trabecular number (1/mm); Tb.Th = trabecular thickness (μm); Tb.Sp = trabecular separation (μm).

Table 2.6. Results of ANCOVA models used to test for possible dose relationships between distance run and bone response, with linetype as the fixed effect, line nested within linetype as a random effect, and body mass and mean daily running distance during the last 6 days of wheel access as covariates. Significant effects are indicated in bold print.

	Linetype	Body Mass	Daily Running Distance
DF	1,6	1,30	1,30
Diaphyseal cortical			
Ps.Ar	0.0581	**0.0005**	0.7203
Ec.Ar	**0.0208**	0.1504	0.5373
Ct.Ar	0.9940	**0.0003**	0.7435
Ct.Th	0.2307	**0.0422**	0.5601
J	0.1747	**<.0001**	0.9846
TMD	**0.0252**	0.2692	0.1301
Metaphyseal cortical			
Ps.Ar	0.3029	**0.0106**	0.6292
Ec.Ar	0.2669	0.0537	0.5185
Ct.Ar	0.8921	**0.0004**	0.6856
Ct.Th	0.4169	0.0644	**0.0178**
J	0.5435	**0.0005**	0.5733
TMD	0.7809	0.1412	0.6412
Metaphyseal trabecular			
BV/TV	0.5957	0.0548	0.0748
Tb.N	0.7995	0.1894	**0.0392**
Tb.Th	0.4327	0.1204	0.3672
Tb.Sp	0.786	0.1041	0.0569
TMD	0.1618	0.2128	0.0741

DF = degrees of freedom; Ps.Ar = periosteal area; Ec.Ar = endocortical area; Ct.Ar = cortical area; Ct.Th = cortical thickness; J = polar moment of area; TMD = tissue mineral density; BV/TV = bone volume fraction; Tb.N = trabecular number; Tb.Th = trabecular thickness; Tb.Sp = trabecular separation.

Table 2.7. Comparison of bone traits within the High Runner linetype, with mini-muscle mice excluded. Significance levels are for ANCOVAs with body mass as a covariate, and line, activity, and the line X activity interaction as fixed factors. Significant differences are indicated in bold print.

Trait	Line	Activity		Line X Activity	Body Mass
DF	3,22	1,22		3,22	1,22
Diaphyseal cortical					
Ps.Ar	0.0608	0.5016	A>S	0.8179	**0.0394**
Ec.Ar	0.5482	**0.0395**	**A>S**	0.852	0.3456
Ct.Ar	**0.0033**	0.0565	S>A	0.3475	0.051
Ct.Th	**0.0232**	**0.016**	**S>A**	0.4637	0.4004
J	**0.0443**	0.6132	S>A	0.6632	**0.0377**
TMD	0.9876	0.103	S>A	0.8262	0.8114
Metaphyseal cortical					
Ps.Ar	**0.0004**	0.4263	A>S	0.6122	**0.0169**
Ec.Ar	**0.0002**	0.1735	A>S	0.6728	**0.0312**
Ct.Ar	0.0531	0.0565	S>A	0.5669	**0.0136**
Ct.Th	**0.0084**	**0.0054**	**S>A**	0.7006	0.4726
J	**0.0123**	0.5588	S>A	0.4923	**0.0054**
TMD	**0.0089**	0.5142	S>A	0.8280	0.7831
Metaphyseal trabecular					
BV/TV	0.704	0.2255	A>S	0.7276	0.6292
Tb.N	0.0846	0.6038	A>S	0.6111	0.9119
Tb.Th	**0.0402**	0.406	A>S	0.1837	0.127
Tb.Sp	0.0647	0.5649	S>A	0.7514	0.6154
TMD	0.1975	0.4031	A>S	0.771	0.6832

DF = degrees of freedom; A = active mice with wheel access; S = sedentary mice without wheel access; Ps.Ar = periosteal area; Ec.Ar = endocortical area; Ct.Ar = cortical area; Ct.Th = cortical thickness; J = polar moment of area; TMD = tissue mineral density; BV/TV = bone volume fraction; Tb.N = trabecular number; Tb.Th = trabecular thickness; Tb.Sp = trabecular separation.

Figure 2.1
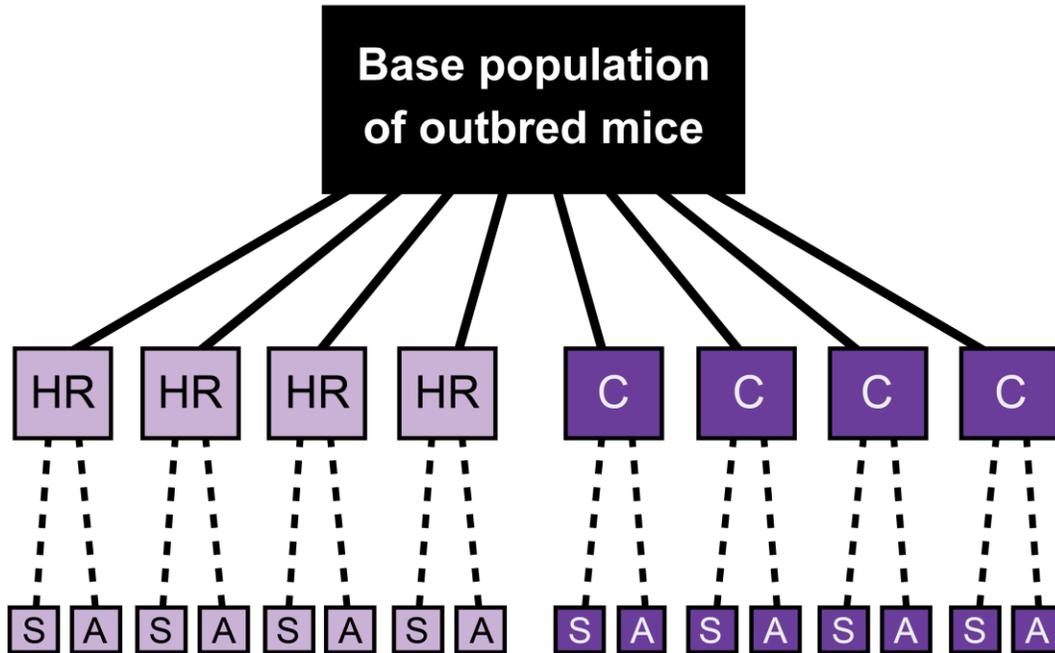
Figure 2.1. Schematic illustrating how the groups of mice employed in the study were established. Solid lines represent 21 generations of either selective breeding for high levels of voluntary wheel running (four replicate High Runner or HR lines) or breeding without regard to amount of wheel running (four replicate control or C lines). Dashed lines represent assignment of individuals within each of the eight lines to either a sedentary (S, no access to a wheel) or active (A, cages attached to wheels) lifestyle.

Figure 2.2
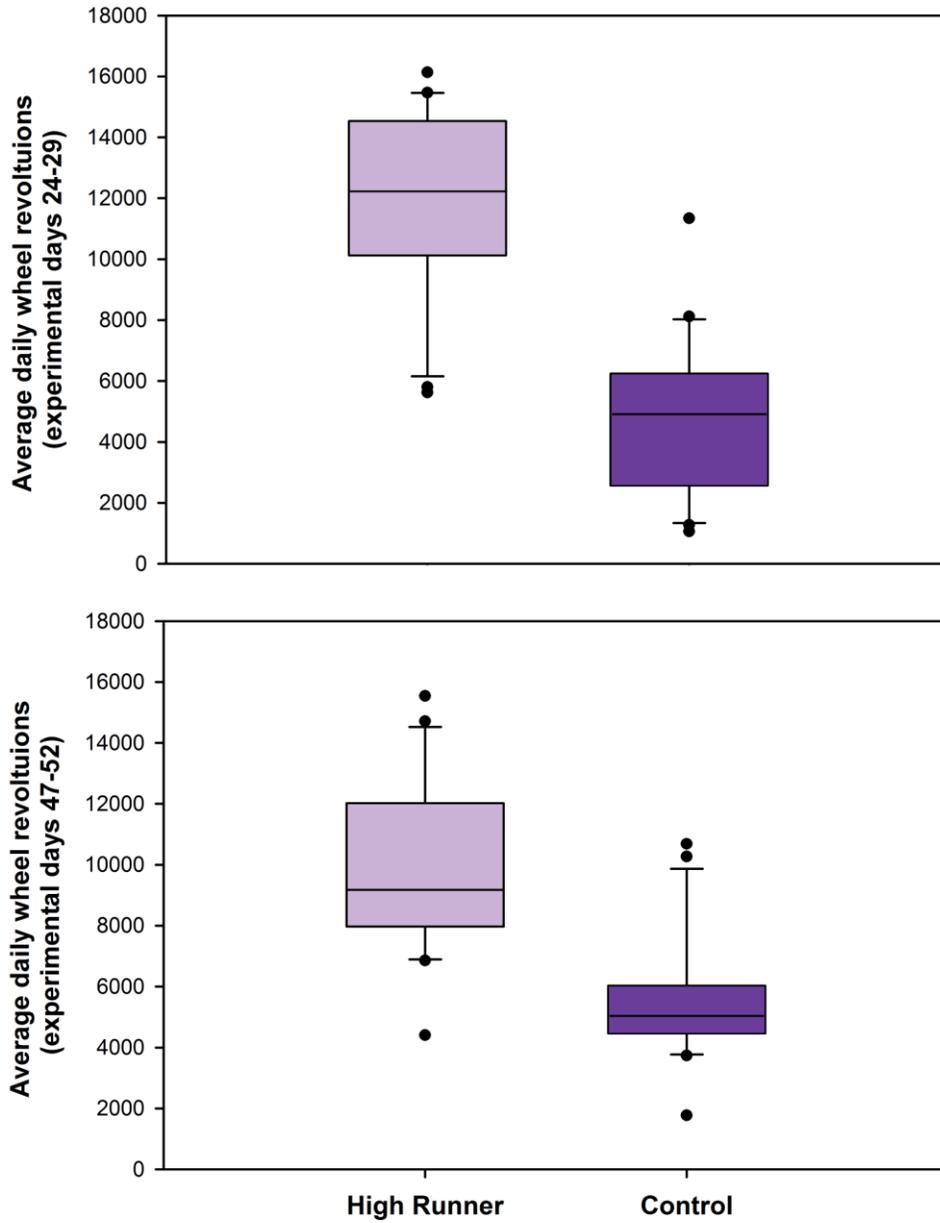
Figure 2.2. Box plots depicting average daily wheel revolutions in High Runner and control mice given wheel access during the middle 6 days (top) and last 6 days (bottom) of the experimental period. See Kelly et al. (2006) for statistical analyses of wheel-running data.

Figure 2.3
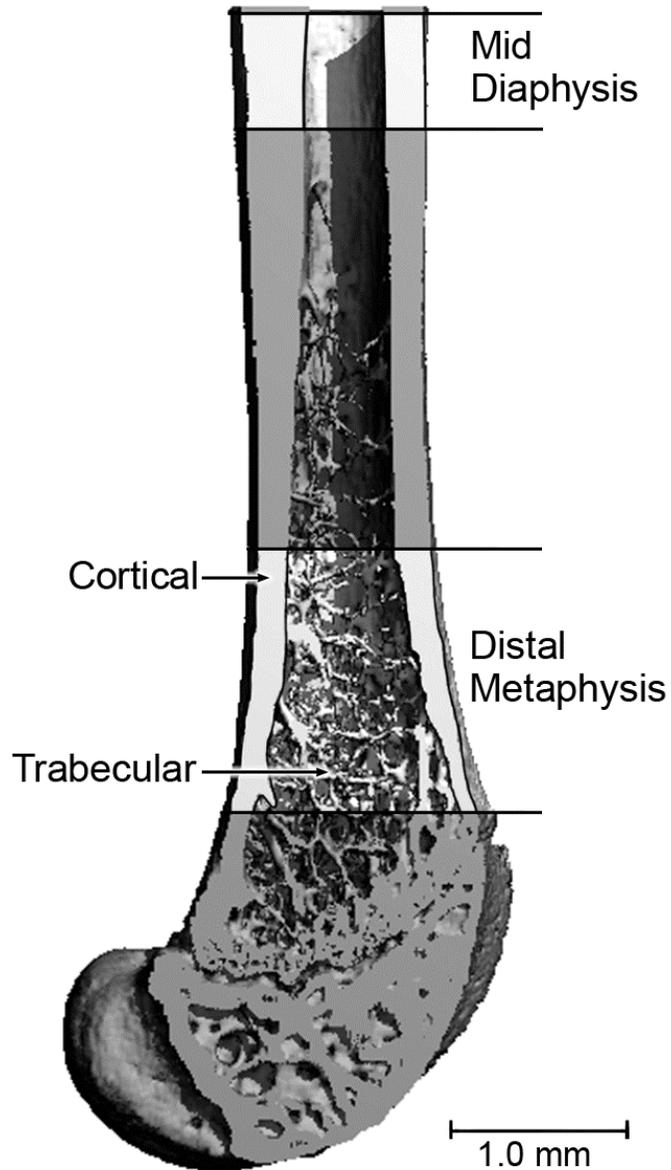
Figure 2.3. Three-dimensional reconstruction of the femur of a High Runner mouse showing the regions in the diaphysis and distal metaphysis that were analyzed using μCT. The diaphyseal region contained only cortical bone and the metaphyseal region contained both cortical and trabecular bone.

Figure 2.4
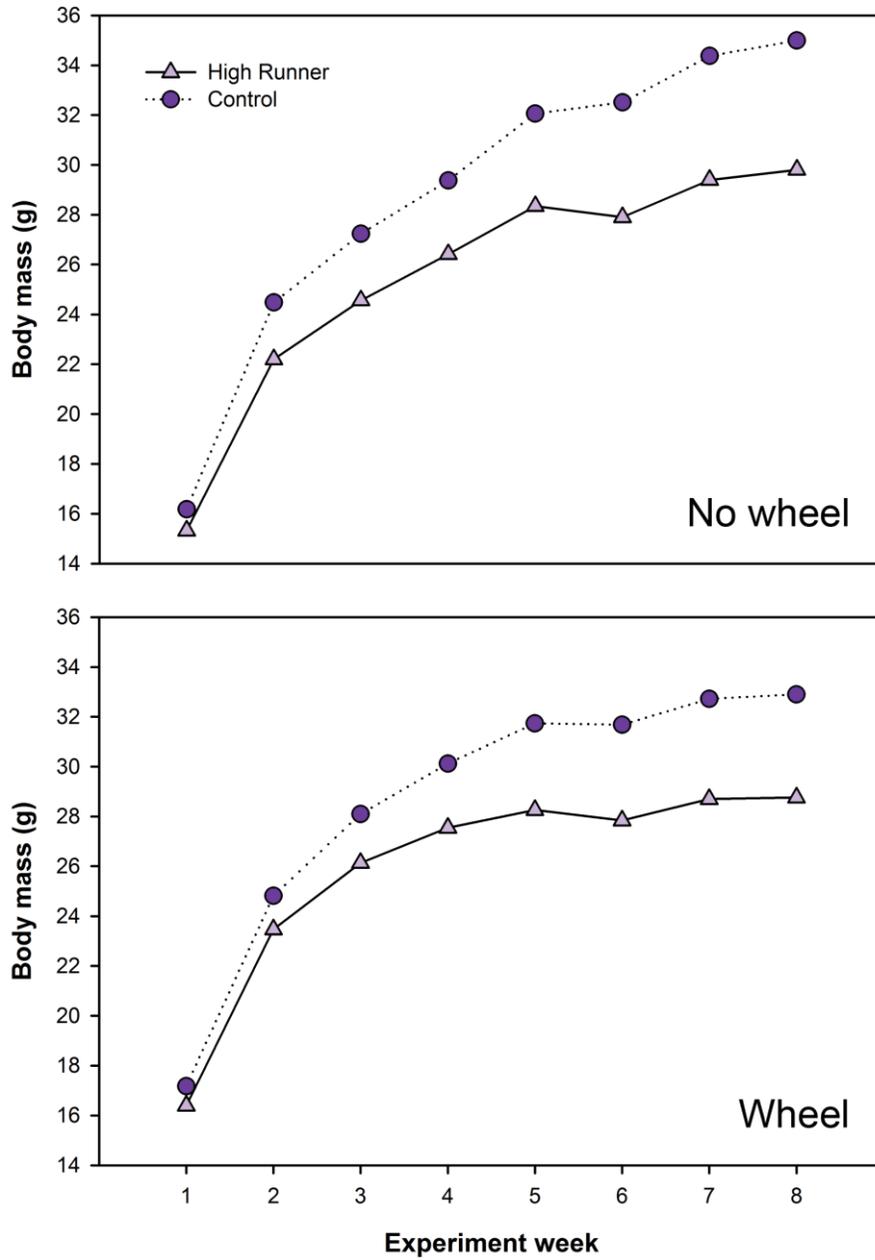
Figure 2.4. Change in body mass throughout the experimental period in High Runner and control mice denied (top) or granted (bottom) access to a running wheel. See Kelly et al. (2006) for statistical analyses of body mass data.

Figure 2.5
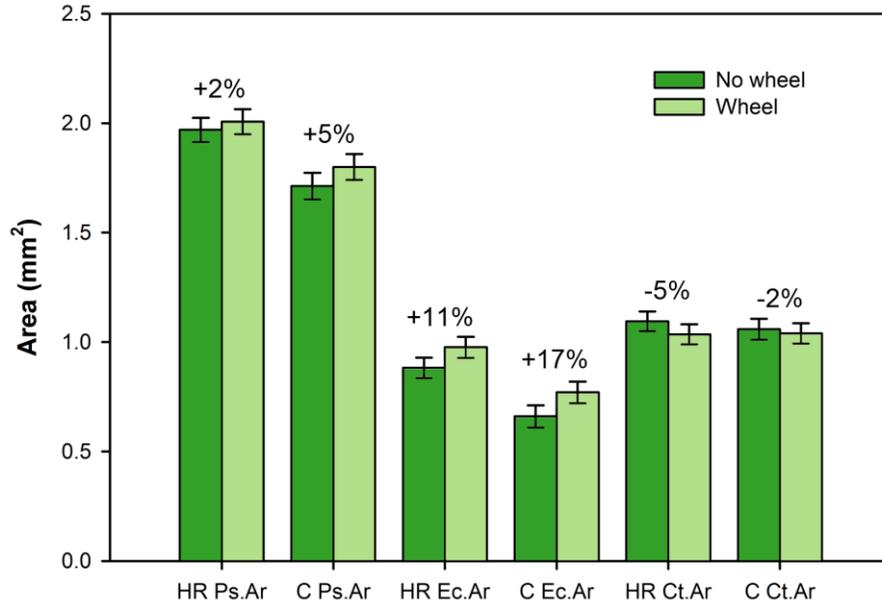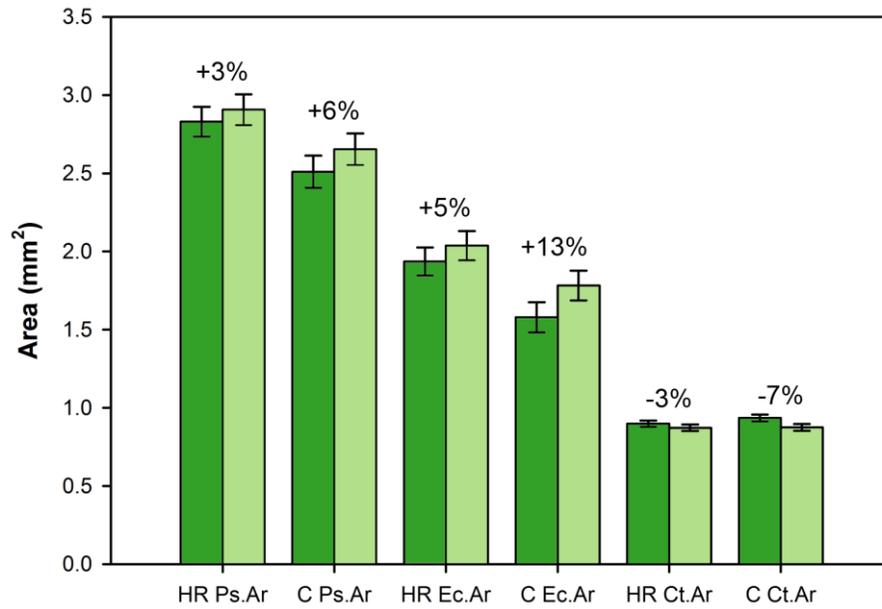
Figure 2.5. Least-squares means and standard errors (corresponding to tests presented in Table 2.1) for periosteal area (Ps.Ar), endocortical area (Ec.Ar), and cortical bone area (Ct.Ar) in the mid-diaphysis (top) and distal metaphysis (bottom). Numbers indicate change associated with access to a wheel. In both regions, wheel access induced moderate periosteal enlargement (diaphysis: $P=0.06$; metaphysis: $P<0.05$), but relatively greater endocortical enlargement (diaphysis and metaphysis: $P<0.01$). The imbalance between periosteal and endocortical expansion led to significantly reduced cortical area in the metaphysis ($P<0.02$), but not in the diaphysis ($P=0.22$).

Figure 2.6
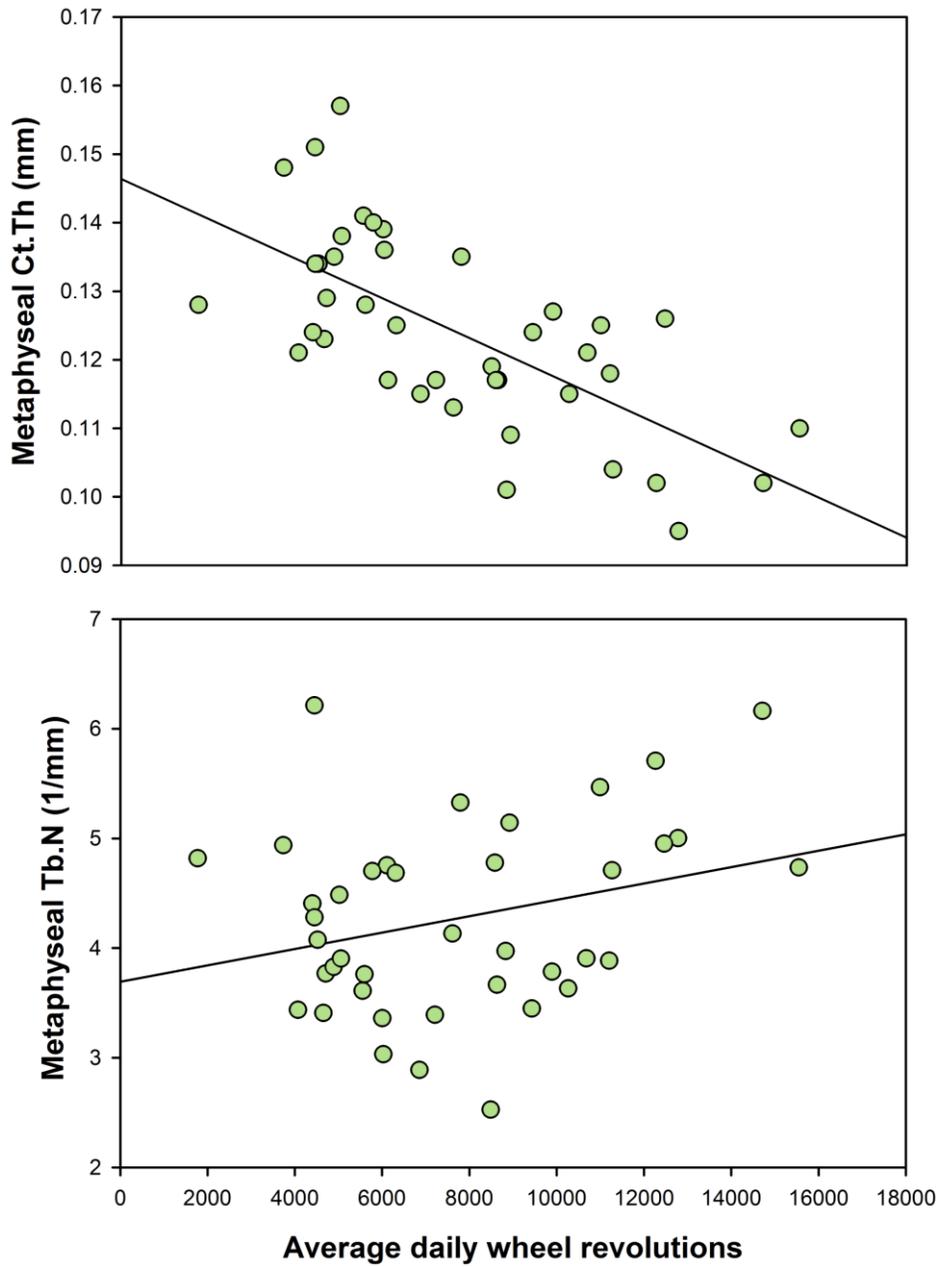
Figure 2.6. Metaphyseal cortical thickness (Ct.Th) (top) and trabecular number (Tb.N) (bottom) in relation to the mean number of daily wheel revolutions during the last 6 days of the experimental period. Lines are least-squares regressions.

Chapter 3

Physical Activity and Genetics as Determinants of Limb Bone Structure:
Insight from Outbred Stocks of Mice

Outbred stocks of mice are often used in biomedical research on the rationale that their genetic architecture models that of human populations (Rice and O'Brien, 1980; Cui et al., 1993; Festing, 2010). By definition, an outbred stock is a closed population of genetically variable animals that is bred to maintain maximum heterozygosity (Hartl, 2001; Chia et al., 2005). Therefore, in outbred mouse stocks, as in human populations, individual animals are genetically heterogeneous, and no two animals are genotypically or phenotypically identical. Commercial mouse breeders such as Harlan Sprague Dawley (HSD) and Charles River Laboratories (CRL) maintain large closed populations of outbred mice consisting of several thousand animals per population that have accumulated numerous recombination events (Yalcin and Flint, 2012). In recent years, large-scale genetic analyses have confirmed that the degree of genetic heterozygosity within many commercial outbred stocks is similar to that which exists within human populations (Yalcin et al., 2010). In addition, it has been shown that substantial genetic variation exists between commercial stocks, with certain stocks differing from each other genetically at least as much as many human populations (Aldinger et al., 2009; Yalcin et al., 2010). Thus, outbred mouse stocks represent an ideal model for examining the degree to which phenotypic traits might vary between genetically distinct populations of heterozygous individuals, and to explore how populational genetic variation may affect phenotypic responsiveness to environmental stimuli.

In this study, to examine the degree to which genetic differences between populations influence limb bone structure and strength, as well as bone's responsiveness to mechanical loading, mice were employed from two commercially available outbred stocks, Hsd:ICR (ICR) and Crl:CD1 (CD1), which are maintained by HSD and CRL, respectively. Growing animals from each stock were either treated with treadmill running exercise for 1 month or served as sedentary controls. These particular stocks were chosen for analysis because their ancestry is

especially well documented (Chia et al., 2005; Yalcin et al., 2010) and their genetic architecture displays important similarities to human populations (Aldinger et al., 2009; Yalcin et al., 2010). Both stocks derive from a small group of non-inbred albino mice imported to the United States from Switzerland in 1926 by Clara J. Lynch, a researcher at the Rockefeller Institute in New York City (Lynch, 1969). Descendants were subsequently sent to other researchers to establish breeding colonies, including one colony at the Fox Chase Cancer Center in Philadelphia during the 1940s (Chia et al., 2005). A portion of that colony was given to the Roswell Park Memorial Institute in upstate New York, which in turn gave animals to CRL in Massachusetts in 1959 to establish the CD1 stock (Rice and O'Brien, 1980). In 1983, HSD in Indianapolis acquired CD1 mice from CRL and started their own colony, the ICR stock (Yalcin et al., 2010). Thus, ICR and CD1 mice have been reproductively isolated since 1983 for at least 120 generations, which would correspond in humans to at least ~3,400 years of genetic separation (Fenner, 2005). Genetic isolation has led to clear population stratification that is comparable to that of human groups (Aldinger et al., 2009). For example, Fst, a measure of genetic diversity between populations, is approximately 0.11 for the ICR and CD1 stocks (Yalcin et al., 2010; Jonathan Flint, Wellcome Trust Centre for Human Genetics, personal communication), whereas closely related human populations typically exhibit values less than 0.05 (Reich et al., 2009), meaning that allele frequency differentiation between ICR and CD1 mice is at least as great as that between many human groups. Since becoming reproductively isolated, the ICR and CD1 stocks have been rigorously managed to preserve genetic diversity (Hartl, 2001). Average heterozygosity in both stocks is approximately 0.30 (Yalcin et al., 2010), which is well within the range of human populations (Conrad et al., 2005).

As in the previous chapter, it is reasoned that if running exercise is found to enhance limb bone morphology in both the ICR and CD1 mice, and genetic differences between stocks have little effect on skeletal structure and bone mechanoresponsiveness, then the results of this study would lend support to the idea held by many anthropologists that the physical activity levels of past human populations can be accurately inferred from variation in limb bone morphology. However, if limb bone structure and bone mechanoresponsiveness are found to be strongly influenced by genetic differences between the outbred stocks, and/or the effects of exercise loading are negligible or negative in either stock, then the results would suggest that prudence is necessary when using limb bone remains to glean information about the physical

activity levels of past human populations.

Materials and Methods

Experimental design

Female mice from ICR and CD1 outbred stocks were acquired from Harlan Sprague Dawley (Indianapolis, IN) and Charles River Laboratories (Wilmington, MA), respectively, at 3 weeks of age (n=46/stock). Non-siblings were requested in order to maximize genetic diversity within samples. Animals were housed individually in standard cages (28 X 17 X 13 cm) and maintained on a 12:12-hr light-dark cycle with free access to water and food (LabDiet 5P00 Prolab RMH 3000; PMI Nutrition Int., Brentwood, MO). At 4 weeks of age, 40 mice from each stock were divided into runners and sedentary controls (n=20/stock/activity group).[‡] Runners were treated with 30 minutes of treadmill running 5 days/week for 4 weeks. Animals were exercised on a Columbus Instruments Exer-3/6 treadmill (Columbus, OH) at a rate of 12 m/min. Sedentary controls were handled but did not run. Home-cage activity was quantified for all 80 animals at the end of weeks 2 and 3 of the exercise program. To enable measurement of dynamic indices of bone formation, animals were injected (i.p.) with calcein (30 mg/kg) on days 16 and 26 of the experimental period.[§] At 8 weeks of age, animals were euthanized by CO_2 inhalation, right hind limb muscles (quadriceps, triceps surae) were dissected and weighed, and hind limb bones (femur, tibia) were extracted and either wrapped in gauze soaked with x1 PBS (right elements for μCT analysis and mechanical testing) or placed in 70% EtOH (left elements for histomorphometry) and stored in a freezer (-20°C). Body mass was recorded weekly throughout the experimental period. Hind limb forces generated in quadrupedal locomotion were measured in the 6 additional mice from each stock between 6 and 7 weeks of age.

Microcomputed tomography

[‡] Sample sizes were determined based on a power analysis that indicated that in a two-way ANOVA an n/cell of 20 mice would produce a power level of >0.99 for the stock X activity interaction, assuming an interaction effect size of 1.13 (Bausell and Li, 2002). The effect size was estimated based on patterns of means and standard deviations reported in previous studies of the effects of running exercise on femoral mid-diaphyseal cortical area in ICR and CD1 mice (Hamrick et al., 2006; Coats et al., 2011).

[§] Histomorphometric data are not reported here.

To quantify limb bone morphology, right femora and tibiae were scanned in distilled water at a 10-μm^3 voxel size (70 kVp, 114 μA, 150-ms integration time) using a μCT 40 scanner (Scanco Medical AG, Brüttisellen, Switzerland). Cortical bone was assessed in 600- and 300-μm-long regions of the femoral and tibial diaphysis, respectively, centered at half bone length. Trabecular bone was assessed in a 1100-μm-long region of the distal femoral metaphysis, starting 850 μm proximal to the growth plate, and in a 600-μm-long region of the proximal tibial metaphysis, starting 500 μm distal to the growth plate. Micro-CT images were calibrated using hydroxyapatite phantoms (Scanco Medical AG). Volumes were segmented using a constrained 3D Gaussian filter to reduce noise (support=1, sigma=0.1 [diaphysis] and 0.5 [metaphysis]) and thresholded to extract the bone phase. The threshold values chosen for cortical and trabecular bone (593.1 and 428.1 mg HA/cm^3, respectively) were determined empirically to achieve maximal concordance between raw and thresholded images. Repeatability of this thresholding method is high (Judex et al., 2004b). Trabecular bone was isolated from the cortical shell using an automated algorithm (Lublinsky et al., 2007). Bone properties were computed using the internal imaging code supplied by the scanner manufacturer, and defined according to Bouxsein et al. (2010). Cortical bone traits included periosteal and endocortical areas (Ps.Ar, Ec.Ar; mm^2), cortical area (Ct.Ar; mm^2), average cortical thickness (Ct.Th; mm), maximal and minimal second moments of area (I$_{max}$, I$_{min}$; mm^4), polar moment of area (J; mm^4), intracortical porosity (Ct.Po; %), and tissue mineral density (TMD; mg HA/cm^3). Trabecular bone traits included bone volume fraction (BV/TV; %), trabecular number (Tb.N; 1/mm), trabecular thickness (Tb.Th; μm), and trabecular separation (Tb.Sp; μm).

Mechanical testing

To determine whether patterns of diaphyseal morphological variation translated to variation in bone strength, diaphyses were loaded in three-point bending to failure using a MTS 858 Mini Bionix II material testing machine (MTS System Corp., Cary, NC) fitted with a 100-N force cell (SMT1-100N; Interface, Inc., Scottsdale, AZ). Tests were conducted at room temperature. Femora were tested in the anteroposterior (AP) direction with the posterior surface in compression, and tibiae were tested in the mediolateral (ML) direction with the lateral surface

in compression (Wallace et al., 2007). Prior to testing, fibulae were removed from tibiae with a scalpel. The loading velocity was 0.05 mm/sec and data were recorded at 100 Hz. Load-displacement curves were used to calculate structural (whole-bone) properties, including ultimate force (F_u; N), yield force (F_y; N), and stiffness (S; N/mm). Yield was defined as the point where the load-displacement curve becomes non-linear (Currey, 2002). Mid-diaphyseal second moments of area about the bending axis (femur: I_{ML}; tibia: I_{AP}), as well as the distance from the bone area centroid to the surface in tension (c), were calculated from μCT images using BoneJ freeware (Doube et al., 2010). Ultimate stress (σ_u; MPa) was calculated as F_u x Lc/4I, yield stress (σ_y; MPa) as F_y x Lc/4I, and Young's modulus (E; MPa) as S x (L^3/48I), where L equals the 6-mm span between the outer supports (Turner and Burr, 1993).

Home-cage activity

Genetic variation in mice has been shown to be associated with different propensities to be active in home cages (e.g., Kaye and Kusy 1995; Malisch et al., 2008, 2009; Preston, 2009). Therefore, home-cage activity of all ICR and CD1 sedentary controls and runners was quantified in order to assess the degree to which cage behavior might affect apparent relationships between bone traits and mechanical loads. Home-cage activity was monitored using a 16-chamber Opto-M3 system (Columbus Instruments), in which each cage was placed into a monitoring apparatus that casted a grid of infrared beams (1.27 cm^2) above the cage floor. No additional stimulus was provided by the monitoring system, and animals maintained free access to water and food. Each animal was monitored on two separate occasions. Monitoring sessions lasted 24 hours, with measurements recorded in 1-hr intervals. Overall home-cage activity was quantified as the total number of times during a 24-hr period that a new infrared beam was broken. Repeated interruptions of individual beams caused by scratching, grooming, or other non-ambulatory movements were disregarded. For each animal, data collected during the two 24-hr sessions were averaged.

Ground reaction forces

To verify that the forces sustained by the hind limbs during quadrupedal locomotion are similar in ICR and CD1 mice, the vertical component of peak ground reaction forces generated by steady state walking and running in the two stocks was measured using a custom-built force plate (Riskin et al., 2009). The plate consists of a stiff 28-cm-long X 28-cm-wide honeycomb fiberfoam surface supported at two opposite ends by aluminum beams with spring blade elements instrumented with strain gages. Signals from strain gages were amplified (2100 system; Vishay Measurements Group, Raleigh, NC), digitized (PCI-6071E; National Instruments, Austin, TX), and saved to a personal computer. The force plate was modified for collection of single-limb contacts by attaching a 90-g wooden strip to the plate surface and concealing the rest of the plate with a wooden runway (Zumwalt et al., 2006). Animals moved within a clear Lexan tunnel placed over the runway (44-cm long X 7-cm wide). Neither the runway nor the tunnel contacted the force plate surface. On each recording day, the relationship between vertical force magnitude and voltage output was determined by applying a series of known weights (5-100 g) to the wooden strip contacting the force plate surface. Regressions of force to voltage were linear ($R^2 > 0.999$). Electronic drift in the baseline output was determined separately for each trial by sampling the signal of the unloaded plate within 2 seconds of limb contact. Animal body mass was measured before each recording session. Ground reaction forces recorded at 1000 Hz and video recorded in lateral view at 500 Hz were synchronized using a ProCapture motion analysis system (Xcitex, Inc., Cambridge, MA). Subject speed was calculated from video as the time interval required for a fixed anatomical landmark (i.e., the nose) to pass between markers on either side of the force plate. Force data were filtered with a 30-Hz low-pass Butterworth filter and extracted using ProAnalyst software (Xcitex, Inc.). Data from between 5 and 10 hind limb contacts were collected per animal (n=47 and 49 steps total for ICR and CD1 mice, respectively).

Statistical analyses

All statistical analyses were performed in R freeware (version 2.15.3; R Core Development Team 2013). Shapiro-Wilk tests were used to determine if data followed a normal distribution, and Levene's tests were used to assess the equality of group variances. Independent-samples t-tests were used to determine whether genetic variation between ICR and CD1 mice led to differences in body composition, bone traits, and home-cage activity levels within each

activity group (e.g., ICR controls vs. CD1 controls), and whether exercise caused differences in traits between runners and controls within each stock (e.g., ICR runners vs. ICR controls). Two-way ANOVAs were also used to assess whether the effect of running on traits differed between ICR and CD1 mice (as indicated by statistically significant stock X activity group interactions). Because significant differences in body mass and bone length were detected among experimental groups, additional tests were performed on the most mechanically relevant diaphyseal structural traits standardized by body size. Specifically, cortical area was standardized by body mass, and area moments were standardized by the product of body mass and bone length (Ruff et al., 1993). Because ICR sedentary controls were found to be significantly less active in their home cages than CD1 controls, linear regression was used to assess the degree to which home-cage activity affected bone parameters in these animals. As speed is a potential confounding factor in ground reaction force studies, Pearson product moment correlation was used to test for an association between speed and hind limb peak vertical ground reaction forces (Wallace and Demes, 2008). The relationship between these variables was found to be non-significant; therefore, independent-samples t-tests were used to assess differences in peak vertical limb forces between the stocks. Significance level for all tests was $P<0.05$. Relative differences between group means were calculated as percent difference $\pm$ standard deviation of the sampling distribution of the relative difference (Holguin et al., 2011).

Results

Body size and composition

At the beginning of the experiment, when mice were 4 weeks of age, body mass was not significantly different among the experimental groups (Table 3.1). In all groups, body mass increased steadily over the course of the experimental period, with the most rapid increase occurring during the first week (Figure 3.1). By 5 weeks of age, ICR sedentary controls weighed significantly less than CD1 controls (P=0.03), and this difference remained significant until the end of the experiment, at which point CD1 controls were 4±2% heavier than ICR controls (P=0.02). In addition, at the end of the experiment, relative to ICR sedentary mice, CD1 controls had 9±4% greater quadriceps mass (P=0.02), 5±2% greater triceps surae mass (P=0.03), and

51

3±1% longer femora and tibiae (P<0.0001) (Table 3.1). At no point during the experiment were body mass differences between ICR and CD1 runners significant, nor were muscle mass differences at the end of the experiment. However, CD1 runners had 2.2±0.7% longer femora (P<0.01) and 1.4±0.5% longer tibiae (P<0.01) compared to ICR runners. In neither stock did treadmill exercise result in significant differences in body mass between sedentary controls and runners at any point during the experiment. Muscle mass was also not significantly affected by running. In the ICR stock, treadmill exercise led to a 1.2±0.5% increase in tibial length (P=0.03), but femoral length was not significantly altered. In the CD1 stock, running did not significantly affect bone length. No significant stock X activity group interactions were detected for any body size or body composition parameter (Table 3.1).

Diaphyseal cortical bone morphology

Significant differences in femoral diaphyseal cortical bone morphology were found between the ICR and CD1 stocks (Tables 3.2 and 3.3; Figures 3.2 and 3.3). Among the sedentary controls, relative to ICR mice, CD1 mice had 15±3% larger periosteal areas (P<0.0001), 13±5% larger endocortical areas (P<0.01), 18±4% larger cortical areas (P<0.0001), 11±4% thicker cortices (P<0.01), 32±8% greater maximal second moments of area (P<0.001), 41±8% greater minimal second moments of area (P<0.00001), and 35±7% greater polar moments of area (P<0.0001) (Table 3.2; Figure 3.2). Significant differences remained detectable when femoral diaphyseal cortical bone parameters were standardized for body size: CD1 sedentary mice had 13±4% larger cortical areas (P<0.001), 22±6% greater maximal second moments of area (P<0.01), 30±6% greater minimal second moments of area (P<0.0001), and 25±6% greater polar moments of area (P<0.001) compared to ICR controls (Table 3.3; Figure 3.3). Interestingly, a different pattern was observed among the animals treated with treadmill exercise (Table 3.2; Figure 3.2). Only two significant stock differences were detected, and CD1 runners were found to have 6±3% thinner cortices (P=0.04) compared to ICR runners, primarily as a result of having 13±5% larger endocortical areas (P<0.01). No significant stock differences were detected among the runners in size-standardized femoral diaphyseal properties (Table 3.3; Figure 3.3).

Treadmill running had a very different effect on femoral diaphyseal cortical bone morphology within the ICR and CD1 stocks (Tables 3.2 and 3.3; Figures 3.4 and 3.5). ICR mice

treated with running exercise had 6±3% larger periosteal areas (P=0.03), 11±3% larger cortical areas (P<0.001), 10±3% thicker cortices (P<0.001), 17±6% greater maximal second moments of area (P<0.01), 16±6% greater minimal second moments of area (P<0.01), and 17±6% greater polar moments of area (P<0.01) compared to ICR sedentary controls (Table 3.2; Figure 3.4). When femoral diaphyseal structural properties were standardized for body size, ICR runners had 10±2% larger cortical areas (P<0.001), 15±5% greater maximal second moments of area (P<0.01), 14±5% greater minimal second moments of area (P<0.01), and 14±4% greater polar moments of area (P<0.01) relative to ICR controls (Table 3.3; Figure 3.5). In contrast, CD1 mice treated with running exercise displayed diminished femoral diaphyseal cortical bone structure relative to CD1 sedentary controls, although differences between activity groups for both raw or size-standardized properties were never significant (Tables 3.2 and 3.3; Figures 3.4 and 3.5). A differential effect of running exercise on femoral diaphyseal morphology in ICR and CD1 mice was further indicated by multiple significant stock X activity group interactions, including for cortical thickness (P<0.001), raw and size-standardized cortical area (P<0.001 and P<0.01, respectively), raw and size-standardized maximal second moments of area (P=0.03 and P=0.04, respectively), raw and size-standardized minimal second moments of area (P=0.01 and P=0.02, respectively), and raw and size-standardized polar moments of area (P=0.02 and P=0.03, respectively) (Tables 3.2 and 3.3).

As in the femur, significant differences in tibial diaphyseal cortical bone structure were detected between the ICR and CD1 stocks (Tables 3.2 and 3.3; Figures 3.2 and 3.3). However, the pattern of stock differences was more consistent across activity groups than it was in the femur. Among the sedentary controls, compared to ICR mice, CD1 mice had 19±3% larger periosteal areas (P<0.00001), 35±6% larger endocortical areas (P<0.000001), 11±3% larger cortical areas (P<0.01), 38±7% greater maximal second moments of area (P<0.00001), 36±8% greater minimal second moments of area (P<0.0001), and 37±7% greater polar moments of area (P<0.00001) (Table 3.2; Figure 3.2). In terms of body size-standardized tibial diaphyseal properties, CD1 sedentary controls had 6±3% larger cortical areas (P=0.03), 28±6% greater maximal second moments of area (P<0.0001), 26±7% greater minimal second moments of area (P<0.001), and 27±6% greater polar moments of area (P<0.0001) relative to ICR controls (Table 3.3; Figure 3.3). Among the animals treated with treadmill running, CD1 mice had 11±3% larger periosteal areas (P<0.0001), 30±5% larger endocortical areas (P<0.000001), 23±5% greater

53

maximal second moments of area (P<0.001), 17±5% greater minimal second moments of area (P<0.01), and 21±5% greater polar moments of area (P<0.001) relative to ICR mice (Table 3.2; Figure 3.2). In addition, CD1 runners had 19±5% greater size-standardized maximal second moments of area (P<0.001), 15±4% greater size-standardized minimal second moments of area (P<0.01), and 18±4% greater size-standardized polar moments of area (P<0.001) compared to ICR runners (Table 3.3; Figure 3.3).

The effect of treadmill running on tibial diaphyseal cortical bone structure also differed between the ICR and CD1 stocks as it did in the femur (Tables 3.2 and 3.3; Figures 3.4 and 3.5). ICR runners had 9±3% larger periosteal areas (P<0.01), 11±3% larger cortical areas (P<0.01), 4±2% thicker cortices (P=0.02), 20±6% greater maximal second moments of area (P<0.01), 21±7% greater minimal second moments of area (P<0.01), and 20±6% greater polar moments of area (P<0.01) compared to ICR sedentary controls (Table 3.2; Figure 3.4). In addition, relative to ICR controls, ICR runners had 10±3% larger size-standardized cortical areas (P<0.01), 17±6% greater maximal second moments of area (P<0.01), 18±6% greater minimal second moments of area (P<0.01), and 17±6% greater polar moments of area (P<0.01) (Table 3.3; Figure 3.5). Unlike in the femur, treadmill running had a positive effect on tibial diaphyseal structure in the CD1 mice, but the effect was not as great as that observed in the ICR mice. Relative to CD1 controls, CD1 runners had 3±1% thicker cortices (P=0.03), 5±2% larger size-standardized cortical areas (P=0.02), and 9±4% greater size-standardized maximal second moments of area (P=0.03) (Tables 3.2 and 3.3; Figures 3.4 and 3.5). No significant stock X activity group interactions were detected for any tibial diaphyseal structural parameter (Tables 3.2 and 3.3).

Diaphyseal cortical bone tissue composition

Differences in femoral and tibial cortical bone tissue mineral density and intracortical porosity were not significant within either activity group or stock, nor were stock X activity group interactions significant (Table 3.2). However, it is noteworthy that ICR mice consistently displayed higher tissue mineral density than CD1 mice within both activity groups.

Metaphyseal trabecular bone morphology

54

Trabecular bone structure in the distal femoral metaphysis differed significantly between the ICR and CD1 stocks (Table 3.4; Figure 3.6). Among the sedentary controls, CD1 mice had 13±6% fewer trabeculae (P<0.01) and 22±7% greater trabecular separation (P<0.01) compared to ICR mice. Similarly, among the mice treated with treadmill exercise, relative to ICR runners, CD1 runners had 31±8% lower trabecular bone quantity (P<0.001), 27±5% fewer trabeculae (P<0.00001), and 41±7% greater trabecular separation (P<0.00001).

Treatment with running exercise affected distal femoral metaphyseal trabecular bone morphology differently in ICR and CD1 mice (Table 3.4; Figure 3.6). Among the ICR mice, running resulted in 24±11% greater trabecular bone quantity (P=0.04), 12±6% more trabeculae (P=0.04), and 12±6% smaller trabecular separation (P=0.03). In contrast, CD1 runners displayed diminished trabecular bone structure relative to CD1 sedentary controls, although differences between activity groups were not significant. A significant stock X activity group interaction was detected for trabecular thickness (P=0.04) such that running had a positive effect on trabecular thickness in ICR mice but a negative effect in CD1 mice.

As in the distal femur, trabecular bone structure in the proximal tibial metaphysis differed significantly between ICR and CD1 mice (Table 3.4; Figure 3.6). Among the sedentary controls, CD1 mice had 13±4% thicker trabeculae (P<0.01) and 13±6% greater trabecular separation (P=0.03) relative to ICR mice. Among the mice treated with treadmill exercise, compared to ICR runners, CD1 runners had 17±5% fewer trabeculae (P<0.01) and 21±6% greater trabecular separation (P<0.01).

Few significant differences in tibial trabecular bone structure were detected between sedentary controls and runners in either stock (Table 3.4; Figure 3.6). In the ICR mice, consistent with the pattern observed in the femur, runners had greater trabecular bone quantity than sedentary controls, but not significantly so (Figure 3.6). The only significant effect of running on tibial trabecular bone structure in the ICR mice was a 9±4% increase in trabecular thickness (P=0.03). No significant effects of running were detected in the CD1 mice, nor were any significant stock X activity group interactions detected for tibial trabecular bone traits.

Diaphyseal strength

Femoral diaphyseal strength differed significantly between the ICR and CD1 stocks (Table 3.5; Figure 3.8), as would be expected based on their diaphyseal structural differences. Among the sedentary controls, relative to ICR mice, CD1 mice displayed 40±7% higher ultimate force (P<0.00001), 45±8% higher yield force (P<0.00001), and 29±8% greater stiffness (P<0.01). Among the mice treated with running exercise, CD1 runners had 16±6% higher yield force (P=0.01) compared to ICR runners.

The effects of treadmill running on femoral diaphyseal strength are also consistent with the patterns detected in diaphyseal morphology, in that the stocks displayed a differential response to exercise (Table 3.5; Figure 3.9). In the ICR stock, running led to 15±5% higher ultimate force (P<0.01), 13±5% higher yield force (P=0.02), and 16±7% greater stiffness (P=0.03). In contrast, relative to CD1 sedentary controls, CD1 runners had 11±5% lower ultimate force (P<0.05), as well as non-significant reductions in yield force and stiffness. The divergent effects of running exercise on femoral diaphyseal strength in ICR and CD1 mice were further indicated by significant stock X activity group interactions for ultimate force (P<0.01), yield force (P=0.01), and stiffness (P=0.03).

Tibial diaphyseal strength also differed significantly between the ICR and CD1 stocks (Table 3.5; Figure 3.8), as again would be expected based on their diaphyseal morphological differences. Among the sedentary controls, CD1 mice exhibited 11±5% higher ultimate force (P<0.05), 12±5% higher yield force (P=0.03), and 12±6% greater stiffness (P=0.4) compared to ICR mice. No significant stock differences were found among the mice treated with treadmill running.

Running exercise affected tibial diaphyseal strength differently in ICR and CD1 mice (Table 3.5; Figure 3.9), as it did tibial diaphyseal structure. In the ICR mice, treadmill running led to a 12±5% increase in ultimate force (P=0.03) and a 14±5% increase in stiffness (P<0.01). In the CD1, tibial diaphyseal strength was not significantly affected by running. Stock X activity group interactions for all tibial diaphyseal strength parameters were non-significant.

Diaphyseal cortical bone tissue strength

Differences in femoral cortical bone tissue ultimate stress, yield stress, and Young's modulus were not significant within either activity group or stock, nor were stock X activity group interactions significant (Table 3.5).

In the tibia, significant differences in cortical bone tissue strength were detected among the ICR and CD1 stocks (Table 3.5). Among the sedentary controls, CD1 mice displayed 9±4% lower ultimate stress (P=0.02) and a 13±6% lower Young's modulus (P=0.03) compared to ICR mice. Among the mice treated with running exercise, relative to ICR runners, CD1 runners exhibited 15±3% lower ultimate stress (P<0.0001), 10±4% lower yield stress (P=0.01), and a 15±5% lower Young's modulus (P<0.01). Treadmill running did not have a significant effect on tibial cortical bone tissue strength in either the ICR or CD1 mice, and no significant stock X activity group interactions were detected for any parameter (Table 3.5).

Home-cage activity

The pattern of home-cage activity throughout a 24-hr period was generally similar among the experimental groups (Figure 3.10). Peak activity occurred ~2-3 hours after the lights were turned off and then declined thereafter. The lowest activity levels occurred during the ~9 hours prior to the lights being turned on. In terms of overall daily home-cage activity levels, CD1 sedentary controls were significantly more activity than ICR controls (P=0.01), but ICR and CD1 runners exhibited similar activity levels. In neither stock were daily home-cage activity levels significantly different between the sedentary controls and runners. In addition, the stock X activity group interaction for daily home-cage activity level was not significant.

Effects of home-cage activity on diaphyseal cortical bone morphology

Given the significant difference in overall home-cage activity level between the ICR and CD1 sedentary controls, linear regression was used to assess the degree to which home-cage activity may have affected differences in femoral and tibial traits detected between the groups (Table 3.6; Figure 3.11). All relationships between bone parameters and average daily ambulatory counts were found to be non-significant. For example, Figure 3.11 illustrates the lack of a strong relationship between body size-standardized diaphyseal structural parameters and

home-cage activity. These results suggest that differences in bone traits between ICR and CD1 sedentary controls can reasonably be attributed to genetic variation between the stocks rather than to bone loading history.

Hind limb peak ground reaction forces

Peak vertical ground reaction forces sustained by the hind limbs during quadrupedal walking and running were not significantly different between ICR and CD1 mice, regardless of whether raw or body mass-standardized forces are considered (Table 3.7; Figure 3.12).

Discussion

The effects of genetic variation at the population level on limb bone structure and strength, as well as bone mechanoresponsiveness, were investigated using mice from two commercial outbred stocks, ICR and CD1. Animals from each stock were either treated with treadmill exercise for 1 month, beginning shortly after weaning, or served as sedentary controls. At the end of the experimental period, cortical and trabecular bone structure were assessed in the femur and tibia with μCT and diaphyseal strength was determined by mechanical testing. Genetic background was found to have a strong influence on nearly all morphological and mechanical parameters analyzed. Among the sedentary controls, CD1 mice displayed significantly enhanced femoral and tibial diaphyseal bone areas and area moments, as well as elevated diaphyseal mechanical strength, relative to ICR mice. Among the animals treated with treadmill exercise, fewer significant stock differences in diaphyseal morphology and strength were detected, although compared to ICR runners, CD1 runners exhibited elevated femoral yield strength, larger tibial periosteal areas, and enhanced tibial area moments. In addition, femoral and tibial trabecular bone morphology were significantly diminished in CD1 runners relative to ICR runners. The somewhat divergent patterns of inter-stock variation detected in the controls and runners can be explained, in large part, by the dramatic difference observed between ICR and CD1 mice in the responsiveness of their bones to treadmill exercise. In the ICR mice, treadmill running led to significantly enhanced diaphyseal bone areas, area moments, and mechanical strength in both the femur and tibia, and to improved trabecular bone morphology in

58

the distal femur. In contrast, in CD1 mice, running had a negative effect (albeit non-significant) on femoral diaphyseal structure, and led to significantly reduced femoral diaphyseal strength. The differential effects of running on ICR and CD1 femora were further indicated by several significant stock X activity group statistical interactions, including for diaphyseal cortical area, area moments, and mechanical strength. In the tibia, running had a moderate positive effect on diaphyseal structure in the CD1 mice, resulting in significantly enhanced size-standardized cortical areas and maximal second moments of area. However, in general, far fewer tibial parameters were significantly improved by running in CD1 mice than in ICR mice, again indicating distinct effects of mechanical loading on the limbs bone of the two stocks.

In terms of cortical bone tissue properties, ICR mice consistently exhibited greater tissue mineral density than CD1 mice, but the differences between stocks were never significant in either the sedentary controls or runners. However, significant stock differences were detected in tibial tissue strength, such that, within both activity groups, ICR mice had stronger cortical tissue than CD1 mice. This highlights the fact that, although tissue mineral density is positively related to tissue strength, they are not proportional to each other (Currey, 1984). Relatively small differences in mineral content can cause major differences in strength. Treadmill running did not lead to significant changes in cortical tissue composition or strength in either stock, which is consistent with cross-sectional studies of human athletes suggesting that exercise loading affects bone morphology to a greater degree than it does tissue-level parameters (e.g., Haapasalo et al., 2000).

As shown by the force plate analyses, peak ground reaction forces sustained by the hind limbs of ICR and CD1 mice during quadrupedal locomotion are similar. Therefore, apparent differences between stocks in bone morphology, strength, and mechanoresponsiveness are not likely to have been affected by variation in external force magnitudes. However, CD1 sedentary controls were found to engage in higher levels of home-cage activity compared to ICR controls, thus introducing the possibility that the enhanced limb bone structural and mechanical properties of CD1 controls relative to ICR controls were caused, in part, by the frequency of loading events and not only alleles directly influencing bone development. Indeed, studies of inbred mice have found that strains exhibiting elevated home-cage activity also tend to display augmented skeletal structure, suggesting that these two phenomena may be causally related (Kaye and Kusy, 1995; Preston, 2009). However, this pattern is not consistent across all inbred strains. For example, B6

mice relative to C3H mice have greatly diminished limb bone morphology (Judex et al., 2004b) but are far more active in their home cages (de Visser et al., 2006). Therefore, the influence of cage activity on the mouse skeleton remains unclear. In this study, to assess the degree to which limb bone structure and strength in ICR and CD1 sedentary controls were affected by home-cage activity, linear regression was used to test for relationships between bone properties and average daily ambulatory counts at the level of individual variation within each stock. Interestingly, in both stocks, cage activity accounted for a remarkably small portion of the total variation in bone structure and strength. R^2 values for all femoral and tibial diaphyseal structural and mechanical properties were less than 0.06, and no relationships between bone parameters and cage activity were significant. Thus, although it is possible that variation in home-cage activity between ICR and CD1 controls contributed to the observed bone morphological and mechanical variation, its contribution is likely to have been minimal relative to genetic factors. Furthermore, it is important to note that in neither stock was home-cage activity significantly different between the sedentary controls and runners, nor was the stock X activity group interaction significant for home-cage activity, meaning that cage behavior is unlikely to have confounded the observed relationships between bone traits and treadmill exercise.

Given that bone properties among the sedentary mice were not greatly influenced by home-cage activity, skeletal differences between ICR and CD1 controls were presumably achieved through stock-specific bone growth regulatory mechanisms semi-independent of mechanical signals. In a study by Price and colleagues (2005) examining variation in limb bone growth patterns among inbred mouse strains, it was found that most genotype-specific bone traits present at 2 months of age were established by 1 month of age. Therefore, bone phenotypic differences between 2-month-old ICR and CD1 controls at the end of the experimental period likely approximate stock differences existing at the onset of the experiment when animals were 1-month old (i.e., 'baseline' phenotypic differences). If so, then distinct baseline skeletal structure may have promoted the differential effects of running exercise on ICR and CD1 limb bones. Specifically, if CD1 mice had enhanced limb bone diaphyseal structure early on in the experiment—as did CD1 controls at the end of the experiment—then equal mechanical loads produced by treadmill running would have engendered higher strains in the less rigid diaphyses of ICR mice and, likewise, may have been more potent stimuli for bone formation (Leppänen et al., 2008). This scenario is consistent with the 'principle of initial value' of exercise training

which states that individuals with low initial values of a physiologic parameter will exhibit the greatest improvement in response to exercise (Winters-Stone and Snow, 2003; Koch et al., 2005). Nevertheless, even if stock-specific skeletal growth patterns contributed to the greater responsiveness of ICR limb bones, this factor alone cannot explain all distinct effects of exercise in the two stocks. For example, enhanced baseline diaphyseal properties in CD1 mice would not account for the significantly *diminished* femoral strength caused by running in this stock, or the non-significant reductions in femoral structural parameters. According to existing models of strain regulation of skeletal structure (Rubin, 1984; Frost, 2003), the most 'detrimental' response of bone to exercise loading should be stasis, not catabolism. In addition, baseline skeletal morphology would not have been responsible for the significant increase in femoral trabecular bone quantity in ICR runners but not CD1 runners, assuming that ICR mice displayed enhanced trabecular structure early in the experiment, as did ICR controls at the end of the experiment. Unfortunately, rigorous evaluation of the role of initial skeletal morphology in dictating bone's response to exercise would require measurements of true baseline bone structure from *in vivo* μCT, which was not logistically possible in this study given the large number of animals that would have had to be scanned roughly concurrently.

In previous studies documenting negative effects of exercise on skeletal structure in humans, the catabolic response has typically been attributed to factors related to organismal energy availability and mineral homeostasis (Scofield and Hecht, 2012), highlighting the complex patterns of tradeoffs and constraints that exist between the skeleton and other systems simultaneously stimulated by exercise. For example, sweating causes calcium loss, which can induce bone resorption (Barry and Kohrt, 2008). More importantly, these studies draw attention to the fact that genetic variants have the capacity to influence the skeleton's response to exercise not only by affecting bone tissue mechanotransduction *per se*, but also by influencing multiple dimensions of whole-organism physiology (Karsenty and Ferron, 2012). For example, genetic polymorphisms regulating exercise-induced endocannabinoid signaling and associated changes in psychological state (e.g., 'runner's high') (Raichlen et al., 2012, 2013) could, hypothetically, affect the skeletal reaction to exercise given the apparent role of endocannabinoids in modulating bone cell activity and bone turnover (Idris and Ralston, 2012). Ultimately, with numerous direct and indirect pathways by which alleles can influence the skeletal effects of physical activity,

exercise studies such as this one are inevitably limited in their ability to elucidate the precise genetic basis of the observed bony responses.

As discussed in Chapter 1, it has been suggested that the limb bones of small animals such as mice should be less responsive to functional loading than the bones of larger animals such as humans due to factors related to skeletal allometry, and, therefore, extrapolating results from small animals to large animals requires caution (e.g., Skedros, 2012). Interestingly, however, in this study, the magnitude of the osteogenic response to treadmill running among the ICR mice was comparable to results obtained from exercise studies involving larger animals such as sheep (e.g., Lieberman and Pearson, 2001; Lieberman et al., 2003; Devlin and Lieberman, 2007; Barak et al., 2011). For example, in a study by Lieberman and colleagues (2003), 3 months of treadmill running by juvenile sheep led to 3%, 12%, and 6% increases in size-standardized diaphyseal cortical bone areas in the femur, tibia, and metatarsal, respectively, whereas in the present study, 1 month of treadmill running by growing ICR mice led to 10% gains in size-standardized diaphyseal cortical areas in both the femur and tibia. In terms of trabecular bone, a study by Barak et al. (2011) found that 1 month of treadmill running by juvenile sheep resulted in 8% and 20% increases in trabecular bone volume fraction in the medial and lateral distal radius, respectively, while in this study, the same duration of exercise treatment in ICR mice caused 24% and 27% gains in trabecular bone quantity in the distal femur and proximal tibia, respectively. Therefore, although there may be sound theoretical reasons to expect body size to affect limb bone mechanoresponsiveness (see Chapter 1), this expectation is not supported by the results of this study. Instead, the present results suggest that experimental data obtained from small animals such as mice may provide valuable insight into the skeletal mechanobiology of larger animals including humans.

If extrapolation of data reported here from mice to humans is warranted, then the results of this study suggest that patterns of limb bone structural variation among paleontological and archaeological human samples likely reflect, to some degree, genetic differences among populations, which greatly limits our ability to accurately infer mechanical loading history from the morphology of limb bone remains. Furthermore, this study illustrates that one way in which genetic differences among populations may exert their influence on the skeleton is by modulating the responsiveness of limb bones to mechanical loads, which means that the magnitude of the functional signal could vary in the limb bones of individuals from different

populations despite similar physical activity levels during life. In sum, the results of this study suggest that prudence is necessary when using limb bone remains to investigate the physical activity levels of human populations living in the past.

Table 3.1. Body size and composition in ICR and CD1 sedentary controls and runners. Values are means ± SD.

Trait	ICR Sedentary	ICR Runner	CD1 Sedentary	CD1 Runner
Initial body mass (g)	18.9 ± 1.5	19.6 ± 1.6	19.0 ± 1.8	19.0 ± 1.7
Final body mass (g)	26.1 ± 1.6	26.4 ± 1.9	27.2 ± 1.6[a]	26.7 ± 1.6
Quadriceps mass (g)	0.162 ± 0.020	0.168 ± 0.017	0.176 ± 0.019[a]	0.171 ± 0.019
Triceps surae mass (g)	0.136 ± 0.011	0.138 ± 0.008	0.143 ± 0.008[a]	0.139 ± 0.010
Femur length (mm)	15.0 ± 0.4	15.1 ± 0.3	15.5 ± 0.3[b]	15.4 ± 0.3[a]
Tibia length (mm)	17.0 ± 0.3	17.2 ± 0.3[c]	17.5 ± 0.4[b]	17.4 ± 0.3[a]

[a] $P<0.01$, [b] $P<0.001$ vs. corresponding ICR mice.

[c] $P<0.05$ vs. corresponding sedentary control mice.

No significant stock X activity group interactions.

Table 3.2. Diaphyseal cortical bone parameters in ICR and CD1 sedentary controls and runners. Values are means ± SD.

Trait	ICR Sedentary	ICR Runner	CD1 Sedentary	CD1 Runner
Femur				
Ps.Ar	1.72 ± 0.13	1.82 ± 0.15^d	1.98 ± 0.22^c	1.94 ± 0.22
Ec.Ar	0.90 ± 0.10	0.91 ± 0.10	1.02 ± 0.16^b	1.03 ± 0.17^b
Ct.Ar[**]	0.82 ± 0.08	0.91 ± 0.08^f	0.96 ± 0.12^c	0.91 ± 0.10
Ct.Th[**]	0.203 ± 0.019	0.223 ± 0.015^f	0.225 ± 0.026^b	0.210 ± 0.023^a
I_{max}[*]	0.210 ± 0.036	0.246 ± 0.043^e	0.276 ± 0.060^c	0.260 ± 0.060
I_{min}[*]	0.125 ± 0.020	0.146 ± 0.024^e	0.176 ± 0.038^c	0.162 ± 0.034
J[*]	0.335 ± 0.054	0.391 ± 0.065^e	0.452 ± 0.096^c	0.422 ± 0.091
TMD	971 ± 14	977 ± 16	970 ± 23	968 ± 21
Po	5.9 ± 1.2	5.9 ± 1.2	5.7 ± 0.9	5.9 ± 0.8
Tibia				
Ps.Ar	0.84 ± 0.08	0.92 ± 0.08^e	1.00 ± 0.09^c	1.02 ± 0.07^c
Ec.Ar	0.26 ± 0.04	0.28 ± 0.04	0.36 ± 0.06^c	0.36 ± 0.05^c
Ct.Ar	0.58 ± 0.06	0.64 ± 0.05^e	0.64 ± 0.05^b	0.66 ± 0.04
Ct.Th	0.208 ± 0.012	0.215 ± 0.007^d	0.206 ± 0.010	0.211 ± 0.006^d
I_{max}	0.060 ± 0.013	0.073 ± 0.012^e	0.084 ± 0.013^c	0.089 ± 0.013^c
I_{min}	0.043 ± 0.009	0.052 ± 0.009^e	0.058 ± 0.012^c	0.061 ± 0.007^b
J	0.103 ± 0.021	0.124 ± 0.020^e	0.141 ± 0.024^c	0.150 ± 0.019^c
TMD	993 ± 23	997 ± 18	983 ± 23	987 ± 14
Po	6.5 ± 1.5	6.1 ± 0.9	6.2 ± 0.9	5.6 ± 1.1

[a] $P<0.05$, [b] $P<0.01$, [c] $P<0.001$ vs. corresponding ICR mice.

[d] $P<0.05$, [e] $P<0.01$, [f] $P<0.001$ vs. corresponding sedentary control mice.

[*] $P<0.05$, [**] $P<0.001$ stock X activity group interaction.

Ps.Ar = periosteal area (mm^2); Ec.Ar = endocortical area (mm^2); Ct.Ar = cortical area (mm^2); Ct.Th = cortical thickness (mm); I_{max} = maximal second moments of area (mm^4); I_{min} = minimal second moments of area (mm^4); J = polar moment of area (mm^4); TMD = tissue mineral density (mg HA/cm^3); Po = intracortical porosity (%).

Table 3.3. Mechanically relevant diaphyseal cortical bone structural parameters in ICR and CD1 sedentary controls and runners, standardized for body size. Values are means ± SD.

Trait	ICR Sedentary	ICR Runner	CD1 Sedentary	CD1 Runner
Femur				
Ct.Ar[**]	31.3 ± 2.1	34.4 ± 2.7[f]	35.4 ± 4.4[c]	33.9 ± 4.0
I_{max}[*]	0.535 ± 0.074	0.614 ± 0.089[e]	0.652 ± 0.129[b]	0.630 ± 0.135
I_{min}[*]	0.320 ± 0.041	0.364 ± 0.050[e]	0.416 ± 0.083[c]	0.391 ± 0.074
J[*]	0.855 ± 0.107	0.977 ± 0.131[e]	1.069 ± 0.204[c]	1.021 ± 0.202
Tibia				
Ct.Ar	22.1 ± 2.2	24.2 ± 1.9[e]	23.6 ± 1.8[a]	24.8 ± 1.5[d]
I_{max}	0.137 ± 0.026	0.160 ± 0.026[e]	0.175 ± 0.024[c]	0.192 ± 0.023[c,d]
I_{min}	0.097 ± 0.018	0.114 ± 0.018[e]	0.122 ± 0.024[c]	0.131 ± 0.013[b]
J	0.233 ± 0.042	0.274 ± 0.042[e]	0.297 ± 0.045[c]	0.322 ± 0.034[c]

[a] $P<0.05$, [b] $P<0.01$, [c] $P<0.001$ vs. corresponding ICR mice.

[d] $P<0.05$, [e] $P<0.01$ [f] $P<0.001$ vs. corresponding sedentary control mice.

[*] $P<0.05$, [**] $P<0.01$ stock X activity group interaction.

Ct.Ar = cortical area; I_{max} = maximal second moments of area; I_{min} = minimal second moments of area; J = polar moment of area. Cortical area is size-standardized by body mass • 100; moments of area are size-standardized by the product of body mass and bone length • 1000.

Table 3.4. Metaphyseal trabecular bone structural parameters in ICR and CD1 sedentary controls and runners. Values are means ± SD.

Trait	ICR Sedentary	ICR Runner	CD1 Sedentary	CD1 Runner
Femur				
BV/TV	15.1 ± 5.7	18.7 ± 5.2^d	13.1 ± 4.9	12.9 ± 4.1^c
Tb.N	5.5 ± 1.1	6.2 ± 0.9^d	4.6 ± 0.9^b	4.5 ± 0.9^c
Tb.Th*	45.2 ± 5.1	48.2 ± 6.1	47.4 ± 4.5	45.8 ± 3.8
Tb.Sp	195 ± 38	172 ± 27^d	237 ± 46^b	242 ± 51^c
Tibia				
BV/TV	12.6 ± 6.4	15.9 ± 5.9	12.7 ± 4.8	13.0 ± 4.0
Tb.N	5.5 ± 1.2	5.9 ± 1.1	4.8 ± 0.8	4.9 ± 0.8^b
Tb.Th	40.5 ± 5.6	44.2 ± 4.8^d	45.7 ± 4.7^b	45.5 ± 3.5
Tb.Sp	198 ± 40	184 ± 32	224 ± 33^a	222 ± 36^b

[a] P<0.05, [b] P<0.01, [c] P<0.001 vs. corresponding ICR mice.

[d] P<0.05 vs. corresponding sedentary control mice.

[*] P<0.05 stock X activity group interaction.

BV/TV = bone volume fraction (%); Tb.N = trabecular number (1/mm); Tb.Th = trabecular thickness (μm); Tb.Sp = trabecular separation (μm).

Table 3.5. Diaphyseal cortical bone mechanical parameters in ICR and CD1 sedentary controls and runners. Values are means ± SD.

Trait	ICR Sedentary	ICR Runner	CD1 Sedentary	CD1 Runner
Femur				
F_u^{**}	14.5 ± 2.4	16.7 ± 2.4[e]	20.3 ± 3.8[c]	18.1 ± 3.0[d]
F_y^{**}	10.1 ± 1.5	11.4 ± 1.9[d]	14.6 ± 3.2[c]	13.2 ± 2.5[a]
S^*	65.0 ± 15.0	75.3 ± 14.2[d]	83.5 ± 18.2[b]	78.1 ± 16.1
σ_u	113 ± 11	116 ± 10	123 ± 26	115 ± 16
σ_y	79.1 ± 9.4	79.4 ± 12.9	88.9 ± 21.1	84.0 ± 16.6
E	2192 ± 505	2191 ± 332	2062 ± 651	2068 ± 529
Tibia				
F_u	15.6 ± 2.7	17.5 ± 2.4[d]	17.3 ± 2.6[a]	17.2 ± 2.2
F_y	12.8 ± 2.2	13.5 ± 1.7	14.4 ± 2.2[a]	14.2 ± 1.5
S	79.0 ± 13.1	90.1 ± 9.3[e]	88.3 ± 15.0[a]	92.5 ± 13.7
σ_u	225 ± 19	227 ± 22	205 ± 32[a]	192 ± 24[c]
σ_y	185 ± 22	177 ± 26	171 ± 29	159 ± 18[a]
E	6119 ± 1042	6235 ± 1024	5309 ± 1168[a]	5310 ± 898[b]

[a] P<0.05, [b] P<0.01, [c] P<0.001 vs. corresponding ICR mice.

[d] P<0.05, [e] P<0.01 vs. corresponding sedentary control mice.

[*] P<0.05, [**] P<0.01 stock X activity group interaction.

F_u = ultimate force (N); F_y = yield force (N); S = stiffness (N/mm); σ_u = ultimate stress (MPa); σ_y = yield stress (MPa); E = Young's modulus (MPa).

Table 3.6. R^2 values from linear regressions of bone parameters versus average daily ambulatory counts in the ICR and CD1 sedentary controls. Signs of regression slopes are in parentheses.

Trait	ICR Femur	CD1 Femur	ICR Tibia	CD1 Tibia
Length	0.057 (-)	0.010 (+)	0.060 (-)	0.038 (+)
Ps.Ar	0.002 (-)	0.004 (+)	0.015 (-)	0.001 (-)
Ec.Ar	0.009 (+)	<0.001 (+)	0.002 (-)	0.029 (-)
Ct.Ar	0.034 (-)	0.010 (+)	0.017 (-)	0.017 (+)
Ct.Th	0.042 (-)	0.006 (+)	0.009 (-)	0.056 (+)
I_{max}	0.007 (-)	<0.001 (+)	0.037 (-)	0.002 (-)
I_{min}	0.037 (-)	0.018 (+)	0.008 (-)	0.001 (+)
J	0.016 (-)	0.004 (+)	0.024 (-)	<0.001 (-)
TMD	<0.001 (+)	0.045 (-)	<0.001 (+)	0.031 (+)
Po	0.004 (+)	0.024 (+)	0.002 (+)	0.012 (+)
Ct.Ar[†]	< 0.001 (-)	0.008 (+)	0.003 (-)	0.009 (+)
I_{max}[†]	< 0.001 (+)	< 0.001 (+)	0.017 (-)	0.011 (-)
I_{min}[†]	0.010 (-)	0.018 (+)	< 0.001 (-)	< 0.001 (-)
J[†]	< 0.001 (-)	0.003 (+)	0.007 (-)	0.004 (-)
BV/TV	0.029 (-)	0.085 (+)	0.018 (-)	0.073 (+)
Tb.N	0.044 (-)	0.086 (+)	0.013 (-)	0.021 (+)
Tb.Th	0.033 (-)	0.188 (+)	0.009 (-)	0.162 (+)
Tb.Sp	0.026 (+)	0.143 (-)	0.010 (+)	0.034 (-)
F_u	0.002 (-)	0.046 (-)	0.002 (-)	0.076 (+)
F_y	0.005 (-)	0.025 (-)	<0.001 (-)	<0.001 (+)
S	<0.001 (-)	<0.001 (+)	0.029 (-)	0.080 (-)
σ_u	0.055 (-)	0.124 (-)	0.157 (+)	0.120 (+)
σ_y	0.057 (-)	0.077 (-)	0.105 (+)	0.014 (+)
E	0.012 (-)	0.012 (-)	0.011 (-)	0.044 (-)

All relationships between bone parameters and average daily ambulatory counts were non-significant.

Ps.Ar = periosteal area; Ec.Ar = endocortical area; Ct.Ar = cortical area; Ct.Th = cortical thickness; I_{max} = maximal second moments of area; I_{min} = minimal second moments of area; J = polar moment of area; BV/TV = bone volume fraction; Tb.N = trabecular number; Tb.Th = trabecular thickness; Tb.Sp = trabecular separation; F_u = ultimate force; F_y = yield force; S = stiffness; σ_u = ultimate stress; σ_y = yield stress; E = Young's modulus.

[†] = body size-standardized. Cortical area is size-standardized by body mass • 100; moments of area are size-standardized by the product of body mass and bone length • 1000.

Table 3.7. Body mass, speed, and hind limb peak vertical ground reaction force data from ICR and CD1 mice employed in force plate analyses (6 mice/stock; n=47 and 49 steps total for ICR and CD1 mice, respectively). Values are means ± SD.

	ICR	CD1
Body mass (g)	24.9 ± 1.0	23.7 ± 1.0[a]
Speed (cm/sec)	46.8 ± 12.3	41.9 ± 13.4
Peak vertical force (N)	0.145 ± 0.026	0.142 ± 0.025
Peak vertical force (% body mass)	59.5 ± 11.1	61.1 ± 11.2

[a] $P<0.001$ vs. ICR mice. All other stock differences were non-significant.

Figure 3.1
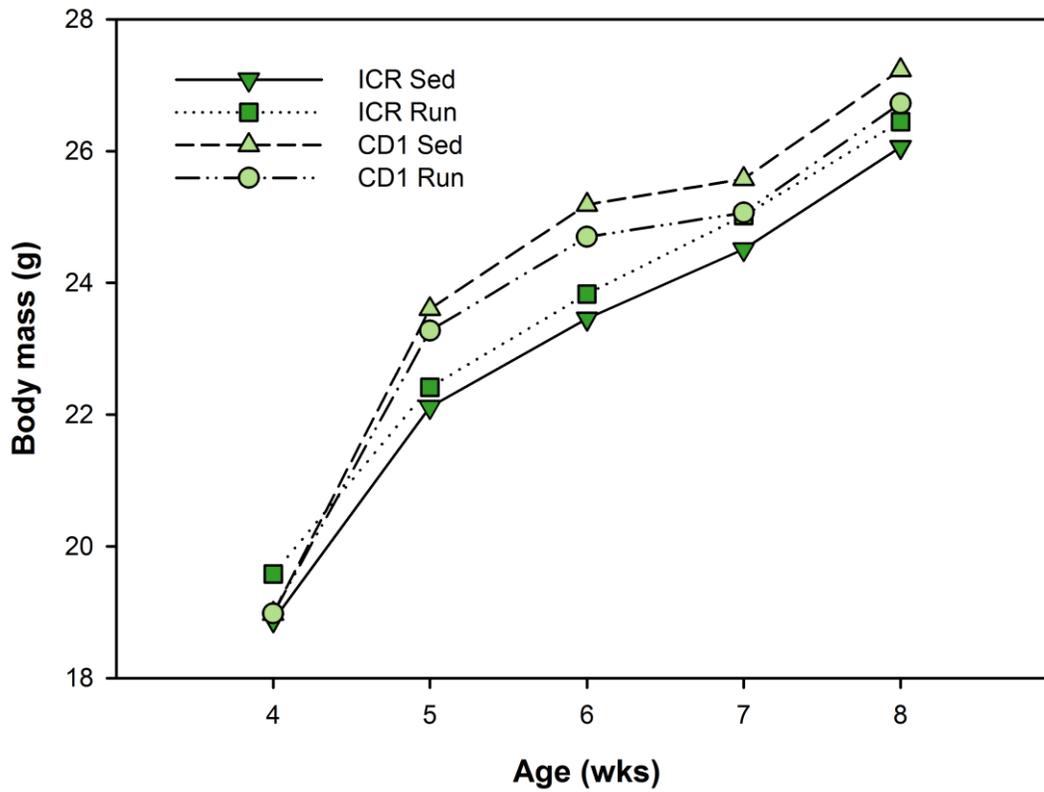
Figure 3.1. Change in body mass over the 4-wk experimental period. At no point were body mass differences between sedentary controls (Sed) and runners (Run) statistically significant in either the ICR or CD1 stock. From 5 weeks of age until the end of the experiment, CD1 sedentary controls were significantly ($P<0.05$) lighter than ICR controls. Body mass differences between ICR and CD1 runners were never significant, and there were no significant stock X activity group interactions.

Figure 3.2
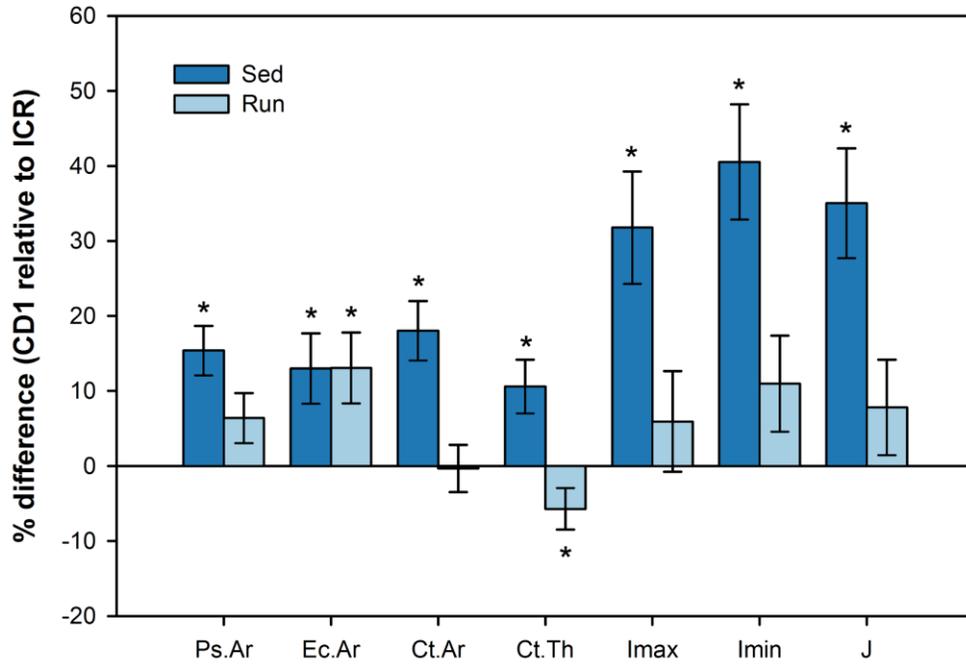
Femur diaphyseal structure
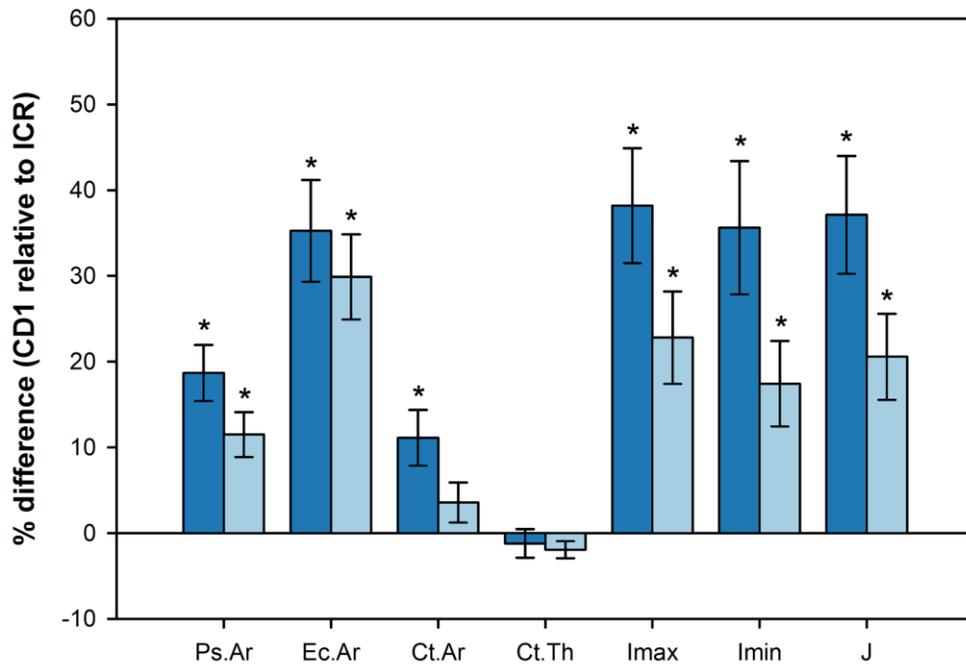
Tibia diaphyseal structure

Figure 3.2. Relative difference in diaphyseal cortical bone structural parameters between ICR and CD1 sedentary controls (Sed) and runners (Run). Bars equal the percent difference between the CD1 mean relative to the ICR mean. Whiskers equal the standard deviation of the sampling distribution of the relative difference. Asterisks indicate statistically significant (P<0.05) differences between stocks. Ps.Ar = periosteal area; Ec.Ar = endocortical area; Ct.Ar = cortical area; Ct.Th = cortical thickness; I_{max} = maximal second moments of area; I_{min} = minimal second moments of area; J = polar moment of area.

Figure 3.3
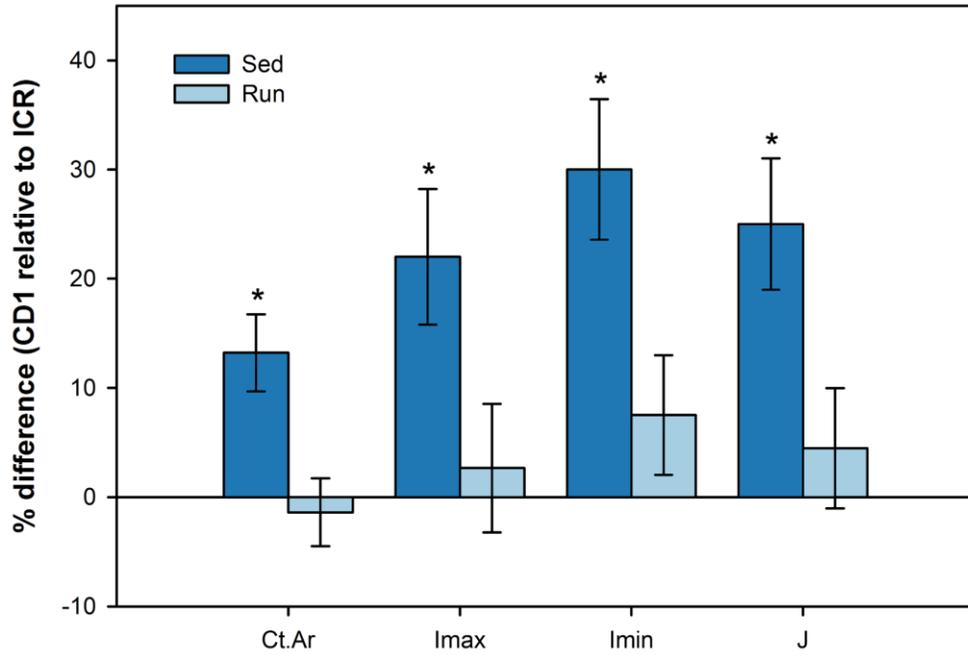
Size-standardized femur diaphyseal structure
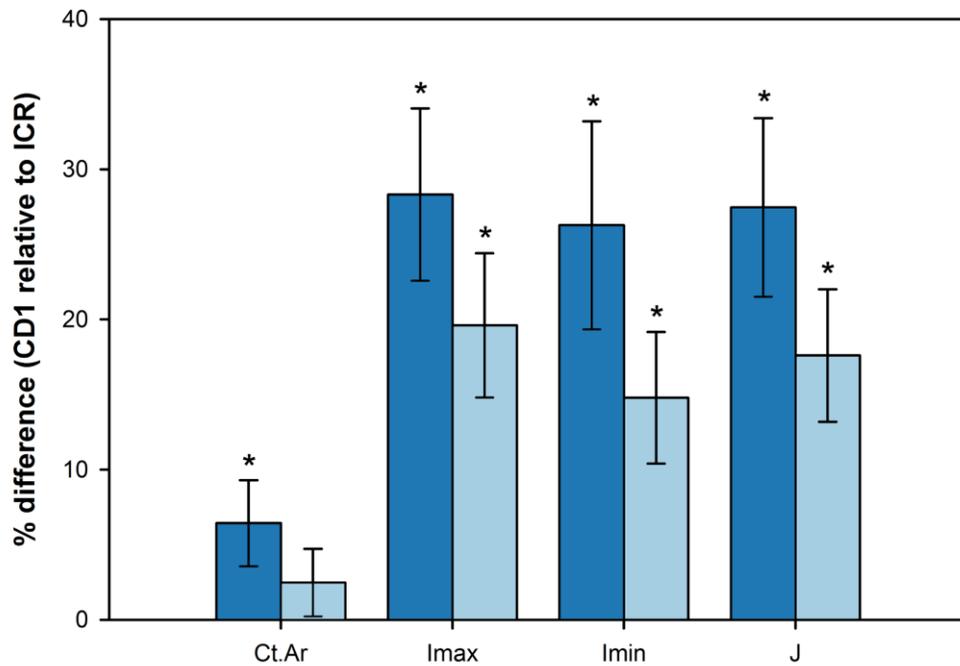
Size-standardized tibia diaphyseal structure

Figure 3.3. Relative difference in mechanically relevant diaphyseal cortical bone structural parameters between ICR and CD1 sedentary controls (Sed) and runners (Run), standardized for body size. Bars equal the percent difference between the CD1 mean relative to the ICR mean. Whiskers equal the standard deviation of the sampling distribution of the relative difference. Asterisks indicate statistically significant ($P<0.05$) differences between stocks. Ct.Ar = cortical area; I_{max} = maximal second moments of area; I_{min} = minimal second moments of area; J = polar moment of area.

Figure 3.4
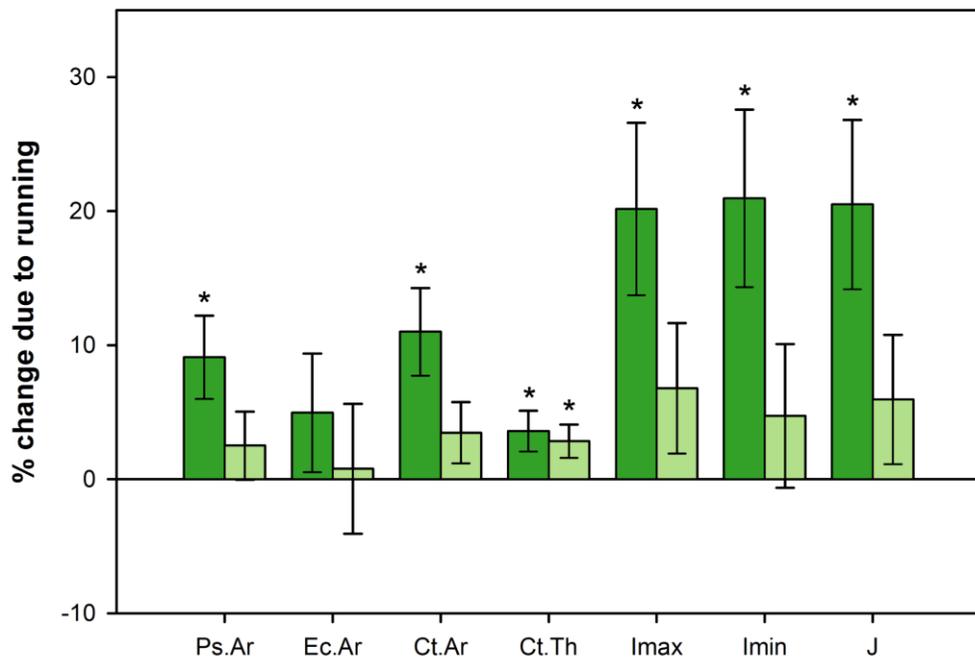
Figure 3.4. Relative difference in diaphyseal cortical bone structural parameters between sedentary controls and runners in the ICR and CD1 stocks. Bars equal the percent difference between the runner mean relative to the sedentary control mean. Whiskers equal the standard deviation of the sampling distribution of the relative difference. Asterisks indicate statistically significant (P<0.05) differences between activity groups. Ps.Ar = periosteal area; Ec.Ar = endocortical area; Ct.Ar = cortical area; Ct.Th = cortical thickness; I_{max} = maximal second moments of area; I_{min} = minimal second moments of area; J = polar moment of area.

Figure 3.5
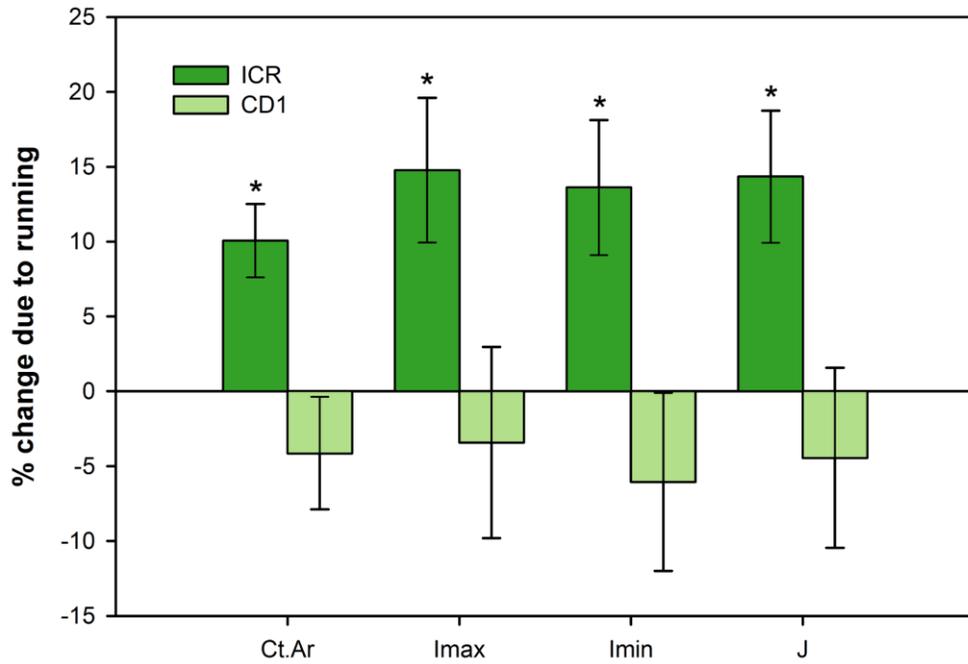
Size-standardized femur diaphyseal structure
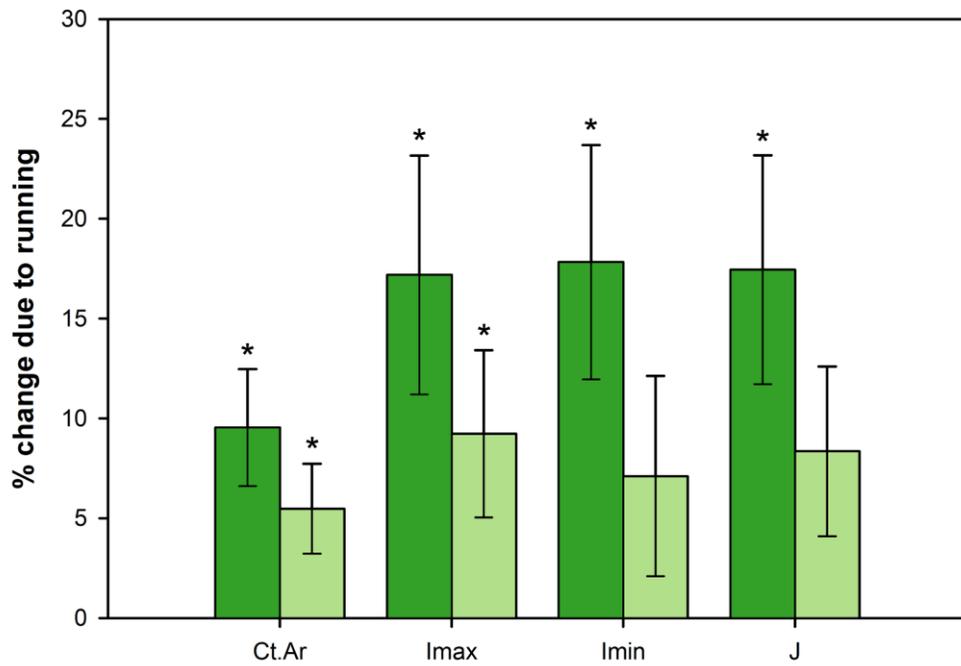
Size-standardized tibia diaphyseal structure

Figure 3.5. Relative difference in mechanically relevant diaphyseal cortical bone structural parameters between sedentary controls and runners in the ICR and CD1 stocks, standardized for body size. Bars equal the percent difference between the runner mean relative to the sedentary control mean. Whiskers equal the standard deviation of the sampling distribution of the relative difference. Asterisks indicate statistically significant (P<0.05) differences between activity groups. Ct.Ar = cortical area; I_{max} = maximal second moments of area; I_{min} = minimal second moments of area; J = polar moment of area.

Figure 3.6
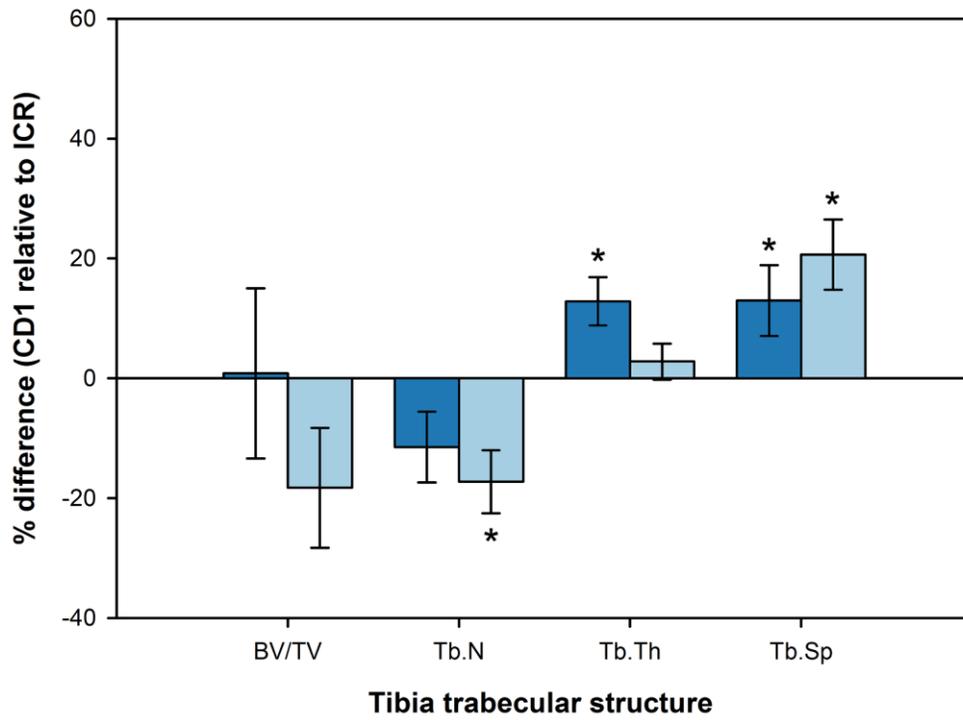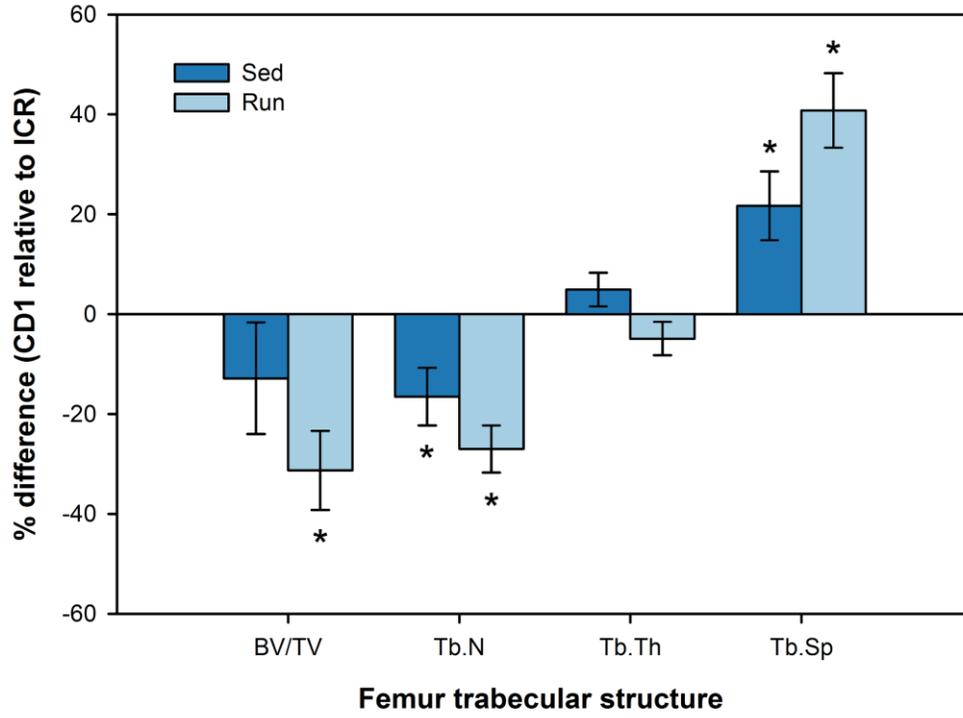
Figure 3.6. Relative difference in metaphyseal trabecular bone structural parameters between ICR and CD1 sedentary controls (Sed) and runners (Run). Bars equal the percent difference between the CD1 mean relative to the ICR mean. Whiskers equal the standard deviation of the sampling distribution of the relative difference. Asterisks indicate statistically significant (P<0.05) differences between stocks. BV/TV = bone volume fraction; Tb.N = trabecular number; Tb.Th = trabecular thickness; Tb.Sp = trabecular separation.

Figure 3.7
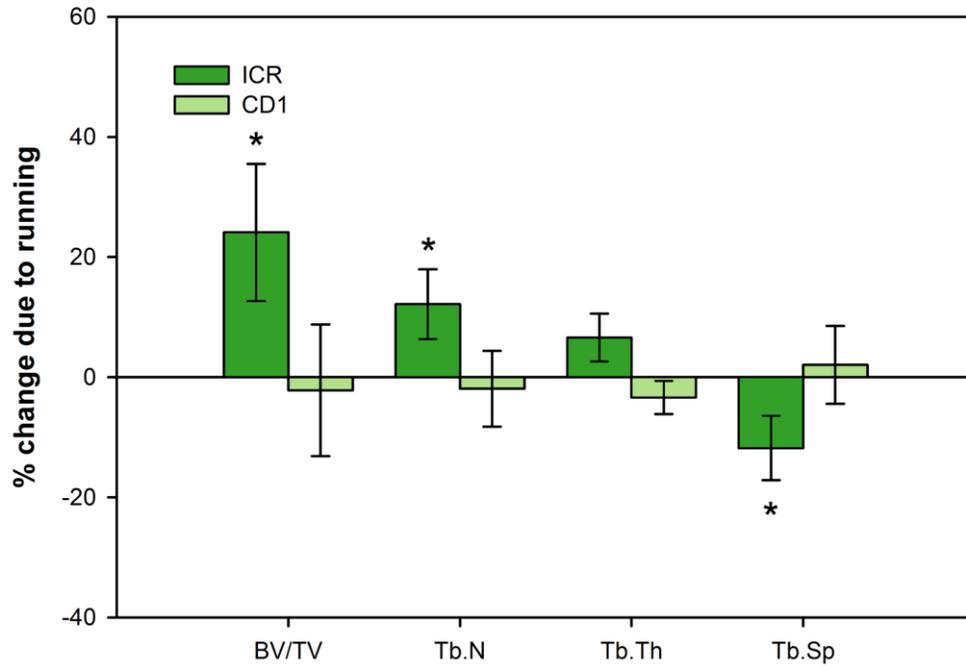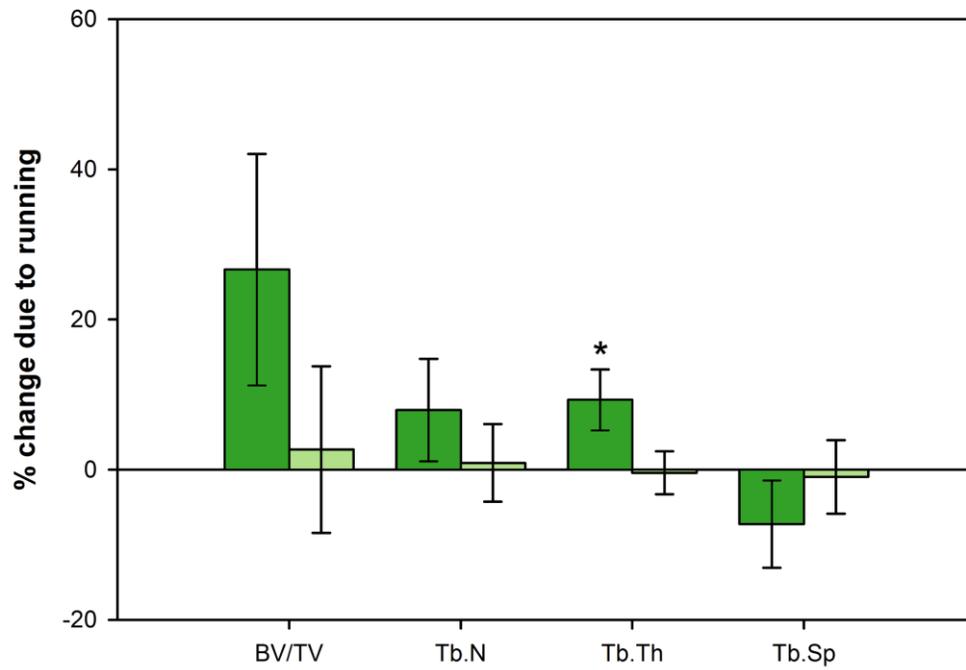
Figure 3.7. Relative difference in metaphyseal trabecular bone structural parameters between sedentary controls and runners in the ICR and CD1 stocks. Bars equal the percent difference between the runner mean relative to the sedentary control mean. Whiskers equal the standard deviation of the sampling distribution of the relative difference. Asterisks indicate statistically significant (P<0.05) differences between activity groups. BV/TV = bone volume fraction; Tb.N = trabecular number; Tb.Th = trabecular thickness; Tb.Sp = trabecular separation.

Figure 3.8
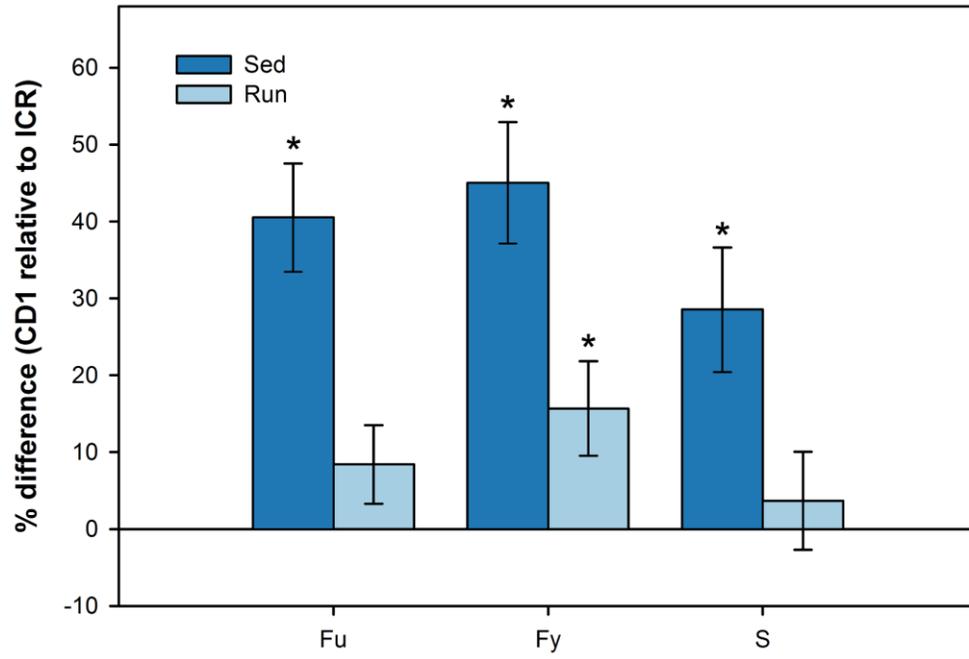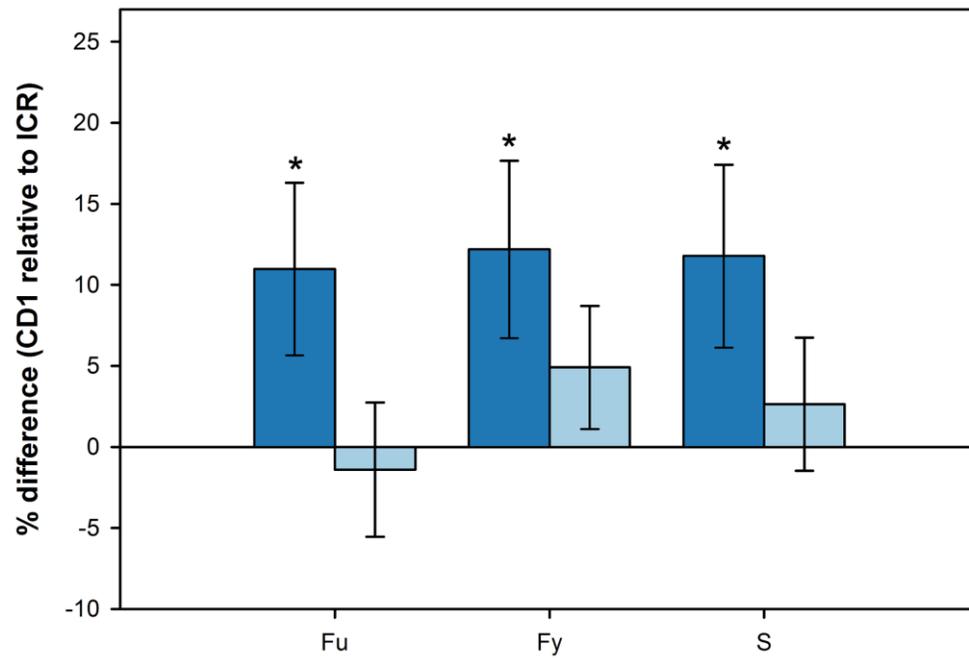
Figure 3.8. Relative difference in diaphyseal cortical bone mechanical parameters between ICR and CD1 sedentary controls (Sed) and runners (Run). Bars equal the percent difference between the CD1 mean relative to the ICR mean. Whiskers equal the standard deviation of the sampling distribution of the relative difference. Asterisks indicate statistically significant (P<0.05) differences between stocks. F_u = ultimate force; F_y = yield force; S = stiffness.

Figure 3.9
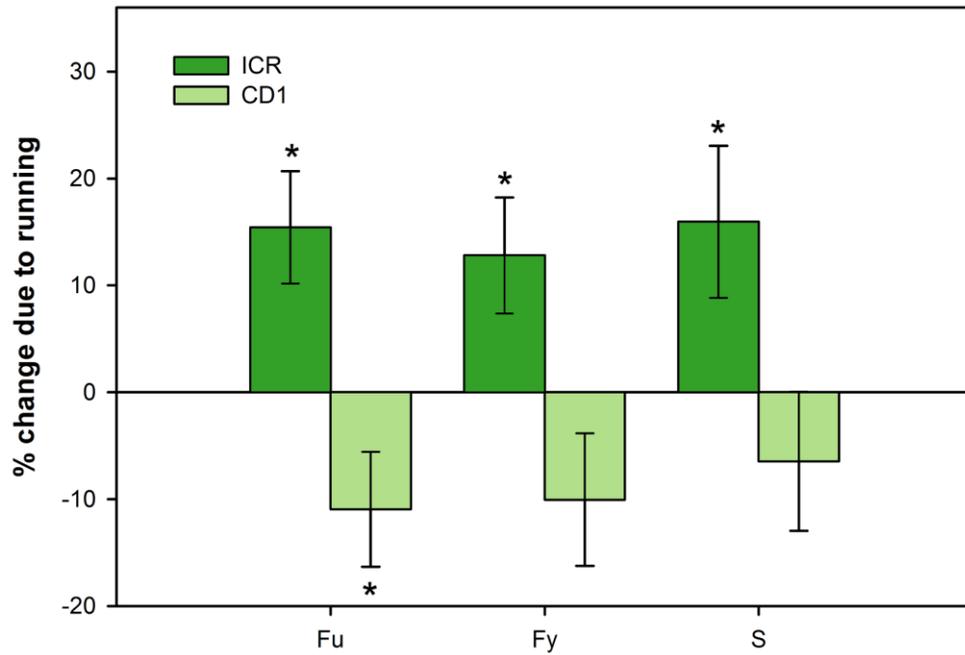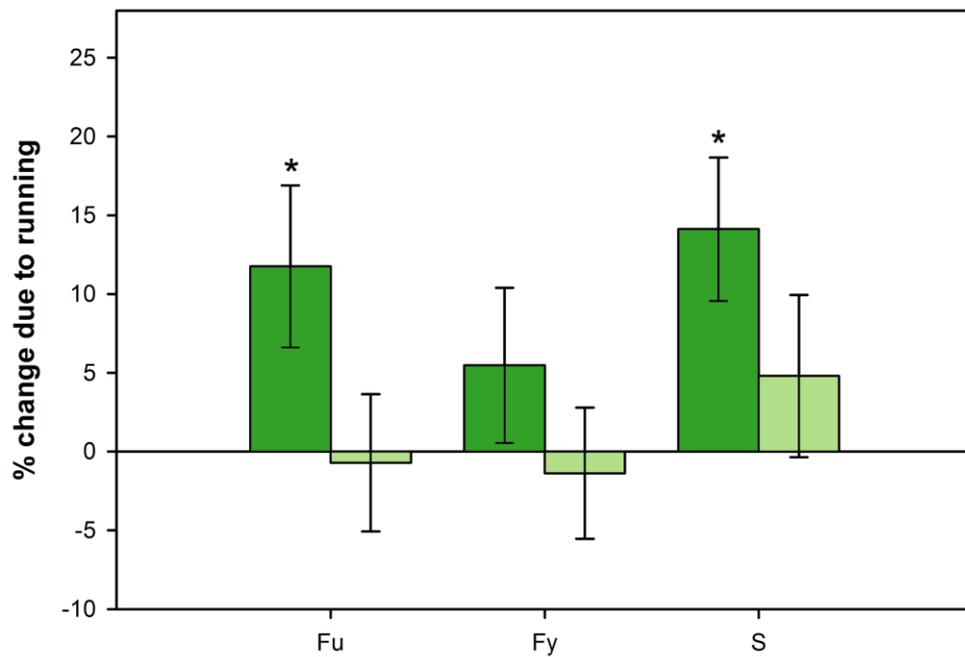
Figure 3.9. Relative difference in diaphyseal cortical bone mechanical parameters between sedentary controls and runners in the ICR and CD1 stocks. Bars equal the percent difference between the runner mean relative to the sedentary control mean. Whiskers equal the standard deviation of the sampling distribution of the relative difference. Asterisks indicate statistically significant (P<0.05) differences between activity groups. F_u = ultimate force; F_y = yield force; S = stiffness.

Figure 3.10
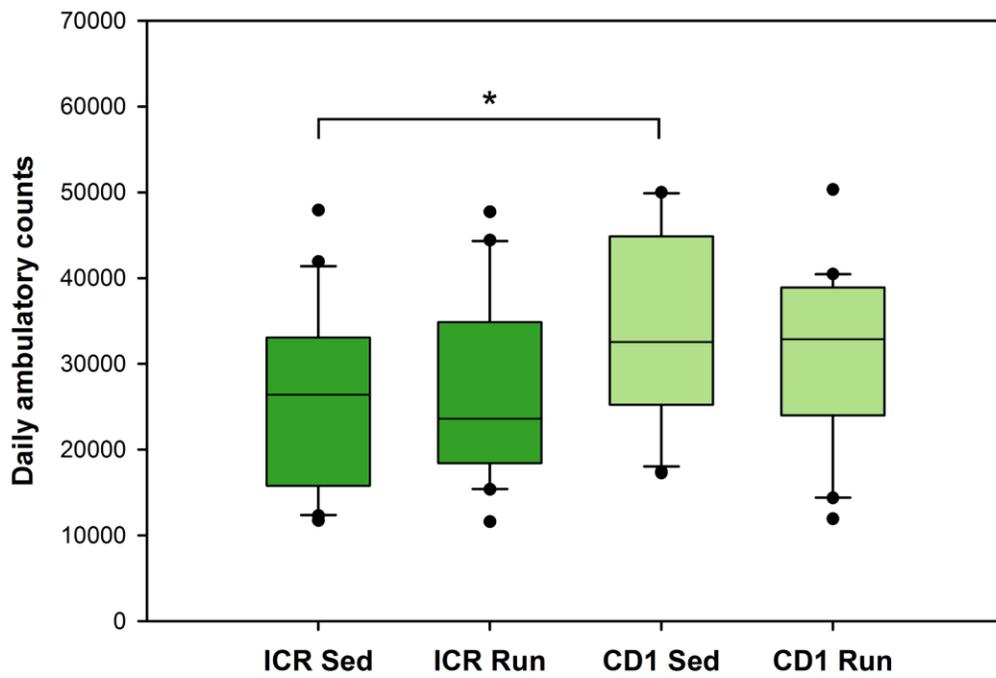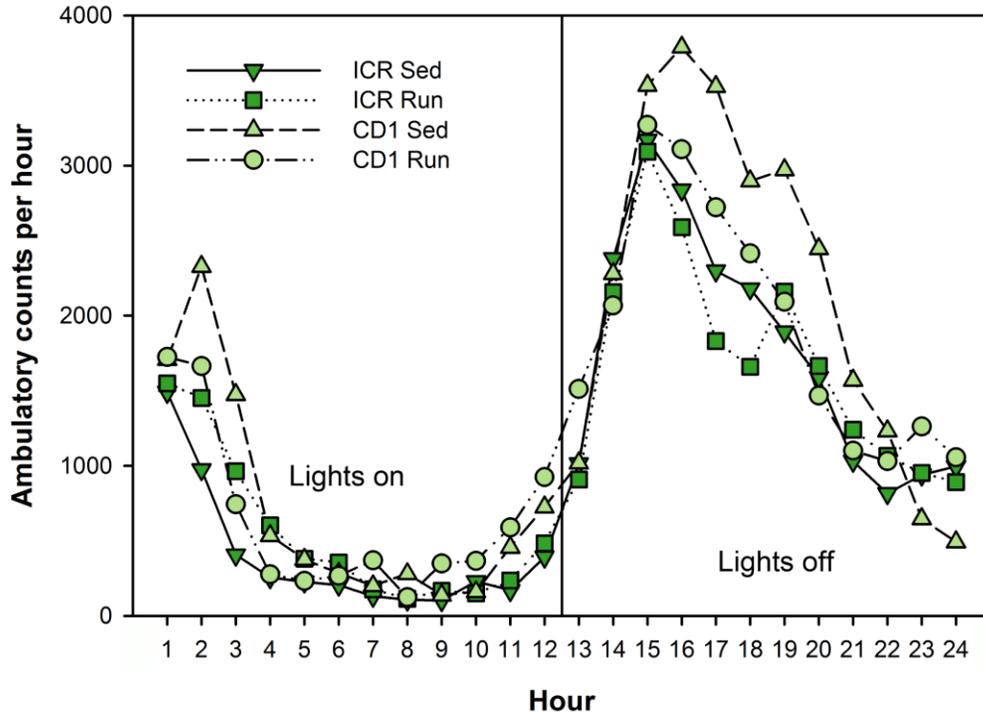
Figure 3.10. Home-cage activity levels in ICR and CD1 sedentary controls (Sed) and runners (Run). Top: Average hourly ambulatory counts throughout a 24-hr period. Bottom: Average total daily ambulatory counts. The asterisk indicates a statistically significant difference in home-cage activity levels between the ICR and CD1 sedentary controls (P=0.01). ICR and CD1 runners exhibited similar activity levels (P=0.25). In neither stock were differences in activity levels between sedentary controls and runners significant (ICR: P=0.76; CD1: P=0.23). The stock X activity group interaction for average daily ambulatory counts was also not significant (P=0.27).

Figure 3.11
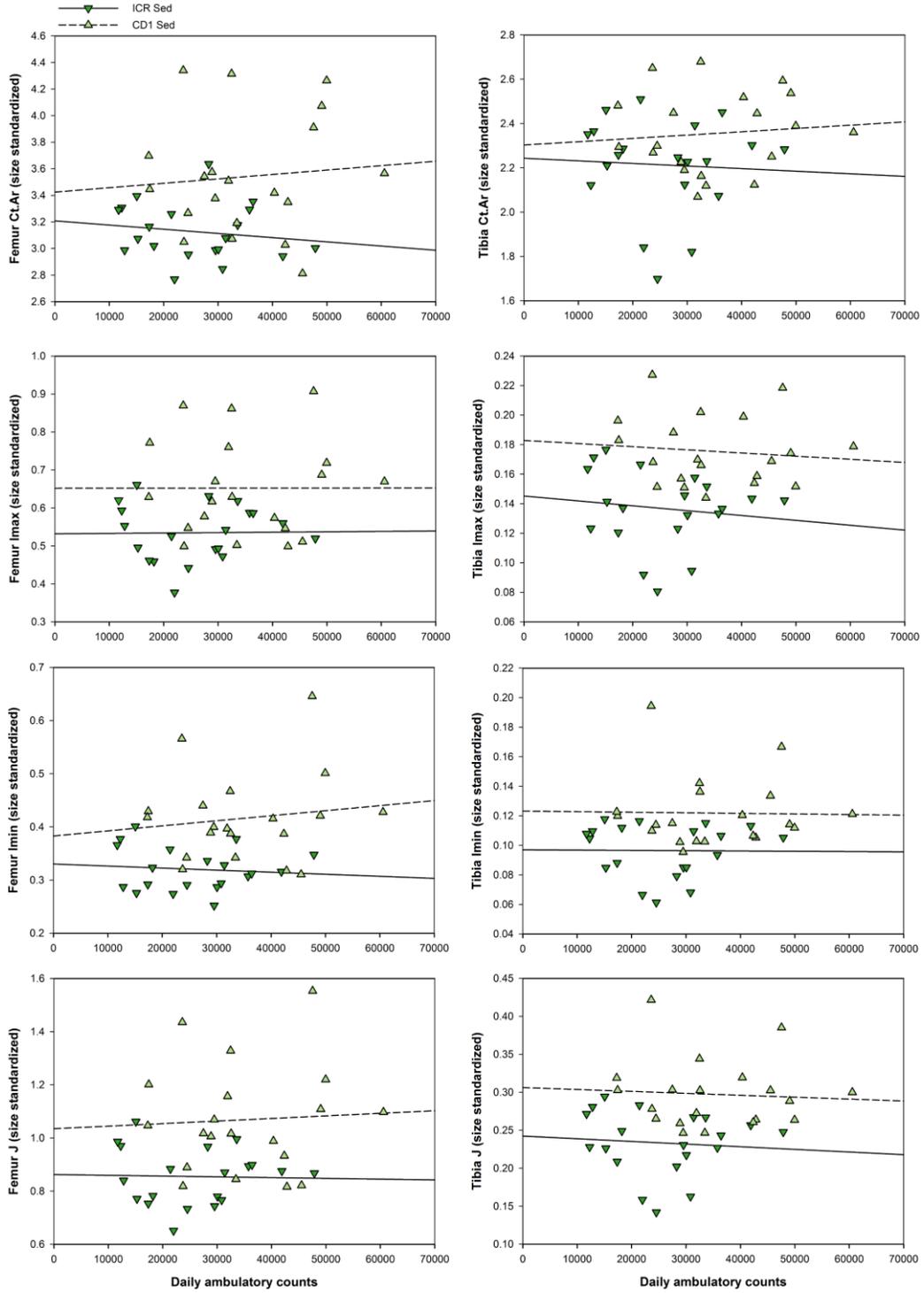
Figure 3.11. Size-standardized mechanically relevant diaphyseal cortical bone structural parameters in relation to average daily home-cage ambulatory counts in the ICR and CD1 sedentary controls (Sed). Lines are least-squares regressions. All relationships were non-significant. Ct.Ar = cortical area; I_{max} = maximal second moments of area; I_{min} = minimal second moments of area; J = polar moment of area. Cortical area is size-standardized by body mass • 100; moments of area are size-standardized by the product of body mass and bone length • 1000.

Figure 3.12
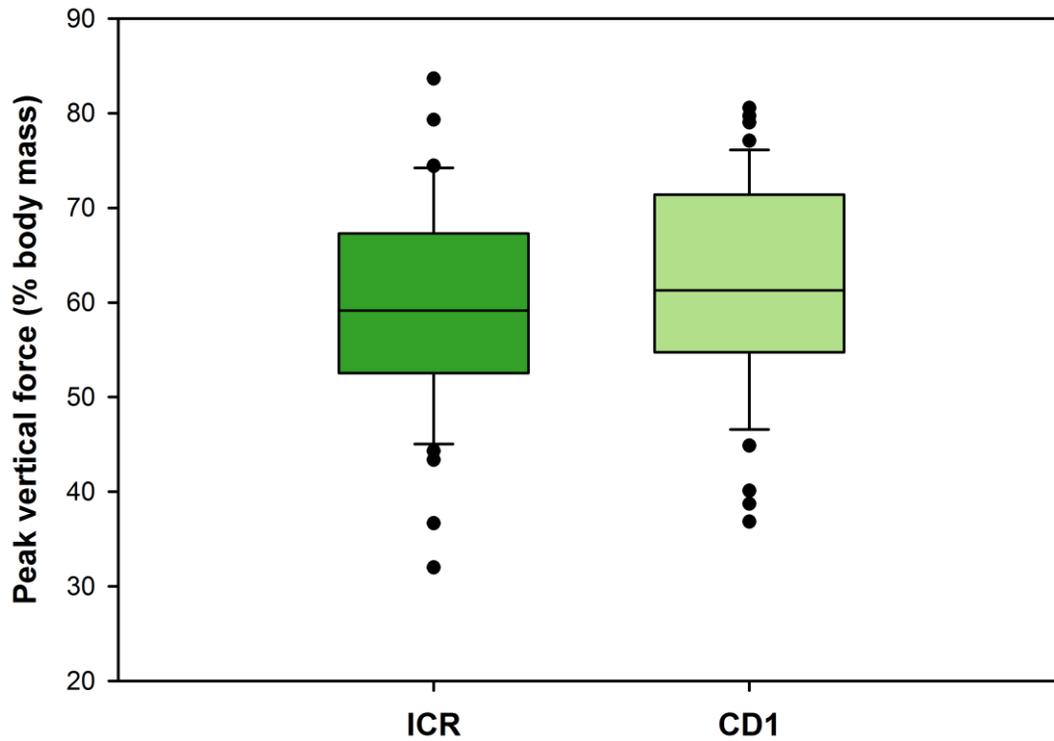
Figure 3.12. Box plots for hind limb peak vertical ground reaction forces (in units of body mass) sustained by quadrupedal locomotion in ICR and CD1 mice**.** The difference between stocks was not statistically significant (P=0.49).

Chapter 4

Functional Significance of Genetic Variation Underlying Limb Bone Diaphyseal Structure[**]

Natural selection favoring particular physical activity levels (or any other complex behavioral trait) would be expected to engender an evolutionary response involving multiple changes in anatomy and physiology, as well as the underlying genetic architecture (Garland and Kelly, 2006). Given the critical role of the skeleton in locomotion, alleles influencing bone structure would presumably be among those especially affected (Middleton et al., 2008b). This idea has not been lost on anthropologists (e.g., Trinkaus et al., 1994; Churchill, 1999; Daegling et al., 2013). For example, discussing the large diaphyseal dimensions characteristic of Pleistocene human limb bones, Churchill (1999:51-52) hypothesized that "heightened skeletal strength…may be expected to positively co-occur in populations with an evolutionary history of high activity." In this scenario, thick limb bone diaphyses among Pleistocene juveniles (e.g., Ruff et al., 1994; Trinkaus and Ruff, 1996; Kondo and Dodo, 2002; Trinkaus et al., 2002; Arsuaga et al., 2007) may be present even at ages prior to the onset of limb loading activities as an evolutionary response to selection acting on earlier members of a lineage for high levels of physical activity. This could also explain some of the variation in limb bone diaphyseal growth patterns documented among children from Holocene populations (e.g., Cowgill and Hager, 2007; Robbins, 2007; Cowgill, 2010). For functional morphologists studying skeletal remains, this would mean that limb bone diaphyseal structure may not necessarily reflect the activity levels of particular individuals, but may nevertheless convey an evolutionary signal providing information about the physical activity levels of their ancestral populations.

To examine the degree to which limb bone diaphyseal structure reflects the physical activity levels of members of a lineage, an experimental evolution approach was again adopted using mice from the selection experiment for high voluntary wheel-running behavior described in Chapter 2 (Swallow et al., 1998; Garland, 2003). As shown in that chapter and in several other

---

[**] This research was published in the *American Journal of Physical Anthropology* (Wallace et al., 2010).

studies of mice from the selection experiment (reviewed in Garland, 2003; Rhodes et al., 2005; Middleton et al., 2008b; Swallow et al., 2009; Garland et al., 2011b), the dramatic (~2.7-fold) increase in daily voluntary wheel running in selected High Runner (HR) mice relative to non-selected control (C) mice has been associated with several correlated responses to selection for high wheel running, including enhancement of limb bone diaphyseal dimensions (at least in HR mice not harboring the mini-muscle allele), suggesting an evolutionary relationship between high levels of physical activity and limb bone morphology (Kelly et al., 2006; Middleton et al., 2010; Chapter 2). Importantly, when the activity levels of HR and C mice are limited by denying them wheel access, HR mice continue to have enhanced limb bone diaphyseal structure. However, as noted previously, selection has also resulted in increased home-cage activity levels in HR mice (Malisch et al., 2008, 2009), thus introducing the possibility that variation detected in limb bone structure between HR and C mice is due to differences in physical activity levels rather than allelic differences shaped by selection that directly influence bone development. To determine if selective breeding for high levels of physical activity alters diaphyseal structure independent of mechanical signals, this study tests for differences in the femoral diaphyseal structure of 1-week-old animals. Differences in diaphyseal structure at 1 week can be assumed to primarily reflect the evolutionary effects of past selection rather than direct mechanical stimuli, given that the onset of locomotion in mice is shortly after day 7 (Williams and Scott, 1954). Following Churchill (1999), it was hypothesized that if genetically determined diaphyseal structure reflects the activity patterns of members of a lineage, then HR mice will have enhanced diaphyseal structure at 1 week compared to non-selected C mice.

Materials and Methods

Study animals

Animals used in this analysis were from a single selected HR line (laboratory designation line 8) and a single non-selected control line (laboratory designation line 2) from generation 45 of selection. At 1 week postnatal, a single male and female from each of 23 families were weighed, euthanized via decapitation, and frozen. The bones of 3 individuals were excluded from the study due to damage sustained during organ extraction. At a later date, carcasses were

defrosted and right and left femora were extracted and preserved in 70% EtOH. Body and triceps surae muscle mass data for these individuals were reported previously (Middleton et al., 2008b). No significant differences in body mass (females: P=0.13; males: P=0.35; Figure 4.1) or triceps surae mass (females: P=0.17; males: P=0.59) or triceps surae mass relative to body mass (females: P=0.81; males: P=0.98) were found between the HR and C mice at 1 week of age.

Microcomputed tomography

Femoral diaphyses were scanned in 70% EtOH at an isometric voxel size of 8 μm (70 kVp, 114 μA, 300-ms integration time) with a μCT 40 scanner (Scanco Medical AG, Brüttisellen, Switzerland). Structural parameters were quantified in a 0.64-mm-long volume of interest (VOI) that was defined at midspan between the growth plates (Figure 4.2). Raw gray scale images (Figure 4.3a, d) were filtered with a constrained 3D Gaussian filter to reduce noise (support=1, sigma=0.1) and segmented with a global threshold of 21% of maximum possible gray scale value (Figure 4.3b, e). This threshold was determined with the help of density histograms, and visual comparison indicated that the 21% value rendered good concordance between the raw and thresholded images. The cortical mask of the diaphyseal VOI was defined with dilation and subsequent erosion operations, filling in holes and connecting fragments to produce continuous periosteal and endocortical contours. The cortical mask edges were checked by overlay on the raw images (Figure 4.3c, f).

Bone properties were computed using a script routine written by Svetlana Lublinsky (Ben-Gurion University of the Negev) in the internal imaging code supplied by the scanner manufacturer and defined according to Bouxsein et al. (2010). Parameters measured included cortical area (Ct.Ar; mm^2), periosteal and endocortical areas (Ps.Ar, Ec.Ar; mm^2), maximal and minimal second moments of area (I_{max}, I_{min}; mm^4), polar moment of area (J; mm^4), tissue mineral density (TMD; mg HA/cm^3), and intracortical porosity (Po; %). Tissue mineral density was quantified using calibration hydroxyapatite phantoms (Scanco Medical AG) for the conversion of linear attenuation of a given voxel to mg HA/cm^3. Area moments and Ct.Ar were quantified excluding all porosities. As noted in Chapter 2, in standard beam analysis, these parameters approximate diaphyseal strength if the material strength of the bone tissue is held constant: Ct.Ar approximates a cross section's internal resistance to axial loads, I_{max} and I_{min} describe resistance

to bending around principal axes, and J describes average bending rigidity and resistance to torsion (Ruff et al., 1993). However, 1-week-old mouse diaphyses consist largely of bone fragments that are irregularly connected via narrow struts (Figure 4.3), violating one of the assumptions of the beam model (at least for bending and torsion) that stress under loading will be distributed linearly across sections (Hibbeler, 1997). Therefore, in this case, area moments should not be interpreted as indicators of strength, but as geometric parameters delineating bone shape (i.e., 'apparent traits'). Visual inspection of the cross sections indicated that the distribution of the intracortical pores was similar in HR and C bones (Figure 4.3). A previous study on ontogenetic series of inbred mouse strains also suggests that the distribution of porosities in developing mouse bones is similar in animals with different genetic backgrounds (Price et al., 2005). Diaphyseal parameters of right and left femora were averaged for each individual to minimize measurement error.

Statistical analyses

Statistical analyses were carried out using SPSS (version 11; Armonk, NY). Males and females were analyzed separately. Descriptive statistics for all parameters were calculated, and data were then converted to natural logarithms for subsequent analyses. While data were distributed approximately normally in both raw and ln space (insignificant Kolmogorov-Smirnoff Z values), logging them slightly improved r^2 values and linearity in regressions (Durbin-Watson statistics closer to 2). Pearson correlations were calculated to test for associations between body mass and bone properties. Areas and area moments were all found to be significantly correlated with body mass; however, TMD and Po were not. For areas and area moments, regression slopes were compared to confirm that associations between body mass and structural parameters were similar between the HR and C groups. All slope differences were found to be non-significant. One-way ANCOVAs were then used to test for differences in areas and area moments between the groups, with body mass as a covariate. For TMD and Po, single classification ANOVAs were used to test for differences between groups. The Levene test statistic was calculated for each sample to determine if the assumption of homogeneous variance was violated. In one case (Ec.Ar; males), the result of this test was significant and additional

96

rank transformation of the data was necessary. Statistical significance was assessed using a 95% criterion (P<0.05), and tests were two-tailed.

Results

Descriptive statistics for body mass and femoral diaphyseal parameters, separated by sex and selection history, are presented in Table 4.1. Body mass-adjusted diaphyseal dimensions were significantly different between selected HR and non-selected C animals (Table 4.2; Figure 4.4). Among both females and males, HR mice had larger mass-adjusted area moments compared to C mice, although the differences were generally greater in females. On average, selected females had 28% greater maximal second moments of area (P<0.001), 37% greater minimal second moments of area (P<0.0001), and 32% greater polar moments of area (P<0.0001). Selected males had 21% greater maximal second moments of area (P<0.01), 22% greater minimal second moments of area (P<0.01), and 21% greater polar moments of area (P<0.01). Compared to controls, HR animals also had larger cortical areas (20% difference in female mass-adjusted means, and 8% difference in male mass-adjusted means); however, the difference was statistically significant only for females (P<0.001; males: P=0.10). Selected and non-selected animals had similar relative endocortical areas (females: P=0.29; males: P=0.10), but selected mice had significantly larger mass-adjusted periosteal areas (females: 13% difference, P<0.001; males: 12% difference, P<0.01). Therefore, differences in cortical area were evidently driven primarily by relatively greater periosteal expansion in the diaphyses of selected animals. Figure 4.5 graphically depicts data for tissue mineral density and intracortical porosity. No significant differences were found in either tissue mineral density (females: P=0.32; males: P=0.37) or porosity (females: P=0.26; males: P=0.25).

Discussion

This study explored the degree to which limb bone diaphyseal structure reflects the historical physical activity levels of members of a lineage (population) using 1-week-old mice selectively bred for high levels of voluntary wheel running. The goal was to determine whether the femora of mice with an 'evolutionary history' of high locomotor activity (i.e., the High

97

Runner or HR mice) were structurally distinct from non-selected control (C) mice prior to the onset of locomotion. As hypothesized, at 1 week postnatal, HR animals had larger body mass-adjusted diaphyseal dimensions, suggesting that selection for high levels of physical activity has led to a concomitant evolutionary enhancement of limb bone diaphyseal structure. Interestingly, it was found that differences between HR and C animals are more pronounced in females than in males, and adult females also run more than males (Garland, 2003). Given that tissue mineral density and intracortical porosity did not significantly differ between HR and C mice, bone tissue strength was presumably similar across the groups. However, for reasons discussed above (see Materials and Methods), it is unclear whether differences in diaphyseal dimensions translate to differences in strength. This would need to be determined by whole-bone mechanical testing. In any case, the results of this study suggest that an evolutionary signal conditioned by ancestral physical activity levels may be discerned in limb bone diaphyses.

An evolutionary signal in limb bone diaphyses is presumably most evident during perinatal development (or at the age selection has been acting if the genes act in an age-specific fashion), and becomes obscured to some degree throughout ontogeny as bones are affected by environmental factors including functional loading. Furthermore, the degree to which adult diaphyseal morphology conveys an evolutionary signal may vary between individuals depending on their initial (baseline) diaphyseal structure and strength (Chapter 3). One might predict that if a genome contains information that 'instructs' cells to produce a larger and stronger diaphysis, then that bone may sustain greater loading without triggering an osteogenic response. This scenario is ostensibly consistent with the results presented in Chapter 3, where CD1 sedentary mice displayed enhanced femoral and tibial diaphyseal structure and strength relative to ICR sedentary mice, and treadmill exercise led to greater improvements in skeletal morphology and strength in ICR mice than CD1 mice (see also Leppänen et al., 2008). Alternatively, it could be argued that adult diaphyseal structure might always primarily reflect the effects of individual physical activity rather than ancestral behavior (genetic background) if bone quantity is regulated by stress control acting in a feedback loop (Ruff et al., 2006). According to this view, individuals born with large diaphyses would need to be highly active throughout life to maintain their elevated diaphyseal structure; otherwise, they would be 'genetically overbuilt' for their 'customary mechanical environment' and would likewise lose bone. This scenario, however, is not supported by the results of Chapter 3, as CD1 mice treated with treadmill running were found

to have enhanced tibial diaphyseal structure relative to ICR runners, despite similar levels of physical activity (i.e., exercise plus home-cage activity). In other words, the effects of genetic background on diaphyseal structure did not disappear as a result of functional loading during life.

The mechanisms responsible for the evolutionary signal detected in this study are elusive. In principle, however, the physical activity profiles of earlier generations could be incorporated into the genome of subsequent generations by the process commonly referred to as 'genetic assimilation' (Waddington, 1961; Price et al., 2003; West-Eberhard, 2003; Pigliucci et al., 2006). In this model, phenotypic traits individually acquired through a plastic response to environmental stimuli, such as some aspects of diaphyseal structure, are later, under the influence of selection, incorporated into an organism's developmental repertoire if the environmental stimulus becomes constant. In the case of limb bones, if there is a shift in the loading environment that elicits a bony response in a given generation (e.g., increased loading associated with high physical activity levels causes individuals to grow large, strong diaphyses), and this new loading environment persists in subsequent generations (e.g., members of the lineage remain highly physically active), then the loading-induced phenotype may become genetically assimilated and constitutively produced. This scenario is consistent with the adaptationist perspective of Churchill (1999) and others (Trinkaus et al., 1994), which predicts that selection favoring high levels of physical activity should cause a concomitant evolutionary increase in diaphyseal size and strength. Thick diaphyses among fossil hominins, juvenile or adult, would thus be interpreted as an evolutionary (cross-generational) adaptation to high physical activity, rather than (only) a plastic response to individual physical activity level.

Alternatively, the evolutionary signal detected in this study need not be interpreted as adaptive. Indeed, from an energetic perspective, elevated bone mass might be considered *maladaptive* for highly physically active animals because it would increase the moment of inertia of their limbs and the metabolic cost of locomotion (Chapter 2). Therefore, increased relative diaphyseal dimensions in HR mice may represent evolutionary 'spandrels' (*sensu* Gould and Lewontin, 1979), genetically associated with physical activity through pleiotropic gene action (e.g., via molecules that regulate both physical activity and bone morphology), rather than adaptations shaped by genetic assimilation. For example, HR mice have lower levels of plasma leptin (especially or possibly only in females; Girard et al., 2007; Vaanholt et al., 2007, 2008), a key molecule in energy metabolism that also affects bone structure (Lee and Karsenty, 2008;

Confavreux et al., 2009; Karsenty and Ferron, 2012). Leptin deficiency has been demonstrated to cause substantial increases in bone quantity (Ducy et al., 2000; Elefteriou et al., 2004; but see Hamrick et al., 2009), suggesting that low leptin levels and high bone quantity in HR mice might be causally related phenomena. Regardless of the specific genes and molecular pathways involved, if the observed differences in diaphyseal structure are non-adaptive and only indirectly related to physical activity, then the results of this study caution against using limb bone diaphyses to infer ancestral physical activity levels. In other words, despite the presence of an evolutionary signal conditioned by ancestral behavior, inferring the latter from the former is not advisable unless they are related through causation and not simple correlation. Otherwise, if HR and C mice were also found to differ in, say, craniofacial morphology, then one would conclude that physical activity levels of fossil taxa could also be reconstructed from these features. Indeed, several inbred strains of mice that differ significantly from one another in terms of physical activity levels (Lightfoot et al., 2004) also have distinct craniofacial morphologies (Cheverud et al., 1991; Vinyard and Payseur, 2008), but these differences are almost certainly not directly related (but see Lieberman, 1996).

This study has assumed that diaphyseal structure in 1-week-old mice is primarily determined by genetics rather than mechanical loads because mice do not actively locomote before this age. However, fetal and perinatal bones do not develop in an environment devoid of mechanical signals. In fact, loads applied through muscle contractions are critical to prenatal skeletal development (Hall and Herring, 1990). Therefore, the differences in diaphyseal structure observed between HR and C mice could be the result of differences in intrauterine and perinatal muscle activity. It is also possible that HR mothers are more physically active during pregnancy than C mothers and that this difference has a positive influence on fetal skeletal growth in HR mice. In this case, differences in perinatal diaphyseal structure would still reflect variation in ancestral physical activity patterns, but would not be the result of genetic inheritance. The activity patterns of pregnant mothers and newborn pups have not yet been examined rigorously, nor have fetal physical activity patterns. However, based on informal observations (by Prof. Garland), HR and C pups appear to be equally sedentary prior to 1 week of age, and this pattern presumably extends to prenatal development as well. Differences in physical activity between pregnant mothers are more likely, but there is currently little experimental evidence suggesting that maternal physical activity influences fetal bone growth directly (i.e., soma to soma). Note

that both the HR and C dams in this study did not have wheel access and that previous behavioral studies have shown that, after giving birth, dams from HR and C lines exhibit similar frequencies of maternal behavior and similar levels of locomotor activity. Litter size or litter mass at birth or at weaning also does not differ between HR and C lines (Girard et al., 2002). In sum, differences in maternal or pre- and perinatal physical activity are unlikely to have significantly influenced the results presented here. It is nevertheless true that at no point during development are phenotypes determined entirely by genetics; environmental factors always have some effect (West-Eberhard, 2003).

An important limitation of this study is that it lacked replication of experimental lines, so it is possible that differences in diaphyseal structure between the selected HR mice and non-selected control mice analyzed here were the result of founder effects and/or random genetic drift rather than the effects of selection (Garland, 2003). Therefore, the results will need to be confirmed by analyses involving all 8 lines from the selection experiment. These preliminary results, however, provide valuable insight into how genetics and phenotypic plasticity might interact in the skeleton over the course of evolution. Genetic background and functional loading both have roles in determining limb bone structure, as demonstrated by the research presented in this dissertation. Functional morphologists would benefit from considering non-mechanical influences on limb bone structure as more than confounding variables, but as potential sources of scientific inquiry.

Table 4.1. Descriptive statistics for body mass and femoral diaphyseal parameters of 1-week-old mice. Values are means ± standard deviations.

Trait	Females		Males	
	High Runner **(n = 10)**	**Control** **(n = 12)**	**High Runner** **(n = 10)**	**Control** **(n = 11)**
BM	4.37 ± 0.46	5.02 ± 1.05	4.61 ± 0.64	5.08 ± 0.67
Ps.Ar	0.6068 ± 0.0692	0.6055 ± 0.1084	0.6611 ± 0.0959	0.6419 ± 0.0770
Ec.Ar	0.3378 ± 0.0486	0.3474 ± 0.0592	0.3964 ± 0.0648	0.3769 ± 0.0399
Ct.Ar	0.1590 ± 0.0289	0.1568 ± 0.0418	0.1545 ± 0.0299	0.1590 ± 0.0253
I_{max}	0.0142 ± 0.0042	0.0148 ± 0.0057	0.0159 ± 0.0052)	0.0159 ± 0.0048
I_{min}	0.0100 ± 0.0027	0.0098 ± 0.0039	0.0107 ± 0.0032	0.0104 ± 0.0026
J	0.0242 ± 0.0069	0.0246 ± 0.0096	0.0266 ± 0.0084	0.0264 ± 0.0073
TMD	722 ± 8	717 ± 15	709 ± 9	713 ± 9
Po	41 ± 2	39 ± 4	42 ± 3	40 ± 3

BM = body mass (g); Ps.Ar = periosteal area (mm^2); Ec.Ar = endocortical area (mm^2); Ct.Ar = cortical area (mm^2); I_{max} = maximal second moments of area (mm^4); I_{min} = minimal second moments of area (mm^4); J = polar moment of area (mm^4); TMD = tissue mineral density (mg HA/cm^3); Po = intracortical porosity (%).

Table 4.2. Results of ANCOVA models used to test for differences in femoral mid-diaphyseal dimensions between 1-week-old mice selectively bred for high voluntary wheel running (High Runner) and non-selected controls, with body mass as a covariate. Values are back-transformed adjusted (least squares) means with 95% confidence intervals in parentheses. Statistically significant differences (P < 0.05) are indicated in bold print.

Trait	Female			Male		
	High Runner (n = 10)	Control (n = 12)	P	High Runner (n = 10)	Control (n = 11)	P
Ps.Ar	0.6396 (0.6131-0.6673)	0.5680 (0.5466-0.5902)	**0.0005**	0.6852 (0.6550-0.7168)	0.6119 (0.5862-0.6387)	**0.0017**
Ec.Ar	0.3501 (0.3232-0.3793)	0.3302 (0.3070-0.3550)	0.2854	0.4070 (0.3797-0.4364)	0.3619 (0.3387-0.3866)	0.1411
Ct.Ar	0.1704 (0.1590-0.1825)	0.1418 (0.1332-0.1509)	**0.0008**	0.1609 (0.1511-0.1713)	0.1494 (0.1407-0.1586)	0.0985
I_{max}	0.0157 (0.0145-0.0170)	0.0123 (0.0115-0.0132)	**0.0002**	0.0168 (0.0153-0.0185)	0.0139 (0.0128-0.0152)	**0.0082**
I_{min}	0.0111 (0.0103-0.0120)	0.0081 (0.0076-0.0087)	**<0.0001**	0.0113 (0.0105-0.0122)	0.0093 (0.0087-0.0100)	**0.0012**
J	0.0269 (0.0249-0.0289)	0.0204 (0.0191-0.0219)	**<0.0001**	0.0282 (0.0259-0.0306)	0.0233 (0.0215-0.0252)	**0.0036**

Ps.Ar = periosteal area (mm^2); Ec.Ar = endocortical area (mm^2); Ct.Ar = cortical area (mm^2); I_{max} = maximal second moments of area (mm^4); I_{min} = minimal second moments of area (mm^4); J = polar moment of area (mm^4).

Figure 4.1
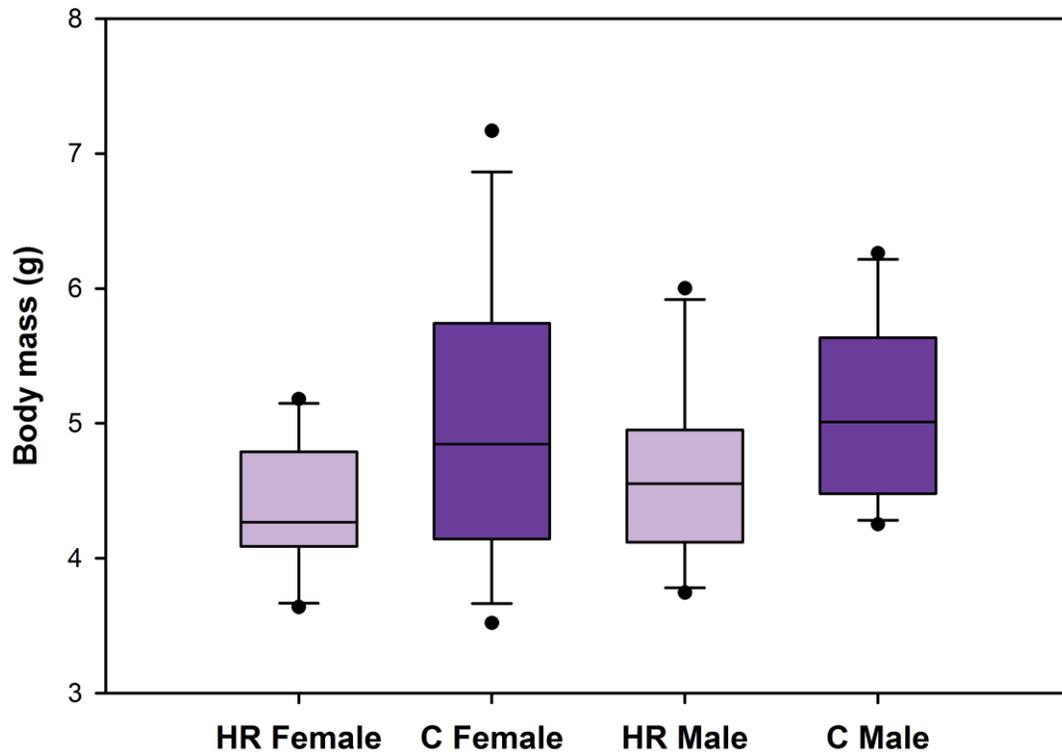
Figure 4.1. Box plots for body mass of 1-week-old selected High Runner (HR) and non-selected control (C) mice. Differences were not statistically significant between HR and C mice for either females or males (Middleton et al., 2008b).

Figure 4.2
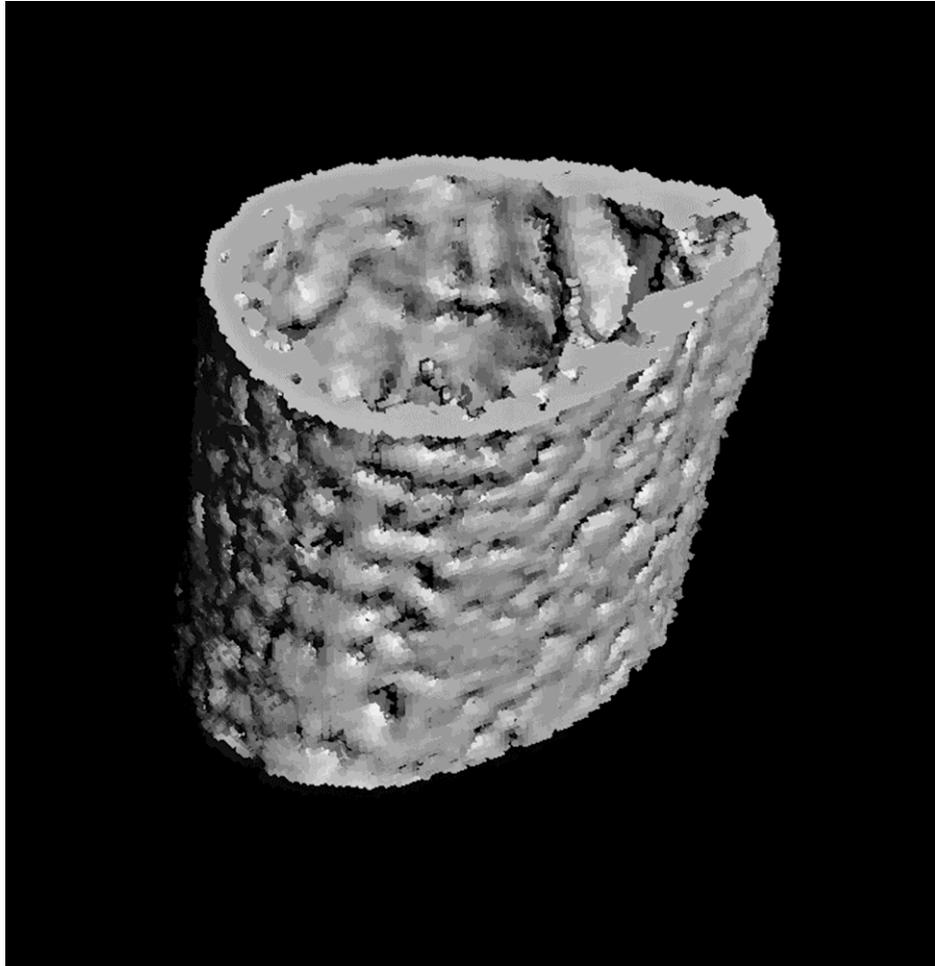
Figure 4.2. Three-dimensional reconstruction of the mid-diaphyseal region of a 1-week-old High Runner mouse femur.

Figure 4.3
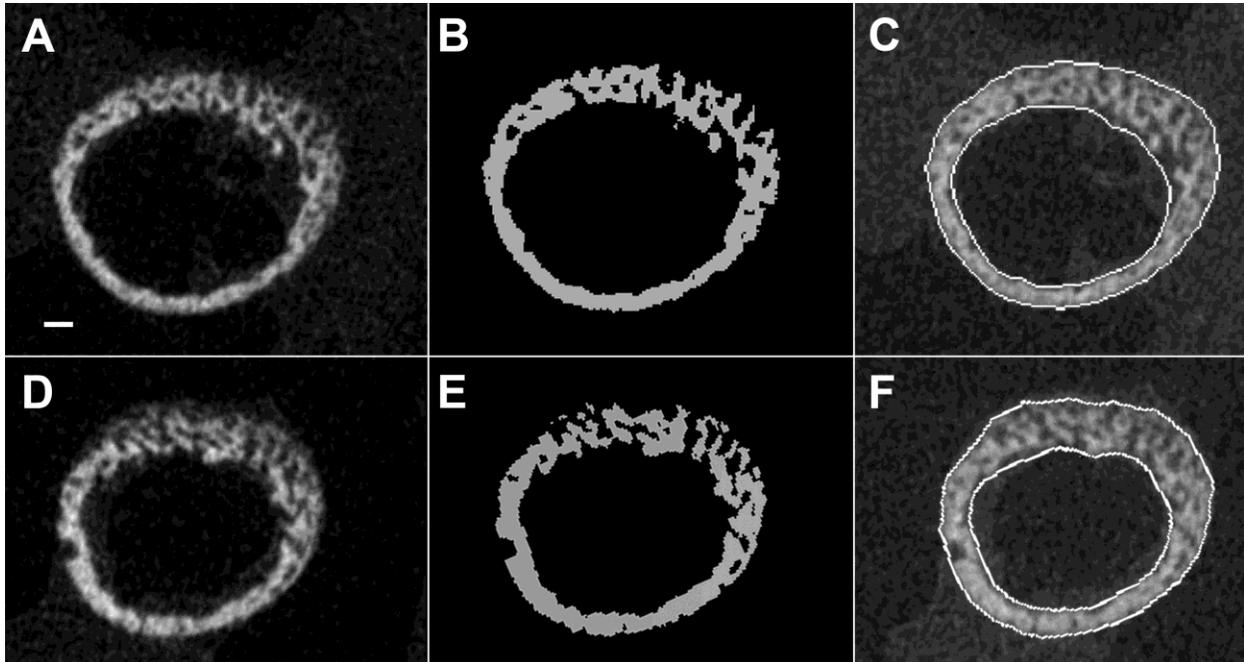
Figure 4.3. Cross sections of 1-week-old mouse femoral mid-diaphyses. A-C: Selected High Runner mouse. D-F: Control mouse. A, D. Gray scale µCT sections. B, E. Segmented bone. C, F. Lines delineating periosteal and endocortical perimeters. Scale bar in A is 100 µm.

Figure 4.4

107
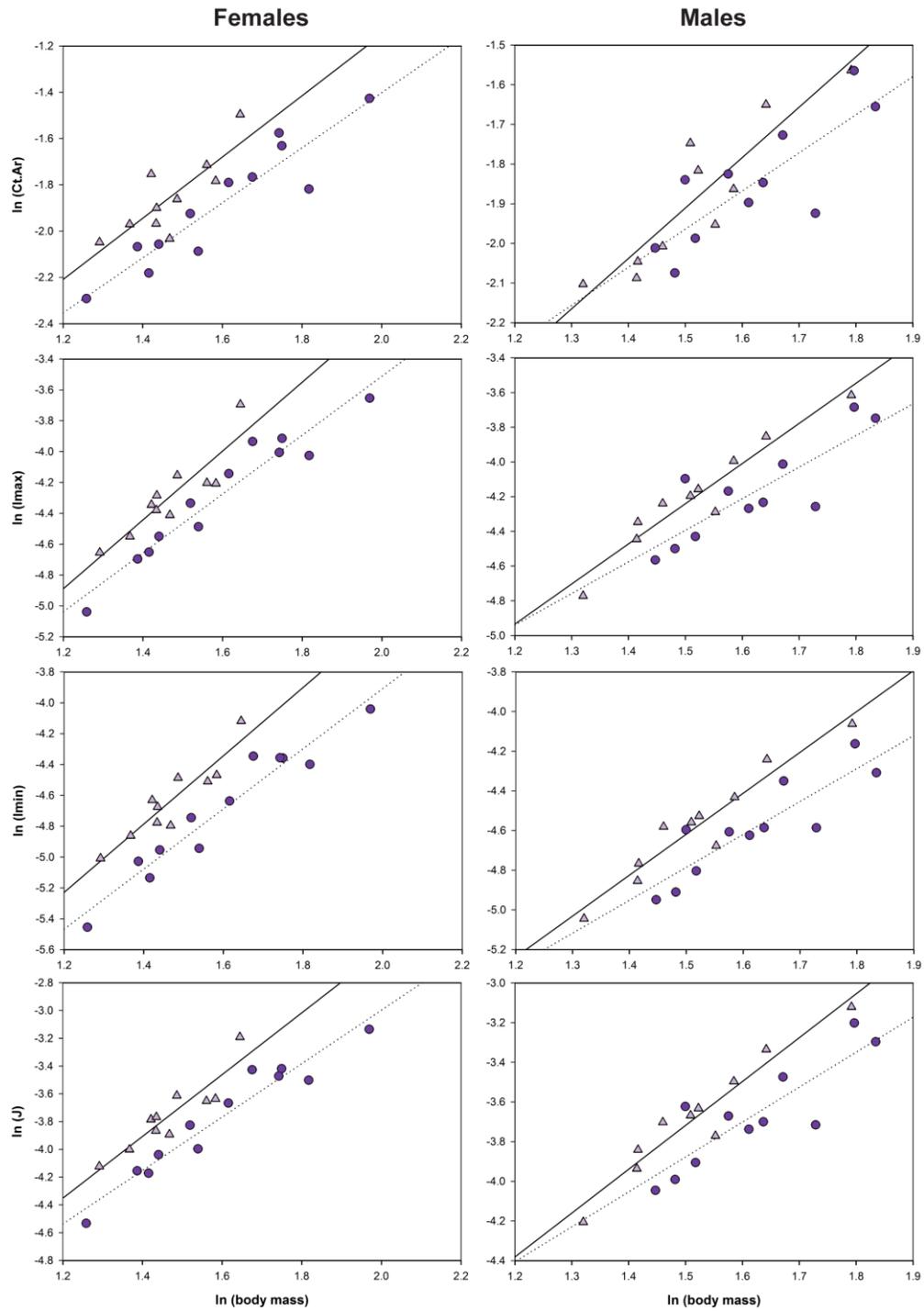
Figure 4.4. Femoral mid-diaphyseal dimensions in relation to body mass. Triangles represent selected High Runner (HR) mice and circles represent non-selected control mice. Lines are least-squares regressions through the selected HR (solid) and control (dotted) samples.

Figure 4.5
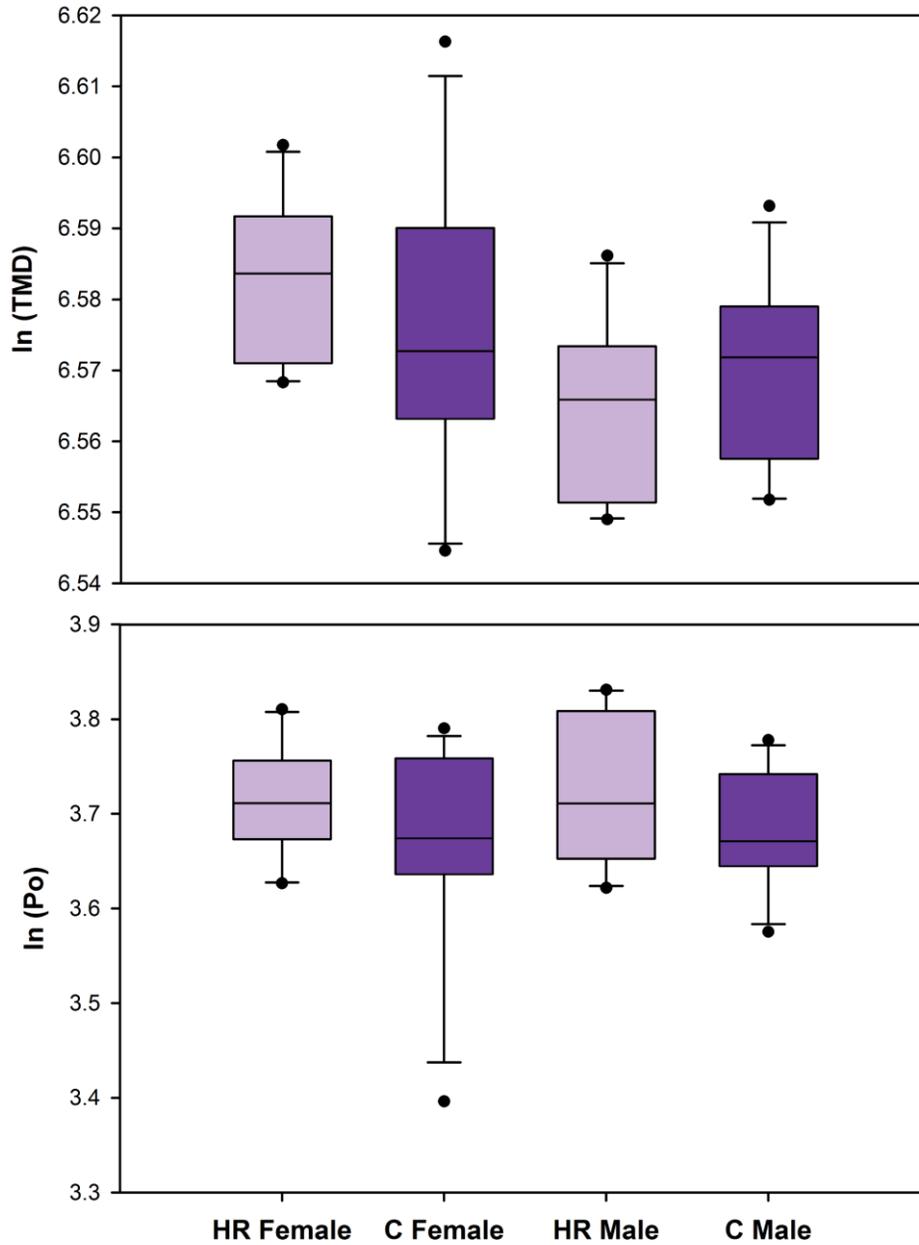
Figure 4.5. Box plots for tissue mineral density (TMD) and intracortical porosity (Po). Differences were not statistically significant between selected High Runner mice and non-selected control mice for either females or males.

Chapter 5

Summary, Significance, and Concluding Remarks

The goals of this dissertation were to clarify (1) the relative importance of genetic background and physical activity in dictating populational variation in limb bone morphology and (2) the degree to which the responsiveness of bone to loading differs between populations. To accomplish these goals, three experiments were conducted using mice as a model organism.

In the first experiment, the simultaneous effects of genetics and physical activity on limb bone structure were examined using mice from a long-term selective breeding experiment for high levels of voluntary wheel running (Swallow et al., 1998; Garland, 2003). Beginning shortly after weaning, males from each of four replicate high runner (HR) lines and four replicate non-selected control (C) lines were either given or denied wheel access for 2 months. At the end of the experiment, μCT was used to quantify femoral morphology at two cortical bone sites (mid-diaphysis, distal metaphysis) and one trabecular bone site (distal metaphysis). Genetic differences among linetypes, lines, and individuals were observed to have a pronounced impact on nearly all morphological parameters analyzed. Femora of HR mice had enlarged shafts, expanded endocortical areas, and mid-diaphyseal shapes suggesting elevated mechanical strength (i.e., larger J values). However, HR mice harboring the MM (mini-muscle) allele (a Mendelian recessive variant that halves hind limb muscle mass) had diminished cortical bone area, shaft shape, and trabecular thickness. Within the HR and C linetypes, replicate lines displayed considerable variation in bone quantity and architecture, with the particular traits affected differing between linetypes and anatomical regions. Wheel running also influenced femoral morphology, although the bone response stimulated by loading did not generally result in improved structure. Running led to moderate periosteal expansion, but relatively greater endocortical enlargement. The disparity between periosteal and endosteal expansion ultimately caused thinner cortices, as well as decreased cortical bone quantity in the metaphysis. Among the mice allowed access to wheels, bone mechanoresponsiveness was broadly independent of exercise dose (distance run) and genetic background (linetype or line). In the mid-diaphysis, the

110

two most mechanically relevant structural parameters (Ct.Ar, J) were unaffected by running. Exercise loading also failed to modify trabecular bone morphology. The results of this experiment demonstrate the strong influence of genetics on limb bone structure. Furthermore, the results underscore the fact that the effects of physical activity on bone morphology can be unpredictable (i.e., loading is not always anabolic).

In the second experiment, the influence of populational genetic variation on limb bone structure and strength, as well as bone mechanoresponsiveness, were examined using mice from two commercial outbred stocks, Hsd:ICR (ICR) and Crl:CD1 (CD1). Large-scale genetic studies have shown that these stocks possess genetic variation that is comparable to that of human populations. Mice from each stock were either treated with a treadmill running regimen for 1 month, beginning shortly after weaning, or served as sedentary controls. Home-cage activity of all animals was monitored during the experiment. Hind limb forces were recorded to confirm that they were alike in the two stocks. Following the experimental period, μCT was used to evaluate cortical bone morphology in femoral and tibial mid-diaphyses and trabecular bone morphology in distal femoral and proximal tibial metaphyses. Diaphyseal strength was measured with mechanical testing. It was found that genetic background strongly influenced nearly all morphological and mechanical traits analyzed. Among the controls, CD1 mice had significantly enhanced femoral and tibial diaphyseal cortical bone quantity and area moments, as well as greater diaphyseal mechanical strength, compared to ICR mice. Among the animals treated with running exercise, fewer significant stock differences in diaphyseal structure and strength were found, although relative to ICR runners, CD1 runners displayed higher femoral yield strength, larger tibial periosteal areas, and augmented tibial area moments. In addition, femoral and tibial trabecular bone structure was significantly deteriorated in CD1 runners compared to ICR runners. The dissimilar patterns of inter-stock variation observed in the controls and runners can be explained, in large part, by the pronounced difference detected between ICR and CD1 mice in their skeletal response to exercise loading. In the ICR mice, treadmill running resulted in significantly enhanced diaphyseal bone areas, area moments, and mechanical strength in both the femur and tibia, and to augmented trabecular bone structure in the distal femur. In contrast, in CD1 mice, the same running regimen had little effect on limb bone cortical and trabecular morphology, and resulted in significantly diminished femoral diaphyseal strength. The differential effects of exercise on ICR and CD1 femora were further indicated by several

significant stock X activity group statistical interactions, including for diaphyseal cortical area, area moments, and mechanical strength. Importantly, in neither stock was body mass, muscle mass, or cage activity level significantly different between runners and controls. Given that most environmental variables were controlled in this experiment, the differential effects of exercise on the limb bones of ICR and CD1 mice can reasonably be attributed to genetic differences between the stocks. In addition to further demonstrating the strong influence of genetics on limb bone structure, the results of this experiment illustrate that one way in which genetic variation between populations can exert its influence on the skeleton is by affecting the responsiveness of bone to loading.

The third experiment explored the possibility that genetic variation underlying limb bone structure is affected by the historical physical activity levels of members of a lineage (population) and might therefore have functional significance in an evolutionary context. In this experiment, 1-week-old mice were employed from the selective breeding experiment for high voluntary wheel running. The goal was to determine whether the femora of mice with an 'evolutionary history' of high levels of physical activity (i.e., HR mice) were morphologically distinct (as indicated by μCT analyses) from non-selected control mice prior to the onset of locomotion. As hypothesized, at 1 week of age, HR mice had augmented femoral diaphyseal bone areas and area moments, suggesting that selection for high levels of physical activity resulted in a concomitant evolutionary enhancement of limb bone diaphyseal morphology. The results of this experiment suggest that limb bone structure may not always only reflect the physical activity levels of particular individuals, but may also convey an evolutionary signal conditioned by ancestral physical activity levels.

Anthropological Significance

The implications of the research described in this dissertation for anthropology are straightforward. First, variation in limb bone structure among populations is not shaped solely by differences in physical activity levels throughout life. Genetic background is also an important determinant of skeletal morphology. Second, physical activity does not *always* augment the skeleton, but can also result in stasis or even diminished structure. Third, the magnitude of the skeletal response to physical activity can vary between populations, such that equal loads can

produce distinct morphological end states. With these three points in mind, anthropologists should be less content to accept that physical activity levels of past human populations can be accurately inferred from skeletal remains. Populations characterized by thick, strong bones may or may not have been highly physically active during life, just as populations characterized by thin, fragile bones may or may not have been sedentary. Moreover, two populations with similar bone structure may have exhibited dramatic differences in physical activity levels during life; and a population with gracile bones may have actually been *more* physically active than a population with enhanced bone structure. This complexity is inconvenient, but it is unavoidable and must be carefully considered when skeletal remains are used to reconstruct past human physical activity. Alas, skeletal morphology may indeed emit a signal related to functional loading history (or perhaps ancestral physical activity levels), but our ability to decipher this functional signal amidst the noise caused by other determinants of bone structure (e.g., genetics, age, sex, nutrition) is limited.

Clinical Significance

Beyond implications for anthropology (and vertebrate functional morphology more generally), the research described in this dissertation, particularly in Chapter 3, may also be pertinent to public health. According to the National Institutes of Health, half of all women and a quarter of men over age 50 will experience an osteoporosis-related bone fracture in their lifetime (http://www.nlm.nih.gov/medlineplus/osteoporosis.html). These fractures are responsible for nearly $20 billion in healthcare costs. Susceptibility to osteoporotic fracture is greatly affected by bone morphology and strength (Albrand et al., 2003). Since skeletal loading is able to induce bone formation and prevent bone loss, clinicians seek to develop technologies and exercise programs that provide healthy doses of mechanical stimulation to the skeleton in order to enhance bone structure and strength (Rubin et al., 2001a; McKay, 2003; Ozcivici et al., 2010). These technologies and interventions are typically designed to be applied broadly across different populations. This strategy may need to be reassessed if bone mechanoresponsiveness varies among human populations as is does between the mouse populations analyzed in Chapter 3. Therapies involving mechanical stimulation of the skeleton are associated with safety risks, particularly exercise programs (Caine et al., 2006; Clark et al., 2008). If the bones of certain

populations are less responsive than others to mechanical loading, then these risks might outweigh the potential benefits of mechanical therapies for these individuals. Therefore, efforts would need to be made to identify those populations that are less responsive, so that alternative strategies, perhaps involving pharmaceuticals, could be adopted to stem age-related bone loss and promote skeletal health in these individuals.

Moving Forward

One of the most iconic images in anthropology is that of a small band of hunter-gatherers trekking through the wilderness (cf. Kelly, 1992). For some, this image is a testament to the triumph of civilization in bestowing leisure upon humanity, while for others, this image conjures up sentimental longing for life in a state of nature with the freedom to roam. Regardless of the emotions inspired by this image, there is little doubt that it reifies a popular narrative about how life in the modern (industrialized) world differs from that of our distant ancestors: we are generally sedentary, and hunter-gatherers "move around a lot" (Lee and DeVore, 1968:11).

Given the common perception of sedentism as a defining characteristic of human 'modernity', it is not surprising that so much anthropological effort has been devoted to deciphering the physical activity levels of populations living in the past. Indeed, over the last half-century, numerous lines of anatomical and archaeological evidence—in addition to gross bone morphology—have been proposed as proxies for human physical activity levels, including entheseal morphology (Villotte et al., 2010), osteoarthritis (Lieverse et al., 2007), stone tool technologies (Kelly, 1992; Wallace and Shea, 2006), and raw material procurement patterns (Féblot-Augustins, 1999). As with gross bone morphology, the validity of many of these purported proxies has often been a source of intense debate. Without a doubt, these discussions have yielded important epistemological contributions to anthropology. However, one senses that, in the throes of disagreement, we may have lost sight of why past human physical activity even matters. In some cases, with multiple lines of anatomical and archaeological evidence available, it may indeed be possible to paint a reasonable picture of past activity. Moving forward, we must remember to ask ourselves: Why is this picture interesting?

The most compelling answers to this question will likely derive from a greater appreciation for how knowledge of past human physical activity adds to our understanding of the

core issues of anthropology, such as the evolutionary forces that shaped humanity, and how our biological past affects the future of our species (Ellison, 2013). For example, it has recently been suggested that high levels of physical activity throughout hominin evolution may have positively affected the evolution of our large brain size and enhanced cognitive function (Raichlen and Polk, 2013). Psychiatric 'diseases of modernity' such as depression and anxiety might be directly related to our current sedentary lifestyle (Hidaka, 2012). Therefore, physical activity levels, past and present, may in some way be responsible for the artistic gifts of melancholy genius offered to us by such humans as Baudelaire, Basquiat, and Bon Iver. That, to me, is interesting.

References

Akhter, M.P., Cullen, D.M., Pedersen, E.A., Kimmel, D.B., and Recker, R.R. (1998). Bone response to in vivo mechanical loading in two breeds of mice. *Calcif. Tissue Int.* 63:442-449.

Akhter, M.P., Cullen, D.M., and Recker, R.R. (2002). Bone adaptation response to sham and bending stimuli in mice. *J. Clin. Densitom.* 5:207-216.

Albrand, G., Munoz, F., Sornay-Rendu, E., DuBoeuf, F., and Delmas, P.D. (2003). Independent predictors of all osteoporosis-related fractures in healthy postmenopausal women: the OFELY study. *Bone* 32:78-85.

Aldinger, K.A., Sokoloff, G., Rosenberg, D.M., Palmer, A.A., and Millen, K.J. (2009). Genetic variation and population substructure in outbred CD-1 mice: implications for genome-wide association studies. *PLoS ONE* 4:e4729.

Alexander, R.M., Jayes, A.S., Maloiy, G.M.O., and Wathuta, E.M. (1979). Allometry of the limb bones of mammals from shrews (Sorex) to elephant (Loxodonta). *J. Zool.* 189:305-314.

Amblard, D., Lafage-Proust, M.H., Laib, A., Thomas, T., Ruegsegger, P., Alexandre C., and Vico, L. (2003). Tail suspension induces bone loss in skeletally mature mice in the C57BL/6J strain but not in the C3H/HeJ strain. *J. Bone Miner. Res.* 18:561-569.

Amtmann, E. (1971). Mechanical stress, functional adaptation, and the variation of structure of the human femur diaphysis. *Ergebn. Anat.* 44:7-89.

Arnsdorf, E.J., Tummala, P., Kwon, R.Y., and Jacobs, C.R. (2009). Mechanically induced osteogenic differentiation—the role of RhoA, ROCKII and cytoskeletal dynamics. *J. Cell Sci.* 122:546-553.

Arsuaga, J.L., Villaverde, V., Quam, R., Martínez, I., Carretero, J.M,, Lorenzo, C., and Gracia, A. (2007). New neandertal remains from Cova Negra (Valencia, Spain). *J. Hum. Evol.* 52:31-58.

Bab, I.A. (2007). Regulation of skeletal remodeling by the endocannabinoid system. *Ann. N.Y. Acad. Sci.* 1116:414-422.

Bab, I., and Zimmer, A. (2008). Cannabinoid receptors and the regulation of bone mass. *Br. J. Pharmacol.* 153:182-188.

Barak, M.M., Lieberman, D.E., and Hublin, J.-J. (2011). A Wolff in sheep's clothing: trabecular bone adaptation in response to changes in joint loading orientation. *Bone* 49:1141-1151.

Barry, D.W., and Kohrt, W.M. (2008). BMD decreases over the course of a year in competitive male cyclists. *J. Bone Miner. Res.* 23:484-491.

Batra, N., and Jiang, J.X. (2012). "INTEGRINating" the connexin hemichannel function in bone osteocytes through the action of integrin α5. *Comm. Integ. Biol.* 5:516-518.

Bausell, R.B., and Li, Y.-F. (2002). *Power Analysis for Experimental Research: A Practical Guide for the Biological, Medical and Social Sciences.* Cambridge: Cambridge University Press.

Behringer, M., Gruetzner, S., McCourt, M., and Mester, J. (2013). Effects of weight-bearing activities on bone mineral content and density in children and adolescents: a meta-analysis. *J. Bone Miner. Res.* DOI: 10.1002/jbmr.2036.

Bertram, J.E.A., and Biewener, A.A. (1988). Bone curvature: sacrificing strength for load predictability? *J. Theor. Biol.* 131:75-92.

Bertram, J.E.A., and Swartz, S.M. (1991). The "law of bone transformation": a case of crying Wolff? *Biol. Rev.* 66:245-273.

Biewener, A.A. (1982). Bone strength in small mammals and bipedal birds: do safety factors change with body size? *J. Exp. Biol.* 98:289-301.

Biewener, A.A. (1990). Biomechanics of mammalian terrestrial locomotion. *Science* 23:1097-1103.

Biewener, A.A., and Taylor, C.R. (1986). Bone strain: a determinant of gait and speed? *J. Exp. Biol.* 123:383-400.

Biewener, A.A., and Bertram, J.E.A. (1993). Skeletal strain patterns in relation to exercise training during growth. *J. Exp. Biol.* 185:51-69.

Biewener, A.A., and Bertram, J.E.A. (1994). Structural response of growing bone to exercise and disuse. *J. Appl. Physiol.* 72:946-955.

Biewener, A.A., Swartz, S.M., and Bertram, J.E.A. (1986). Bone modeling during growth: dynamic strain equilibrium in the chick tibiotarsus. *Calcif. Tissue Int.* 39:390-395.

Bonewald, L.F. (2006). Mechanosensation and transduction in osteocytes. *Bonekey Osteovision* 3:7-15.

Bonjour, J.-P., Chevalley, T., Rizzoli, R., and Ferrari, S. (2007). Gene-environment interactions in the skeletal response to nutrition and exercise during growth. *Med. Sport Sci.* 51:64-80.

Bourrin, S., Genty, C., Palle, S., Gharib, C., and Alexandre, C. (1994). Adverse effects of strenuous exercise: a densiometric and histomorphometric study in the rat. *J. Appl. Physiol.* 76:1999-2005.

Bouxsein, M.L., Boyd, S.K., Christiansen, B.A., Guldberg, R.E., Jepsen, K.J., and Müller, R. (2010). Guidelines for assessment of bone microstructure in rodents using micro-computed tomography. *J. Bone Miner. Res.* 25:1468-1486.

Bridges, P.S. (1989). Changes in activities with the shift to agriculture in the southeastern United States. *Curr. Anthropol.* 30:385-394.

Brodt, M.D., and Silva, M.J. (2010). Aged mice have enhanced endocortical response and normal periosteal response compared with young-adult mice following 1 week of axial tibial compression. *J. Bone Miner. Res.* 25:2006-2015.

Brotherstone, S., and Goddard, M. (2005). Artificial selection and maintenance of genetic variance in the global dairy cow population. *Phil. Trans. R. Soc. B* 360:1479-1488.

Brothwell, D. (1975). Adaptive growth rate changes as a possible explanation for the distinctiveness of the neanderthalers. *J. Archaeol. Sci.* 2:161-163.

Buhl, K.M., Jacobs, C.R., Turner, R.T., Evans, G.L., Farrell, P.A., and Donahue, H.J. (2001). Aged bone displays an increased responsiveness to low-intensity resistance exercise. *J. Appl. Physiol.* 90:1359-1364.

Burger, E.H., and Klein-Nulend, J. (1999). Mechanotransduction in bone – role of the lacunocanalicular network. *FASEB J.* 13:S101-S112.

Burr, D.B., Milgrom, C., Fyhrie, D., Forwood, M., Nyska, M., Finestone, A., Hoshaw, S., Saiag, E., and Simkin, A. (1996). In vivo measurement of human tibial strains during vigorous activity. *Bone* 18:405-410.

Burrows, M., Nevill, A.M., Bird, S., and Simpson, D. (2003). Physiological factors associated with low bone mineral density in female endurance runners. *Br. J. Sports Med.* 37:67-71.

Cardadeiro, G., Baptista, F., Ornelas, R., Janz, K.F., and Sardinha, L.B. (2012). Sex specific association of physical activity on proximal femur BMD in 9 to 10 year-old children. *PLoS ONE* 7:e50657.

Caine, D., DiFiori, J., and Maffulli, N. (2006). Physeal injuries in children's and youth sports: reasons for concern? *Br. J. Sports Med.* 40:749-760.

Carrano, M.T. (1999). What, if anything, is a cursor? Categories versus continua for determining locomotor habit in mammals and dinosaurs. *J. Zool. Lond.* 247:29-42.

Carrier, D.R. (1984). The energetic paradox of human running and hominid evolution. *Curr. Anthropol.* 25:483-495.

Carter, D.R. (1984). Mechanical loading histories and cortical bone remodeling. *Calcif. Tissue Int.* 36(Suppl 1):19-24.

Carter, D.R., and Beaupré, G.S. (2001). *Skeletal Function and Form: Mechanobiology of Skeletal Development, Aging and Regeneration.* Cambridge: Cambridge University Press.

Case, N., and Rubin, J. (2010). Beta-catenin – a supporting role in the skeleton. *J. Cell. Biochem.* 110:545-553.

Chen, Z., Qi, L., Beck, T.J., Robbins, J., Wu, G., Lewis, C.E., Cauley, J.A., Wright, N.C., and Seldin, M.F. (2011). Stronger bone correlates with African admixture in African-American women. *J. Bone Miner. Res.* 26:2307-2316.

Cheverud, J.M., Hartman, S.E., Richtsmeier, J.T., and Atchley, W.R. (1991). A quantitative genetic analysis of localized morphology in mandibles of inbred mice using finite element scaling analysis. *J. Craniofac. Genet. Dev. Biol.* 11:122-137.

Chia, R., Achilli, F., Festing, M.F.W., and Fisher, E.M.C. (2005). The origins and uses of mouse outbred stocks. *Nat. Genet.* 37:1181-1186.

Churchill, S.E. (1999). Cold adaptation, heterochrony, and neandertals. *Evol. Anthropol.* 7:46-60.

Clark, E.M., Ness, A.R., and Tobias, J.H. (2008). Vigorous physical activity increases fracture risk in children irrespective of bone mass: a prospective study of the independent risk factors for fractures in healthy children. *J. Bone Miner. Res.* 23:1012-1022.

Coats, B.R., Middleton, K.M., Kelly, S.A., and Garland, T. Jr. (2011). Cross-sectional limb bone geometry in mice bred for high levels of voluntary wheel running. *Integr. Comp. Biol.* 51(Suppl 1):e176.

Confavreux, C.B., Levine, R.L., and Karsenty, G. (2009). A paradigm of integrative physiology, the crosstalk between bone and energy metabolisms. *Mol. Cell. Endocrinol.* 310:21-29.

Conrad, D.F., Jakobsson, M., Coop, G., Wen, X., Wall, J.D., Rosenberg, N.A., and Pritchard, J.K. (2006). A worldwide survey of haplotype variation and linkage disequilibrium in the human genome. *Nat. Genet.* 38:1251-1260.

Copes, L. (2012). Comparative and experimental investigations of cranial robusticity in Mid-Pleistocene hominins. PhD dissertation. Arizona State University.

Cowgill, L.W. (2010). The ontogeny of Holocene and Late Pleistocene human postcranial strength. *Am. J. Phys. Anthropol.* 141:16-37.

Cowgill, L.W., and Hager, L,D. (2007). Variation in the development of postcranial robusticity: an example from Çatalhöyük, Turkey. *Int. J. Osteoarchaeol.* 17:235-252.

Cui, S., Chesson, C., and Hope, R. (1993). Genetic variation within and between strains of outbred Swiss mice. *Lab. Anim.* 27:116-123.

Currey, J.D. (1979). Mechanical properties of bone tissues with greatly differing functions. *J. Biomech.* 12:313-319.

Currey, J.D. (1984). Effects of differences in mineralization of the mechanical properties of bone. *Phil. Trans. R. Soc. Lond. B* 304:509-518.

Currey, J.D. (2002). *Bones: Structure and Mechanics.* Princeton: Princeton University Press.

Currey, J.D., and Alexander, R. McN. (1985). The thickness of the walls of tubular bones. *J. Zool. Lond.* 206:453-468.

Currey, J.D., and Butler, G. (1975). The mechanical properties of bone tissue in children. *J. Bone Jt. Surg.* 57A:810-814.

Daegling, D.J., Judex, S., Ozcivici, E., Ravosa, M.J., Taylor, A.B., Grine, F.E., Teaford, M.F., and Ungar, P.S. (2013). Feeding mechanics, diet, and dietary adaptations in early hominins. *Am. J. Phys. Anthropol.* 151:356-371.

Dalsky, G.P., Stocke, K.S., Ehsani, A.A., Slatopolsky, E., Lee, W.C., and Birge, S.J. Jr. (1988). Weight-bearing exercise training and lumbar bone mineral content in postmenopausal women. *Ann. Inter. Med.* 108:824-828.

Daly, R.M. (2007). The effect of exercise on bone mass and structural geometry during growth. *Med. Sport Sci.* 51:33-49.

Danielson, M.E., Beck, T.J., Lian, Y., Karlamangla, A.S., Greendale, G.A., Ruppert, K., Lo, J., Greenspan, S., Vuga, M., and Cauley, J.A. (2013). Ethnic variability in bone geometry as assessed by hip structure analysis: findings from the hip strength across the menopausal transition study. *J. Bone Miner. Res.* 28:771-779.

Darwin, C. (1859). *On the Origin of Species by Means of Natural Selection, or the Preservation of Favoured Races in the Struggle for Life.* London: John Murray.

de Visser, L., van den Bos, R., Kuurman, W.W., Kas, M.J.H., and Spruijt, B.M. (2006). Novel approach to the behavioral characterization of inbred mice: automated home cage observations. *Genes Brain Behav.* 5:458-466.

Demes, B. (2007). *In vivo* bone strain and bone functional adaptation. *Am. J. Phys. Anthropol.* 133:717-722.

Demes, B., Stern, J.T. Jr., Hausman, M.R., Larson, S.G., McLeod, K.J., and Rubin, C.T. (1998). Patterns of strain in the macaque ulna during functional activity. *Am. J. Phys. Anthropol.* 106:87-100.

Demes, B., Qin, Y.-Z., Stern, J.T. Jr., Larson, S.G., and Rubin, C.T. (2001). Patterns of strain in the macaque tibia during functional loading. *Am. J. Phys. Anthropol.* 116:257-265.

Demissie, S., Dupuis, J., Cupples, L.A., Beck, T.J., Kiel, D.P., and Karasik, D. (2007). Proximal hip geometry is linked to several chromosomal regions: genome-wide linkage results from the Framingham Osteoporosis Study. *Bone* 40:743-750.

Devlin, M.J. (2011). Estrogen, exercise, and the skeleton. *Evol. Anthropol.* 20:54-61.

Devlin, M.J., and Lieberman, D.E. (2007). Variation in estradiol level affects cortical bone growth in response to mechanical loading in sheep. *J. Exp. Biol.* 210:602-613.

Dhamrait, S.S., James, L., Brull, D.J., Myerson, S., Hawe, E., Pennell, D.J., World, M., Humphries, S.E., Haddad, F., and Montgomery, H.E. (2003). Cortical bone resorption during exercise is interleukin-6 genotype-dependent. *Eur. J. Appl. Physiol.* 89:21-25.

DiGirolamo, D.J., Kiel, D.P., and Esser, K.A. (2013). Bone and skeletal muscle: neighbors with close ties. *J. Bone Miner. Res.* 28:1509-1518.

Dlugosz, E.M., Chappell, M.A., McGillivray, D.G., Syme, D.A., and Garland, T. Jr. (2009). Locomotor trade-offs in mice selectively bred for high voluntary wheel running. *J. Exp. Biol.* 212:2612-2618.

Donahue, S.W., Jacobs, C.R., and Donahue, H.J. (2001). Flow-induced calcium oscillations in rat osteoblasts are age, loading frequency, and shear stress dependent. *Am. J. Physiol. Cell Physiol.* 281:C1635-C1641.

Ducy, P., Amling, M., Takeda, S., Priemel, M., Schilling, A.F., Beil, F.T., Shen, J., Vinson, C., Rueger, J.M., and Karsenty, G. (2000). Leptin inhibits bone formation through a hypothalamic relay: a central control of bone mass. *Cell* 100:197-207.

Duncan, R.L. (1998). Mechanotransduction and mechanosensitive ion channels in osteoblasts. In *Signal Transduction: Single Cell Techniques* (eds. B. Van Duijn and A. Wiltink), pp. 125-134. Berlin: Springer.

Elefteriou, F., Takeda, S., Ebihara, K., Magre, J., Patano, N., Ae Kim, C., Ogawa, Y., Liu, X., Ware, S.M., Craigen, W.J., Robert, J.J., Vinson, C., Nakao, K., Capeau, J., and Karsenty, G. (2004). Serum leptin level is a regulator of bone mass. *Proc. Natl. Acad. Sci. U.S.A.* 101:3258-3263.

Ellison, P.T. (2013). Integration under the big tent. *Am. J. Phys. Anthropol.* 151:505.

Estrada, K., Styrkarsdottir, U., Evangelou, E., Hsu, Y.H., Duncan, E.L., Ntzani, E.E., Oei, L., Albagha, O.M., Amin, N., Kemp, J.P., Koller, D.L., Li, G., Liu, C.T., Minster, R.L., Moayyeri, A., Vandenput, L., Willner, D., Xiao, S.M., Yerges-Armstrong, L.M., Zheng, H.F., Alonso, N., Eriksson, J., Kammerer, C.M., Kaptoge, S.K., Leo, P.J., Thorleifsson, G., Wilson, S.G., Wilson, J.F., Aalto, V., Alen, M., Aragaki, A.K., Aspelund, T., Center, J.R., Dailiana, Z., Duggan, D.J., Garcia, M., Garcia-Giralt, N., Giroux, S., Hallmans, G., Hocking, L.J., Husted, L.B., Jameson, K.A., Khusainova, R., Kim, G.S., Kooperberg, C., Koromila, T., Kruk, M., Laaksonen, M., Lacroix, A.Z., Lee, S.H., Leung, P.C., Lewis, J.R., Masi, L., Mencej-Bedrac, S., Nguyen, T.V., Nogues, X., Patel, M.S., Prezelj, J., Rose, L.M., Scollen, S., Siggeirsdottir, K., Smith, A.V., Svensson, O., Trompet, S., Trummer, O., van Schoor, N.M., Woo, J., Zhu, K., Balcells, S., Brandi, M.L., Buckley, B.M., Cheng, S., Christiansen, C., Cooper, C., Dedoussis, G., Ford, I., Frost, M., Goltzman, D., González-Macías, J., Kähönen, M., Karlsson, M., Khusnutdinova, E., Koh, J.M., Kollia, P., Langdahl, B.L., Leslie, W.D., Lips, P., Ljunggren, Ö., Lorenc, R.S., Marc, J., Mellström, D., Obermayer-Pietsch, B., Olmos, J.M., Pettersson-Kymmer, U., Reid, D.M., Riancho, J.A., Ridker, P.M., Rousseau, F., Slagboom, P.E., Tang, N.L., Urreizti, R., Van Hul, W., Viikari, J., Zarrabeitia, M.T., Aulchenko, Y.S., Castano-Betancourt, M., Grundberg, E., Herrera, L., Ingvarsson, T., Johannsdottir, H., Kwan, T., Li, R., Luben, R., Medina-Gómez, C., Palsson, S.T., Reppe, S., Rotter, J.I., Sigurdsson, G., van Meurs, J.B., Verlaan, D., Williams, F.M., Wood, A.R., Zhou, Y., Gautvik, K.M., Pastinen, T., Raychaudhuri, S., Cauley, J.A., Chasman, D.I., Clark, G.R., Cummings, S.R., Danoy, P., Dennison, E.M., Eastell, R., Eisman, J.A., Gudnason, V., Hofman, A., Jackson, R.D., Jones, G., Jukema, J.W., Khaw, K.T., Lehtimäki, T., Liu, Y., Lorentzon, M., McCloskey, E., Mitchell, B.D., Nandakumar, K., Nicholson, G.C., Oostra, B.A., Peacock, M., Pols, H.A., Prince, R.L., Raitakari, O., Reid, I.R., Robbins, J., Sambrook, P.N., Sham, P.C., Shuldiner, A.R., Tylavsky, F.A., van Duijn, C.M., Wareham, N.J., Cupples, L.A., Econs, M.J., Evans, D.M., Harris, T.B., Kung, A.W., Psaty, B.M., Reeve, J., Spector, T.D., Streeten, E.A., Zillikens, M.C., Thorsteinsdottir, U., Ohlsson, C., Karasik, D., Richards, J.B., Brown, M.A., Stefansson, K., Uitterlinden, A.G., Ralston, S.H., Ioannidis, J.P., Kiel, D.P., and Rivadeneira, F. (2012). Genome-wide meta-analysis identifies 56 bone mineral density loci and reveals 14 loci associated with risk of fracture. *Nat. Genet.* 44:491-501.

Farber, C.R., Kelly, S.A., Baruch, E., Yu, D., Hua, K., Nehrenberg, D.L., Pardo-Manuel de Villena, F., Buus, R.J., Garland, T. Jr., and Pomp, D. (2011). Identification of quantitative trait loci influencing skeletal architecture in mice: emergence of *Cdh11* as a primary candidate gene regulating femoral morphology. *J. Bone Miner. Res.* 26:2174-2183.

Féblot-Augustins, J. (1999). Raw material transport patterns and settlement systems in the European Lower and Middle Palaeolithic: continuity, change and variability. In *The Middle Palaeolithic Occupation of Eutrope* (eds. W. Roebroeks and C. Gamble), pp.193-214. Leiden: University of Leiden.

Fenner, J.N. (2005). Cross-cultural estimation of the human generation interval for use in genetics-based population divergence studies. *Am. J. Phys. Anthropol.* 128:415-423.

Ferguson, V.L., Ayers, R.A., Bateman, T.A., and Simske, S.J. (2003). Bone development and age-related bone loss in male C57BL/6J mice. *Bone* 33:387-398.

Festing, M.F.W. (2010). Inbred strains should replace outbred stocks in toxicology, safety testing, and drug development. *Toxicol. Pathol.* 38:681-690.

Forwood, M.R. (1996). Inducible cyclo-oxygenase (COX-2) mediates the induction of bone formation by mechanical loading in vivo. *J. Bone Miner. Res.* 11:1688-1693.

Forwood, M.R. (2008). Physical activity and bone development during childhood: insights from animal models. *J. Appl. Physiol.* 105:334-341.

Fritton, S.P., McLeod, K.J., and Rubin, C.T. (2000). Quantifying the strain history of bone: spatial uniformity and self-similarity of low-magnitude strains. *J. Biomech*. 33:317-325.

Frost, H.M. (2003). Bone's mechanostat: a 2003 update. *Anat. Rec.* 275A:1081-1101.

Garland, T. Jr. (2003). Selection experiments: an under-utilized tool in biomechanics and organismal biology. In *Vertebrate Biomechanics and Evolution* (eds. V.L. Bels, J.P. Gasc, and A. Casinos), pp. 23-56. Oxford: BIOS.

Garland, T. Jr., and Freeman, P.W. (2005). Selective breeding for high endurance running increases hindlimb symmetry. *Evolution* 59:1851-1854.

Garland, T. Jr., and Kelly, S.A. (2006). Phenotypic plasticity and experimental evolution. *J. Exp. Biol. 209*:2344-2361.

Garland, T. Jr., and Rose, M.R. (2009). *Experimental Evolution: Concepts, Methods, and Applications of Selection Experiments*. Berkeley: University of California Press.

Garland, T. Jr., Morgan, M.T., Swallow, J.G., Rhodes, J.S., Girard, I, Belter, J.G., and Carter, P.A. (2002). Evolution of a small-muscle polymorphism in lines of house mice selected for high activity levels. *Evolution* 56:1267-1275.

Garland, T. Jr., Kelly, S.A., Malisch, J.L., Kolb, E.M., Hannon, R.M., Keeney, B.K., Van Cleave, S.L., and Middleton, K.M. (2011a). How to run far: multiple solutions and sex-specific responses to selective breeding for high voluntary activity levels. *Proc. Roy. Soc. B* 278:574-581.

Garland, T. Jr., Schutz, H., Chappell, M.A., Keeney, B.K., Meek, T.H., Copes, L.E., Acosta, W., Drenowatz, C.R., Maciel, C., van Dijk, G., Kotz, C.M., and Eisenmann, J.C. (2011b). The biological control of voluntary exercise, spontaneous physical activity and daily energy expenditure in relation to obesity: human and rodent perspectives. *J. Exp. Biol.* 214:206-229.

Gartland, A., Skarratt, K.K., Hocking, L.J., Parsons, C., Stokes, L., Jørgensen, N.R., Fraser, W.D., Reid, D.M., Gallagher, G.A., and Wiley, J.S. (2012). Polymorphisms in the P2X7 receptor gene are associated with low lumbar spine bone mineral density and accelerated bone loss in post-menopausal women. *Eur. J. Hum. Genet.* 20:559-564.

Girard, I., Swallow, J.G., Carter, P.A., Koteja, P., Rhodes, J.S., and Garland T. Jr. (2002). Maternal-care behavior and life-history traits in house mice (*Mus domesticus*) artificially selected for high voluntary wheel-running activity. *Behav. Processes* 57:37-50.

Girard, I., Rezende, E.L., and Garland, T. Jr. (2007). Leptin levels and body composition of mice selectively bred for high voluntary locomotor activity. *Physiol. Biochem. Zool.* 80:568-579.

Glatt, V., Canalis, E., Stadmeyer, L., and Bouxsein, M. (2007). Age-related changes in trabecular architecture differ in female and male C57BL/6J mice. *J. Bone Miner. Res.* 22:1197-1207.

Goodship, A.E., and Cunningham, J.L. (2001). Pathophysiology of functional adaptation of bone in remodeling and repair *in vivo*. In *Bone Mechanics Handbook* (ed. S. Cowin), pp. 26:1-31. Boca Raton: CRC Press.

Gould, S.J., and Lewontin, R.C. (1979). The spandrels of San Marco and the Panglossian paradigm: a critique of the adaptationist programme. *Proc. R. Soc. Lond. B* 205:581-598.

Gross, T.S., McLeod, K.J., and Rubin, C.T. (1992). Characterizing bone strain distributions in vivo using three triple rosette strain gages. *J. Biomech.* 25:1081-1087.

Gross, T.S., Edwards, J.L., McLeod, K.J., and Rubin, C.T. (1997). Strain gradients correlate with sites of periosteal bone formation. *J. Bone Miner. Res.* 12:982-988.

Guderley, H., Houle-Leroy, P., Diffee, G.M., Camp, D.M., and Garland, T. Jr. (2006. Morphometry, ultrastructure, myosin isoforms, and metabolic capacities of the "mini muscles" favored by selection for high activity in house mice. *Comp. Biochem. Physiol. B* 144:271-282.

Guderley, H., Joanisse, D.R., Mokas, S., Bilodeau, G.M., and Garland, T. Jr. (2008). Altered fibre types in gastrocnemius muscle of high wheel-running selected mice with the mini-muscle phenotypes. *Comp. Biochem. Physiol. B* 149:490-500.

Haapasalo, H., Kontulainen, S., Sievänen, H., Kannus, P., Järvinen, M., and Vuori, I. (2000). Exercise-induced bone gain is due to enlargement in bone size without a change in volumetric bone density: a peripheral quantitative computed tomography study of the upper arms of male tennis players. *Bone* 27:351-357.

Hall, B.K., and Herring, S.W. (1990). Paralysis and growth of the musculoskeletal system in the embryonic chick. *J. Morphol.* 206:45-56.

Hamrick, M.W., Skedros, J.G., Pennington, C., and McNeil, P.L. (2006). Increased osteogenic response to exercise in metaphyseal versus diaphyseal cortical bone. *J. Musculoskelet. Neuronal Interact.* 6:258-263.

Hamrick, M.W., Della-Fera, M.A., Baile, C.A., Pollock, N.K., and Lewis, R.D. (2009). Body fat as a regulator of bone mass: experimental evidence from animal models. *Clinc. Rev. Bone Miner. Metab.* 7:224-229.

Han, Y., Cowin, S.C., Schaffler, M.B., and Weinbaum, S. (2004). Mechanotransduction and strain amplification in osteocyte cell processes. *Proc. Natl. Acad. Sci. U.S.A.* 101:16689-16694.

Hartl, D.L. (2001). Genetic management of outbred laboratory rodent populations. Wilmington, MA: Charles River Laboratories. Technical document.

Hartmann, J., Garland, T. Jr., Hannon, R.M., Kelly, S.A., Muñoz, G., and Pomp, D. (2008). Fine mapping of "mini-muscle," a recessive mutation causing reduced hind-limb muscle mass in mice. *J. Hered.* 99:679-687.

Havill, L.M., Mahaney, M.C., Binkley T.L., and Specker, B.L. (2007). Effects of genes, sex, age, and activity on BMC, bone size, and areal and volumetric BMD. *J. Bone Miner. Res.* 22:737-746.

Hetland, M.L., Haarbo, J., and Christiansen, C. (1993). Low bone mass and high bone turnover in male long distance runners. *J. Clin. Endocrinol. Metab.* 77:770-775.

Hibbeler, R.C. (1997). *Mechanics of Materials.* Upper Saddle River, NJ: Prentice Hall.

Hidaka, B.H. (2012). Depression as a disease of modernity: explanations for increasing prevalence. *J. Affect. Disord.* 140:205-214.

Hillam, R.A. (1996). Response of bone to mechanical load and alterations in circulating hormones. PhD dissertation. University of Bristol.

Hind, K., and Burrows, M. (2007). Weight-bearing exercise and bone mineral accrual in children and adolescents: a review of controlled trials. *Bone* 40:14-27.

Hoey, D.A., Chen, J.C., and Jacobs, C.R. (2012). The primary cilium as a novel extracellular sensor in bone. *Front. Endocrinol.* 3:75.

Holguin, N., Uzer, G., Chaing, F.-P., Rubin, C., and Judex, S. (2011). Brief daily exposure to low-intensity vibration mitigates the degradation of the intervertebral disc in a frequency-specific manner. *J. Appl. Physiol.* 111:1846-1853.

Holt, B.M. (2003). Mobility in Upper Paleolithic and Mesolithic Europe: evidence from the lower limb. *Am. J. Phys. Anthropol.* 122:200-215.

Houle-Leroy, P., Guderley, H., Swallow, J.G., and Garland, T. Jr. (2003). Artificial selection for high activity favors mighty mini-muscles in house mice. *Am. J. Physiol. Reg. Integr. Comp. Physiol.* 284:R433-R443.

Huang, C., and Ogawa, R. (2010). Mechanotransduction in bone repair and regeneration. *FASEB J.* 24:3625-3632.

Hung, C.T., Pollack, C.R., Reilly, T.M., and Brighton, C.T. (1995). Real-time calcium response of cultured bone cells to fluid flow. *Clin. Orthop. Relat. Res.* 265-269.

Idris, A.I., and Ralston, S.H. (2012). Role of cannabinoids in the regulation of bone remodeling. *Front. Endocrinol.* 3:136.

Jacobs, C.R., Temiyasathit, S., and Castillo, A.B. (2010). Osteocyte mechanobiology and pericellular mechanics. *Annu. Rev. Biomed. Eng.* 12:369-400.

Jepsen, K.J., Hu, B., Tommasini, S.M., Courtland, H.W., Price, C., Terranova, C.J., and Nadeau, J.H. (2007). Genetic randomization reveals functional relationships among morphologic and tissue-quality traits that contribute to bone strength and fragility. *Mamm. Genome* 18:492-507.

Joo, Y.I., Sone, T., Fukunaga, M., Lim, S.G., and Onodera, S. (2003). Effects of endurance exercise on three-dimensional trabecular bone microarchitecture in young growing rats. *Bone* 33:485-493.

Judex, S., and Zernicke, R.F. (2000a). High-impact exercise and growing bone: relation between high strain rates and enhanced bone formation. *J. Appl. Physiol.* 88:2183-2191.

Judex, S., and Zernicke, R.F. (2000b). Does the mechanical milieu associated with high-speed running lead to adaptive changes in diaphyseal growing bone? *Bone* 26:153-159.

Judex, S., and Carlson, K.J. (2009). Is bone's response to mechanical signals dominated by gravitational loading? *Med. Sci. Sports Exerc.* 41:2037-2043.

Judex, S., Gross, T.S., and Zernicke, R.F. (1997). Stain gradients correlate with sites of exercise-induced bone-forming surfaces in the adult skeleton. *J. Bone Miner. Res.* 12:1737-1745.

Judex, S., Donahue, L.R., and Rubin, C. (2002). Genetic predisposition to low bone mass is paralleled by an enhanced sensitivity to signals anabolic to the skeleton. *FASEB J.* 16:1280-1282.

Judex, S., Garman, R., Squire, M., Busa, B., Donahue, L.R., and Rubin, C. (2004a). Genetically linked site-specificity of disuse osteoporosis. *J. Bone Miner. Res.* 19:607-613.

Judex, S., Garman, R.A., Squire, M.E., Donahue, L.R., and Rubin, C.T. (2004b). Genetically based influences on the site-specific regulation of trabecular and cortical bone

morphology. *J. Bone Miner. Res.* 19:600-606.

Judex, S., Lei, X., Han, D., and Rubin, C. (2007). Low-magnitude mechanical signals that stimulate bone formation in the ovariectomized rat are dependent on the applied frequency but not on the strain magnitude. *J. Biomech.* 40:1333-1339.

Judex, S., Zhang, W., Donahue, L.R., and Ozcivici, E. (2013). Genetic loci that control the loss and regain of trabecular bone during unloading and reambulation. *J. Bone Miner. Res.* 28:1537-1549.

Jurmain, R., Cardoso, F.A., Henderson, C., and Villotte, S. (2012). Bioarchaeology's Holy Grail: the reconstruction of activity. In *A Companion to Paleopathology* (ed. A.L. Grauer), pp. 531-552. West Sussex: John Wiley and Sons.

Kaye, M., and Kusy, R.P. (1995). Genetic lineage, bone mass, and physical activity in mice. *Bone* 17:131-135.

Karsenty, G. (2003). The complexities of skeletal biology. *Nature* 423:316-318.

Karsenty, G., and Ferron, M. (2012). The contribution of bone to whole-organism physiology. *Nature* 481:314-320.

Keeney, B.K., Raichlen, D.A., Meek, T.H., Thomas, H., Wijeratne, R.S., Middleton, K.M., Gerdeman, G.L., and Garland, T. Jr. (2008). Differential response to a selective cannabinoid receptor antagonist (SR141716: rimonabant) in female mice from lines selectively bred for high voluntary wheel-running behavior. *Behav. Pharmacol.* 19:812-820.

Keeney, B.K., Meek, T.H., Middleton, K.M., Holness, L.F., and Garland, T. Jr. (2012). Sex differences in cannabinoid receptor-1 (CB1) pharmacology in mice selectively bred for high voluntary wheel-running behavior. *Pharmacol. Biochem. Behav.* 101:528-537.

Kelly, R.L. (1992). Mobility/sedentism: concepts, archaeological measures, and effects. *Annu. Rev. Anthropol.* 21:43-66.

Kelly, S.A., Czech, P.P., Wight, J.T., Blank, K.M., and Garland, T. Jr. (2006). Experimental evolution and phenotypic plasticity of hindlimb bones in high-activity house mice. *J. Morphol.* 267:360-374.

Kemp, T.J., Bachus, K.N., Nairn, J.A., and Carrier, D.R. (2005). Functional trade-offs in the limb bones of dogs selected for running versus fighting. *J. Exp. Biol.* 208:3475-3482.

Kennedy, G.E. (1985). Bone thickness in *Homo erectus*. *J. Hum. Evol.* 14:699-708.

Kesavan, C., Mohan, S., Oberholtzer, S., Wergedal, J.E., and Baylink, D.J. (2005). Mechanical loading-induced gene expression and BMD changes are different in two inbred mouse strains. *J. Appl. Physiol.* 99:1951-1957.

Kesavan, C., Mohan, S., Srivastava, A.K., Kapoor, S., Wergedal, J.E., Yu, H., and Baylink, D.J. (2006). Identification of genetic loci that regulate bone adaptive response to mechanical loading in C57BL/6J and C3H/HeJ mice intercross. *Bone* 39:634-643.

Klein-Nulend, J., Semeins, C.M., Ajubi, N.E., Nijweide, P.J., and Burger, E.H. (1995). Pulsating fluid flow increases nitric oxide (NO) synthesis by osteocytes but not periosteal fibroblasts—correlation with prostaglandin upregulation. *Biochem. Biophys. Res. Comm.* 217:640-648.

Koch, L.G., Green, C.L., Lee, A.D., Hornyak, J.E., Cicila, G.T., and Britton, S.L. (2005). Test of the principle of initial value in rat genetic models of exercise capacity. *Am. J. Regul. Integr. Comp. Physiol.* 288:R466-R472.

Kodama, Y., Dimai, H.P., Wergedal, J., Sheng, M., Malpe, R., Kutilek, S., Beamer, W., Donahue, L.R., Rosen, C., Baylink, D.J., and Farley, J. (1999). Cortical tibial bone volume in two strains of mice: effects of sciatic neurectomy and genetic regulation of bone response to mechanical loading. *Bone* 25:183-190.

Kodama, Y., Umemura, Y., Nagasawa, S., Beamer, W.G., Donahue, L.R., Rosen, C.R., Baylink, D.J., and Farley, J.R. (2000). Exercise and mechanical loading increase periosteal bone formation and whole bone strength in C57BL/6J mice but not C3H/Hej mice. *Calcif. Tissue Int.* 66:298-306.

Kondo, O., and Dodo, Y. (2002). Postcranial bones of the Neanderthal child of the burial No. 1. In *Neanderthal Burials: Excavations of the Dederiyeh Cave, Afrin, Syria* (eds. T. Akazawa and S. Muhesen), pp. 139-214. Kyoto: International Research Center for Japanese Studies.

Kriemler, S., Zahner, L., Puder, J.J., Braun-Fahrländer, C., Schindler, C., Farpour-Lambert, N.J., Kränzlin, M., and Rizzoli, R. (2008). Weight-bearing bones are more sensitive to physical exercise in boys than in girls during pre- and early puberty: a cross-sectional study. *Osteoporos. Int.* 19:1749-1758.

Kummer, B. (1959). *Bauprinzipien des Säugerskeletes.* Stuttgart: Georg Thieme Verlag.

Kummer, B. (1972). Biomechanics of bone: mechanical properties, functional structure, functional adaptation. In *Biomechanics: Its Foundations and Objectives* (eds. Y.C. Fung, N. Perrone, and M. Anliker), pp. 237-271. Englewood Cliffs, NJ: Prentice-Hall.

Kwon, R.Y., Hoey, D.A., and Jacobs, C.R. (2011). Mechanobiology of primary cilia. In *Cellular and Biomolecular Mechanics and Mechanobiology* (ed. A. Gefen), pp. 99-124. Heidelberg: SpringerLink.

Lambert, A., Puymerail, L., Chaumoitre, K., and Schmitt, A. (2013). Analyse fonctionnelle des adaptations osseuses du squelette post crânien au Néolithique en Provence. *Bull. Mém. Soc. Anthropol. Paris* DOI:10.1007/s13219-013-0083-9.

Lang, T., LeBlanc, A.D., Evans, H., Lu, Y., Genant, H., and Yu, A. (2004). Cortical and trabecular bone mineral loss from the spine and hip in long-duration space flight. *J. Bone Miner. Res.* 19:1006-1012.

Langier, P., Novikov, V., Elmann-Larsen, B., and Berger, G. (2000). Quantitative ultrasound imaging of the calcaneus: precision and variation during a 120-day bed rest. *Calcif. Tissue Int.* 66:16-21.

Lanyon, L.E. (1981). Locomotor loading and functional adaptation in limb bones. *Symp. Zool. Soc. Lond.* 48:305-329.

Lanyon, L.E. (1987). Functional strain in bone tissue as an objective, and controlling stimulus for adaptive bone remodeling. *J. Biomech.* 20:1083-1093.

Lanyon, L.E. (1993). Osteocytes, strain detection, bone modeling and remodeling. *Calcif. Tissue Int.* 53(Suppl 1):S102-S106.

Lanyon, L.E., and Rubin, C.T. (1984). Static vs dynamic loads as an influence on bone remodelling. *J. Biomech.* 17:897-906.

Lau, K.H.W., Kapur, S., Kesavan, C., and Baylink, D.J. (2006). Up-regulation of the Wnt, estrogen receptor, insulin-like growth factor-I, and bone morphogenetic protein pathways in C57BL/6J osteoblasts as opposed to C3H/HeJ osteoblasts in part contributes to the differential response to fluid shear. *J. Biol. Chem.* 281:9576-9588.

LeBlanc, A.D., Schneider, V.S., Evans, H.J., Engelbretson, D.A., and Krebs, JM. (1990). Bone mineral loss and recovery after 17 weeks of bed rest. *J. Bone Miner. Res.* 5:843-850.

Lee, N.K., and Karsenty, G. (2008). Reciprocal regulation of bone and energy metabolism. *Trends Endocrinol. Metab.* 19:161-166.

Lee, R.B., and DeVore, I. (1968). *Man the Hunter.* Chicago: Aldine.

Leppänen, O.V., Sievänen, H., Jokihaara, J., Pajamäki, I., Kannus, P., and Järvinen, T.L.N. (2008). Pathogenesis of age-related osteoporosis: impaired mechano-responsiveness of bone is not the culprit. *PLoS ONE* 3:e2540.

Leslie, W.D. (2012). Ethnic differences in bone mass—clinical implications. *J. Clin. Endocrinol. Metab.* 97:4329-4340.

Li, J.Z., Absher, D.M., Tang, H., Southwick, A.M., Casto, A.M., Ramachandran, S., Cann, H.M., Barsh, G.S., Feldman, M., Cavalli-Sforza, L.L., and Myers, R.M. (2008). Worldwide human relationships inferred from genome-wide patterns of variation. *Science* 319:1100-1104.

Li, K.C., Zernicke, R.F., Barnard, R.J., and Li, A.F.Y. (1991). Differential response of rat limb bones to strenuous exercise. *J. Appl. Physiol.* 70:554-560.

Lieberman, D.E. (1996). How and why humans grow thin skulls: experimental evidence for systemic cortical robusticity. *Am. J. Phys. Anthropol.* 101:217-236.

Lieberman, D.E. (1997). Making behavioral and phylogenetic inferences from hominid fossils: considering the developmental influences of mechanical forces. *Annu. Rev. Anthropol.* 26:185-210.

Lieberman, D.E. (2000). Comment on 'Activity, climate, and postcranial robusticity: implications for modern human origins and scenarios of adaptive change.' *Curr. Anthropol.* 41:594-595.

Lieberman, D.E., and Crompton, A.W. (1998). Responses of bone to stress: constraints on symmorphosis. In *Principles of Animal Design* (eds. E.R. Weibel, C.R. Taylor, and L. Bolis), pp. 78-86. Cambridge: Cambridge University Press.

Lieberman, D.E., and Pearson, O.M. (2001). Trade-off between modeling and remodeling responses to loading in the mammalian limb. *Bull. Mus. Comp. Zool.* 156:269-282.

Lieberman, D.E., Devlin, M.J., and Pearson, O.M. (2001). Articular surface area responses to mechanical loading: effects of exercise, age, and skeletal location. *Am. J. Phys. Anthropol.* 116:266-277.

Lieberman, D.E., Pearson, O.M., Polk, J.D., Demes, B., and Crompton, A.W. (2003). Optimization of bone growth and remodeling in response to loading in tapered mammalian limbs. *J. Exp. Biol.* 206:3125-3138.

Lieberman, D.E., Polk, J.D., and Demes, B. (2004). Predicting long bone loading from cross-sectional geometry. *Am. J. Phys. Anthropol.* 123:156-171.

Lieverse, A.R., Weber, A.W., Bazaliiskii, V.I., Goriunova, O.I., and Savel'ev, N.A. (2007). Osteoarthritis in Siberia's Cis-Baikal: skeletal indicators of hunter-gatherer adaptation and cultural change. *Am. J. Phys. Anthropol.* 132:1-16.

Lightfoot, J.T., Turner, M.J., Daves, M., Vordermark, A., and Kleeberger, S.R. (2004). Genetic influence on daily wheel running activity level. *Physiol. Genomics* 19:270-276.

Litzenberger, J.B., Kim, J.B., Tummala, P., and Jacobs, C.R. (2010). Beta1 integrins mediate mechanosensitive signaling pathways in osteocytes. *Calcif. Tissue Int.* 86:325-332.

Liu, D., Genetos, D.C., Shao, Y., Geist, D.J., Li, J., Ke, H.Z., Turner, C.H., and Duncan, R.L. (2008). Activation of extracellular-signal regulated kinase (ERK1/2) by fluid shear is Ca^{2+}- and ATP-dependent in MC3T3-E1 osteoblasts. *Bone* 42:644-652.

Liu, Y.-Z., Wilson, S.G., Wang, L., Liu, Y.-G., Guo, Y.-F., Li, J., Yan, H., Deloukas, P., Soranzo, N., Chinnapen-Horsley, U., Cervino, A., Williams, F.M., Xiong, D.-H., Zhang, Y.-P., Jin, T.-B., Levy, S., Papasian, C.J., Drees, B.M., Hamilton, J.J., Recker, R.R., Spector, T.D., and Deng, H.-W. (2008). Identification of *PLCL1* gene for hip bone size variation in females in a genome-wide association study. *PLoS ONE* 3:e3160.

Lovejoy, C.O., Meindl, R.S., Ohman, J.C., Heiple, K.G., and White, T.D. (2002). The Maka femur and its bearing on the antiquity of human walking: applying contemporary concepts of morphogenesis to the human fossil record. *Am. J. Phys. Anthropol.* 119:97-133.

Lovejoy, C.O., McCollum, M.A., Reno, P.L., and Rosenman, B.A. (2003). Developmental biology and human evolution. *Annu. Rev. Anthropol.* 32:85-109.

Lublinsky, S., Ozcivici, E., and Judex, S. (2007). An automated algorithm to detect the trabecular-cortical bone interface in micro-computed tomographic images. *Calcif. Tissue Int.* 81:285-293.

Luu, Y.K., Capilla, E., Rosen, C.H., Gilsanz, V., Pessin, J.E., Judex, S., and Rubin, C.T. (2009). Mechanical stimulation of mesenchymal stem cell proliferation and differentiation promotes osteogenesis while preventing dietary-induced obesity. *J. Bone Miner. Res.* 24:50-61.

Lynch, C.J. (1969). The so-called Swiss mouse. *Lab. Anim. Care* 19:214-220.

Ma, H., Torvinen, S., Silvennoinen, M., Rinnankoski-Tuikka, R., Kainulainen, H., Morko, J., Peng, Z., Kujala, U.M., Rahkila, P., and Suominen, H. (2010). Effects of diet-induced obesity and voluntary wheel running on bone properties in young male C57BL/6J mice. *Calcif. Tissue Int.* 86:411-419.

Ma, H., Turpeinen, T., Silvennoinen, M., Torvinen, S., Rinnankoski-Tuikka, R., Kainulainen, H., Timonen, J., Kujala, U.M., Rahkila, P., and Suominen, H. (2011). Effects of diet-induced obesity and voluntary wheel running on the microstructure of the murine distal femur. *Nutr. Metab.* 8:1.

Macdonald, H.M., Kontulainen, S.A., Khan, K.M., and McKay, H.A. (2007). Is a school-based physical activity intervention effective for increasing tibial bone strength in boys and girls? *J. Bone Miner. Res.* 22:434-446.

Macdonald, H.M., Ashe, M.C., and McKay, H.A. (2009). The link between physical activity and bone strength across the lifespan. *Int. J. Clin. Rheumatol.* 4:437-463.

MacDougall, J.D., Webber, C.E., Martin, J., Ormerod, S., Chesley, A., Younglai, E.V., Gordon, C.L., and Blimke, C.J.R. (1992). Relationship among running mileage, bone density, and serum testosterone in male runners. *J. Appl. Physiol.* 73:1165-1170.

Maggiano, I.S., Schultz, M., Kierdorf, H., Sosa, T.S., Maggiano, C.M., and Blos, V.T. (2008). Cross-sectional analysis of long bones, occupational activities and long-distance trade of

the Classic Maya from Xcambó—archaeological and osteological evidence. *Am. J. Phys. Anthropol.* 136:470-477.

Main, R.P. (2007). Ontogenetic relationships between in vivo strain environment, bone histomorphometry and growth in the goat radius. *J. Anat.* 210:272-293.

Malisch, J.L., Breuner, C.W., Gomes, F.R., Chappell, M.A., and Garland, T. Jr. (2008). Circadian pattern of total and free corticosterone concentrations, corticosteroid-binding globulin, and physical activity in mice selectively bred for high voluntary wheel-running behavior. *Gen. Comp. Endocrinol.* 156:210-217.

Malisch, J.L., Breuner, C.W., Kolb, E.M., Wada, H., Hannon, R.M., Chappell, M.A., Middleton, K.M., and Garland, T. Jr. (2009). Behavioral despair and home-cage activity in mice with chronically elevated baseline corticosterone concentrations. *Behav. Genet.* 39:192-201.

Manolagas, S.C., and Almeida, M. (2007). Gone with the Wnts: β-catenin, T-cell factor, forkhead box O, and oxidative stress in age-dependent diseases of bone, lipid, and glucose metabolism. *Mol. Endocrinol.* 21:2605-2614.

Marchi, D., Sparacello, V.S., Holt, B.M., and Formicola, V. (2006). Biomechanical approach to the reconstruction of activity patterns in Neolithic Western Liguria, Italy. *Am. J. Phys. Anthropol.* 131:447-455.

Marchi, D., Sparacello, V.S., and Shaw, C.N. (2011). Mobility and lower limb robusticity of a pastoralist Neolithic population from north-western Italy. In *Human Bioarchaeology of the Transition to Agriculture* (eds. R. Pinhasi and J.T. Stock), pp. 317-346. New York: Wiley-Blackwell.

Marsh, R.L., Ellerby, D.J., Carr, J.A., Henry, H.T., and Buchanan, C.I. (2004). Partitioning the energetics of walking and running: swinging the limbs is expensive. *Science* 303:80-83.

Martin, R.B., Burr, D.B., and Sharkey, N.A. (1998). *Skeletal Tissue Mechanics.* New York: Springer.

Matsuda, J.J., Zernicke, R.F., Vailas, A.C., Pedrini, V.A., Pedrini-Mille, A., and Maynard, J.A. (1986). Structural and mechanical adaptation of immature bone to strenuous exercise. *J. Appl. Physiol.* 60:2028-2034.

McKay, H.A. (2003). Lessons learned from school-based intervention trials: UBC Healthy Bones Studies. *J. Musculoskel. Neuronal Interact.* 3:341-344.

Meek, T.H., Eisenmann, J.C., and Garland, T. Jr. (2010). Western diet increases wheel running in mice selectively bred for high voluntary wheel running. *Int. J. Obesity* 34:960-969.

Mencej-Bedrač, S., Preželj, J., Komadina, R., Vindišar, F., and Marc, J. (2011). -1227C>T polymorphism in the *pleiotrophin* gene promoter influences bone mineral density in postmenopausal women. *Mol. Genet. Metabol.* 103:76-80.

Middleton, K.M., Shubin, C.E., Moore, D.C., Carter, P.A., Garland, T. Jr., and Swartz, S.M. (2008a). The relative importance of genetics and phenotypic plasticity in dictating bone morphology and mechanics in aged mice: evidence from an artificial selection experiment. *Zoology* 111:135-147.

Middleton, K.M., Kelly, S.A., and Garland, T. Jr. (2008b). Selective breeding as a tool to probe skeletal response to high voluntary locomotor activity in mice. *Integr. Comp. Biol.* 48:394-410.

Middleton, K.M., Goldstein, B.D., Gudun, P.R., Waters, J.F., Kelly, S.A., Swartz, S.M., and Garland, T. Jr. (2010). Variation in within-bone stiffness measured by nanoindentation in mice bred for high levels of voluntary wheel running. *J. Anat.* 216:121-131.

Morgan, T.J., Garland, T. Jr., and Carter, P.A. (2003). Ontogenies in mice selected for high voluntary wheel-running activity. I. Mean ontogenies. *Evolution* 57:646-657.

Mori, T., Okimoto, N., Sakai, A., Okazaki, Y., Nakura, N., Notomi, T., and Nakamura, T. (2003). Climbing exercise increases bone mass and trabecular bone turnover through transient regulation of marrow osteogenic and osteoclastogenic potentials in mice. *J. Bone Miner. Res.* 18:2002-2009.

Morimoto, N., Ponce de León, M.S., and Zollikofer, C.P.E. (2011). Exploring femoral diaphyseal shape variation in wild and captive chimpanzees by means of morphometric mapping: a test of Wolff's Law. *Anat. Rec.* 294:589-609.

Mosley, J.R., and Lanyon, L.E. (2002). Growth rate rather than gender determines the size of the adaptive response of the growing skeleton to mechanical strain. *Bone* 30:314-319.

Nehrenberg, D.L., Hua, K., Estrada-Smith, D., Garland, T. Jr., and Pomp, D. (2009). Voluntary exercise and its effects on body composition depend on genetic selection history. *Obesity* 17:1402-1409.

Newhall, K.M., Rodnick, K.J., van der Meulen, M.C., Carter, D.R., and Marcus, R. (1991). Effects of voluntary exercise on bone mineral content in rats. *J. Bone Miner. Res.* 6:289-296.

Nicolella, D.P., Moravits, D.E., Gale, A.M., Bonewald, L.F., and Lankford, J. (2006). Osteocyte lacunae tissue strain in cortical bone. *J. Biomech.* 39:1735-1743.

Nikander, R., Sievänen, H., Heinonen, A., Daly, R.M., Uusi-Rasi, K., and Kannus, P. (2010). Targeted exercise against osteoporosis: a systematic review and meta-analysis for optimising bone strength throughout life. *BMC Med.* 8:47.

Notomi, T., Okazaki, Y., Okimoto, N., Saitoh, S., Nakamura, T., and Suzuki, M. (2000). A comparison of resistance and aerobic training for mass, strength and turnover of bone in growing rats. *Eur. J. Appl. Physiol.* 83:469-474.

O'Connor, J.A., Lanyon, L.E., and MacFie, H. (1982). The influence of strain rate on adaptive bone remodelling. *J. Biomech.* 15:767-781.

Ohman, J.C., and Lovejoy, C.O. (2003). Asymmetry in the humeri of tennis players: 'Wolff's Law' or not? *Am. J. Phys. Anthropol.* S36:161.

O'Neill, M.C., and Dobson, S.D. (2008). The degree and pattern of phylogenetic signal in primate long-bone structure. *J. Hum. Evol.* 54:309-322.

Ozcivici, E., Luu, Y.K., Adler, B., Qin, Y.-X., Rubin, J., Judex, S., and Rubin, C.T. (2010). Mechanical signals as anabolic agents in bone. *Nat. Rev. Rheumatol.* 6:50-59.

Pahlavani, MA., and Vargas, D.M. (2000). Influence of aging and caloric restriction on activation of Ras/MAPK, calcineurin, and CaMK-IV activities in rat T cells. *Proc. Soc. Exp. Biol. Med.* 223:163-169.

Pauwels, F. (1965). *Gesammelte Abhandlungen zur funktionellen Anatomie des Bewegungsapparates.* Berlin: Springer-Verlag.

Pearson, O.M. (2000). Activity, climate, and postcranial robusticity: implications for modern human origins and scenarios of adaptive change. *Curr. Anthropol.* 41:569-607.

Pearson, O.M., and Lieberman, D.E. (2004). The aging of Wolff's "law": ontogeny and responses to mechanical loading in cortical bone. *Yearbook Phys. Anthropol.* 47:63-99.

Pigliucci, M., Murren, C.J., and Schlichting, C.D. (2006). Phenotypic plasticity and evolution by genetic assimilation. *J. Exp. Biol.* 209:2362-2367.

Plochocki, J.H., Rivera, J.P., Zhang, C., and Ebba, S.A. (2008). Bone modeling response to voluntary exercise in the hindlimb of mice. *J. Morphol.* 269:313-318.

Preston, H.M. (2009). Effects of exercise and genetic strain on bone strength, musculoskeletal gene expression and activity levels in C57BL/6J and DBA/2J adult female mice. PhD dissertation. Pennsylvania State University.

Preuschoft, H. (1973). Functional anatomy of the upper extremity. *The Chimpanzee* 6:34-120.

Price, C., Herman, B.C., Lufkin, T., Goldman, H.M., and Jepsen, K.J. (2005). Genetic variation in bone growth patterns defines adult mouse bone fragility. *J. Bone Miner. Res.* 20:1983-1991.

Price, T.D., Quarnstrom, A., and Irwin, D.E. (2003). The role of phenotypic plasticity in driving genetic evolution. *Proc. R. Soc. Lond. B* 270:1433-1440.

Qin, X.-Y., Rubin, C.T., and McLeod, K.J. (1998). Nonlinear dependence of loading intensity and cycle number in the maintenance of bone mass and morphology. *J. Orthop. Res.* 16:482-489.

Raichlen, D.A., and Polk, J.D. (2013). Linking brains and brawn: exercise and the evolution of human neurobiology. *Proc. Roy. Soc. B* 280:20122250.

Raichlen, D.A., Foster, A.D., Gerdeman, G.L., Seillier, A., and Giuffrida, A. (2012). Wired to run: exercise-induced endocannabinoid signaling in humans and cursorial mammals and the evolution of the runner's high. *J. Exp. Biol.* 215:1331-1336.

Raichlen, D.A., Foster, A.D., Seillier, A., Giuffrida, A., and Gerdeman, G.L. (2013). Exercise-induced endocannabinoid signaling is modulated by intensity. *Eur. J. Appl. Physiol.* 113:869-875.

Ralston, S.H. (2010). Genetics of osteoporosis. *Ann. N.Y. Acad. Sci.* 1192:181-189.

Rawlinson, S.C.F., El Haj, A.J., Minter, S.L., Tavares, I.A., Bennett, A., and Lanyon, L.E. (1991). Loading-related increases in prostaglandin production in cores of adult canine cancellous bone in vitro: a role for prostacyclin in adaptive bone remodeling? *J. Bone Miner. Res.* 6:1345-1351.

Rawlinson, S.C.F., Mosley, J.R., Suswillo, R.F.L., Pitsillides, A.A., and Lanyon, L.E. (1995). Calvarial and limb bone cells in organ and monolayer culture do not show the same early responses to dynamic mechanical strain. *J. Bone Miner. Res.* 10:1225-1232.

Reich, D., Thangaraj, K., Patterson, N., Price, A.L., and Singh, L. (2009). Reconstructing Indian population history. *Nature* 461:489-494.

Rhodes, J.S., Gammie, S.C., and Garland, T. Jr. (2005). Neurobiology of mice selected for high voluntary wheel-running activity. *Integr. Comp. Biol.* 45:438-455.

Rice, M.C., and O'Brien, S.J. (1980). Genetic variance of laboratory outbred Swiss mice. *Nature* 283:157-161.

Richards, J.B., Zheng, H.-F., and Spector, T.D. (2012). Genetics of osteoporosis from genome-wide association studies: advances and challenges. *Nat. Rev. Genet.* 13:577-588.

Riddle, R.C., and Donahue, H.J. (2009). From streaming potentials to shear stress: 25 years of bone cell mechanotransduction. *J. Orthop. Res.* 27:143-149.

Riskin, D.K., Bahlman, J.W., Hubel, T.Y., Ratcliffe, J.M., Kunz, T.H., and Swartz, S.M. (2009). Bats go head-under-heels: the biomechanics of landing on a ceiling. *J. Exp. Biol.* 212:945-953.

Robbins, G. (2007). Population dynamics, growth and development in Chalcolithic sites of the Deccan Peninsula, India. PhD dissertation. University of Oregon.

Robling, A.G., and Turner, C.H. (2002). Mechanotransduction in bone: genetic effects on mechanosensitivity in mice. *Bone* 31:562-569.

Robling, A.G., Li, J., Shultz, K.L., Beamer, W.G., and Turner, C.H. (2003). Evidence for a skeletal mechanosensitivity gene on mouse chromosome 4. *FASEB J.* 17:324-326.

Robling, A.G., Warden, S.J., Shultz, K.L., Beamer, W.G., and Turner, C.H. (2007). Genetic effects on bone mechanotransduction in congenic mice harboring bone size and strength quantitative trait loci. *J. Bone Miner. Res.* 22:984-991.

Roux, W. (1881). *Der Kampf der Theile im Organismus.* Leipzig: Verlag von Wilhelm Engelmann.

Rubin, C.T. (1984). Skeletal strain and the functional significance of bone architecture. *Calcif. Tissue Int.* 36:S11-S18.

Rubin, C.T., and Lanyon, L.E. (1982). Limb mechanics as a function of speed and gait: a study of functional strains in the radius and tibia of horse and dog. *J. Exp. Biol.* 101:187-211.

Rubin, C.T., and Lanyon, LE. (1984a). Regulation of bone formation by applied dynamic loads. *J. Bone Jt. Surg.* 66A:397-402.

Rubin, C.T., and Lanyon, L.E. (1984b). Dynamic strain similarity in vertebrates: an alternative to allometric limb bone scaling. *J. Theor. Biol.* 107:321-327.

Rubin, C.T., and Lanyon, L.E. (1985). Regulation of bone mass by mechanical strain magnitude. *Calcif. Tissue Int.* 37:411-417.

Rubin, C.T., Bain, S.D., and McLeod, K.J. (1992). Suppression of the osteogenic response in the aging skeleton. *Calcif. Tissue Int.* 50:306-313.

Rubin, C.T., Sommerfeldt, D.W., Judex, S., and Qin, Y.-X. (2001a). Inhibition of osteopenia by low magnitude, high-frequency mechanical stimuli. *Drug Discovery Today* 6:848-858.

Rubin, C., Turner, A.S., Bain, S., Mallinckrodt, C., and McLeod, K. (2001b). Anabolism: low mechanical signals strengthen long bones. *Nature* 412:603-604.

Rubin, C., Turner, A.S., Mallinckrodt, C., Jerome, C., McLeod, K., and Bain, S. (2001c). Mechanical strain, induced noninvasively in the high-frequency domain, is anabolic to cancellous bone, but not cortical bone. *Bone* 30:445-452.

Rubin, C., Xu, G., and Judex, S. (2001d). The anabolic activity of bone tissue, suppressed by disuse, is normalized by brief exposure to extremely low magnitude mechanical stimuli. *FASEB J.* 15:2225-2229.

Rubin, C.T., Recker, R., Raab, D., Ryaby, J., McCabe, J., and McLeod, K.J. (2004). Prevention of post-menopausal bone loss by a low-magnitude, high-frequency mechanical stimuli: a clinical trial assessing compliance, efficacy and safety. *J. Bone Miner. Res.* 19:343-351.

Rubin, C.T., Seeherman, H., Qin, Y.-X., and Gross, T.S. (2013). The mechanical consequences of load bearing in the equine third metacarpal across speed and gait: the nonuniform distributions of normal strain, shear strain, and strain energy density. *FASEB J.* 27:1887-1894.

Rubin, J., Rubin, C., and Jacobs, C.R. (2006). Molecular pathways mediating mechanical signaling in bone. *Gene* 367:1-16.

Rubin, J., Schwartz, Z., Boyan, B.D., Fan, X., Case, N., Sen, B., Drab, M., Smith, D., Aleman, M., Wong, K.L., Yao, H., Jo, H., and Gross, T.S. (2007). Caveolin-1 knockout mice have increased bone size and stiffness. *J. Bone Miner. Res.* 22:1408-1418.

Ruff, C.B. (2005). Mechanical determinants of bone form: insights from skeletal remains. *J. Musculoskelet. Neuronal Interact.* 5:202-212.

Ruff, C.B., Larsen, C.S., and Hayes, W.C. (1984). Structural changes in the femur with the transition to agriculture on the Georgia coast. *Am. J. Phys. Anthropol.* 64:124-136.

Ruff, C.B., Trinkaus, E., Walker, A., and Larsen, C.S. (1993). Postcranial robusticity in *Homo*. I: temporal trends and mechanical interpretation. *Am. J. Phys. Anthropol.* 91:21-53.

Ruff, C.B., Walker, A., and Trinkaus, E. (1994). Postcranial robusticity in *Homo*. III: ontogeny. *Am. J. Phys. Anthropol.* 93:35-54.

Ruff, C.B., Holt, B., and Trinkaus, E. (2006). Who's afraid of the big bad Wolff?: "Wolff's Law" and bone functional adaptation. *Am. J. Phys. Anthropol.* 129:484-498.

Saxon, L.K., Jackson, B.F., Sugiyama, T., Lanyon, L.E., and Price, J.S. (2011). Analysis of multiple bone responses to graded strains above functional levels, and to disuse, in mice *in vivo* show that the human Lrp5 G171V High Bone Mass mutation increases the osteogenic response to loading but that lack of Lrp5 activity reduces it. *Bone* 49:184-193.

Schmitt, D., Zumwalt, A.C., and Hamrick, M.W. (2010). The relationship between bone mechanical properties and ground reaction forces in normal and hypermuscular mice. *J. Exp. Zool.* 313A:339–351.

Scofield, K.L., and Hecht, S. (2012). Bone health in endurance athletes: runners, cyclists, and swimmers. *Curr. Sports Med. Rep.* 11:328-334.

Shackelford, L.L. (2007). Regional variation in the postcranial robusticity of late Upper Paleolithic humans. *Am. J. Phys. Anthropol.* 133:655-668.

Shaw, C.N., and Stock, J.T. (2009). Intensity, repetitiveness, and directionality of habitual adolescent mobility patterns influence the tibial diaphysis morphology of athletes. *Am. J. Phys. Anthropol.* 140:149-159.

Shaw, C.N., and Stock, J.T. (2013). Extreme mobility in the Late Pleistocene? Comparing limb biomechanics among fossil *Homo*, varsity athletes and Holocene foragers. *J. Hum. Evol.* 64:242-249.

Simons, K., and Toomre, D. (2000). Lipid rafts and signal transduction. *Nat. Rev. Mol. Cell. Biol.* 1:31-39.

Skedros, J.G. (2012). Interpreting load history in limb-bone diaphysis: important considerations and their biomechanical foundations. In *Bone Histology: An Anthropological Perspective* (eds. C. Crowder and S. Stout), pp. 153-220. Boca Raton: CRC Press.

Sládek, V., Berner, M., and Sailer, R. (2006). Mobility in Central European Late Eneolithic and Early Bronze Age: tibial cross-sectional geometry. *J. Archaeol. Sci.* 33:470-482.

Smith, F.H., Falsetti, A.B., and Donnelly, S.M. (1989). Modern human origins. *Yearbook Phys. Anthropol.* 32:35-68.

Snow-Harter, C., Bouxsein, M.L., Lewis, B.T., Carter, D.R., and Marcus, R. (1992). Effects of resistance and endurance exercise on bone mineral status of young women: a randomized exercise intervention trial. *J. Bone Miner. Res.* 7:761-769.

Squire, M., Donahue, L.R., Rubin, C., and Judex, S. (2004). Genetic variations that regulate bone morphology in the male mouse skeleton do not define its susceptibility to mechanical unloading. *Bone* 35:1353-1360.

Srinivasan, S., Agans, S.C., King, K.A., Moy, N.Y., Poliachik, S.L., and Gross, T.S. (2003). Enabling bone formation in the aged skeleton via rest-inserted mechanical loading. *Bone* 33:946-955.

Srinivasan, S., Ausk, B.J., Poliachik, S.L., Warner, S.E., Richardson, T.S., and Gross, T.S. (2007). Rest-inserted loading rapidly amplifies the response of bone to small increases in strain and load cycles. *J. Appl. Physiol.* 102:1945-1952.

Srinivasan, S., Ausk, B.J., Prasad, J., Threet, D., Bain, S.D., Richardson, T.S., and Gross, T.S. (2010). Rescuing loading induced bone formation at senescence. *PLoS Comp. Biol.* 6:e1000924.

Srinivasan, S., Gross, T.S., and Bain, S.D. (2012). Bone mechanotransduction may require augmentation in order to strengthen the senescent skeleton. *Aging Res. Rev.* 11:353-360.

Stock, J.T., Bazaliiskii, V.I., Goriunova, O.I., Savel'ev, N.A., and Weber, A.W. (2010). Skeletal morphology, climatic adaptation, and habitual behavior among mid-Holocene Cis-Baikal populations. In *Prehistoric Hunter-Gatherers of the Baikal Region, Siberia: Bioarchaeological Studies of Past Life Ways* (eds. A. Weber, M.A. Katzenberg, and T.G. Schurr), pp. 193-216. Philadelphia: University of Pennsylvania Museum of Archaeology and Anthropology.

Stock, J.T., O'Neill, M.C., Ruff, C.B., Zabecki, M., Shackelford, L., and Rose, J.C. (2011). Body size, skeletal biomechanics, mobility and habitual activity from the Late Palaeolithic to the mid-Dynastic Nile Valley. In *Human Bioarchaeology of the Transition to Agriculture* (eds. R. Pinhasi and J.T. Stock), pp. 347-367. New York: Wiley-Blackwell.

Styrkarsdottir, U., Halldorsson, B.V., Gudbjartsson, D.F., Tang, N.L., Koh, J.M., Xiao, S.M., Kwok, T.C., Kim, G.S., Chan, J.C., Cherny, S., Lee, S.H., Kwok, A., Ho, S., Gretarsdottir, S., Kostic, J.P., Palsson, S.T., Sigurdsson, G., Sham, P.C., Kim, B.J., Kung, A.W., Kim, S.Y., Woo, J., Leung, P.C., Kong, A., Thorsteinsdottir, U., and Stefansson, K. (2010). European bone mineral density loci are also associated with BMD in East-Asian populations. *PLoS ONE* 5:e13217.

Sugiyama, T., Meakin, L.B., Browne, W.J., Galea, G.L., Price, J.S., and Lanyon, L.E. (2012). Bones' adaptive response to mechanical loading is essentially linear between the low strains associated with disuse and the high strains associated with the lamellar/woven bone transition. *J. Bone Miner. Res.* 27:1784-1793.

Suuriniemi, M., Mahonen, A., Kovanen, V., Alén, M., Lyytikäinen, A., Wang, Q., Kröger, H., and Cheng, S. (2004). Association between exercise and pubertal BMD is modulated by estrogen receptor α genotype. *J. Bone Miner. Res.* 19:1758-1765.

Suuriniemi, M., Souminen, H., Mahonen, A., Alen, M., and Cheng, S. (2007). Estrogen receptor alpha polymorphism modifies the association between childhood exercise and bone mass: follow-up study. *Pediatr. Exerc. Sci.* 19:444-458.

Swallow, J.G., Carter, P.A., and Garland, T. Jr. (1998). Artificial selection for increased wheel-running behavior in house mice. *Behav. Genet.* 28:227-237.

Swallow, J.G., Koteja, P., Carter, P.A., and Garland, T. Jr. (1999). Artificial selection for increased wheel-running activity in house mice results in decreased body mass at maturity. *J. Exp. Biol.* 202:2513-2520.

Swallow, J.G., Koteja, P., Carter, P.A., and Garland, T. Jr. (2001). Food consumption and body composition in mice selected for high wheel-running activity. *J. Comp. Physiol. B* 171:651-659.

Swallow, J.G., Hayes, J.P., Koteja, P., and Garland, T. Jr. (2009). Selection experiments and experimental evolution of performance and physiology. In *Experimental Evolution: Concepts, Methods, and Applications of Selection Experiments* (eds. T. Garland Jr. and M.R. Rose), pp. 301-351. Berkeley: University of California Press.

Syme, D.A., Evashuk, K., Grintuch, B., Rezende, E.L., and Garland, T. Jr. (2005). Contractile abilities of normal and "mini" triceps surae muscles from mice (*Mus domesticus*) selectively bred for high voluntary wheel running. *J. Appl. Physiol.* 99:1308-1316.

Tajima, O., Ashizawa, N., Ishii, T., Amagai, H., Mashimo, T., Liu, L.J., Saitoh, S., Tokuyama, K., and Suzuki, M. (2000). Interaction of the effects between vitamin D receptor polymorphism and exercise training on bone metabolism. *J. Appl. Physiol.* 88:1271-1276.

Thompson, J.N. (2013). *Relentless Evolution.* Chicago: University of Chicago Press.

Thompson, W.R., Rubin, C.T., and Rubin, J. (2012). Mechanical regulation of signaling pathways in bone. *Gene* 503:179-193.

Tommasini, S.M., Nasser, P., Hu, B., and Jepsen, K.J. (2008). Biological coadaptation of morphological and composition traits contributes to mechanical functionality and skeletal fragility. J. Bone Miner. Res. 23:236-246.

Trinkaus, E. (1997). Appendicular robusticity and the paleobiology of modern human emergence. *Proc. Natl. Acad. Sci. U.S.A.* 94:13367-13373.

Trinkaus, E., and Ruff, C. (1996). Early modern human remains from eastern Asia: the Yamashita-cho 1 immature postcrania. *J. Hum. Evol.* 30:299-314.

Trinkaus, E., Churchill, S.E., Villemeur, I., Riley, K.G., Heller, J.A., and Ruff, C.B. (1991). Robusticity *versus* shape: the functional interpretation of Neandertal appendicular morphology. *J. Anthropol. Soc. Nippon* 99:257-278.

Trinkaus, E., Churchill, S.E., and Ruff, C.B. (1994). Postcranial robusticity in *Homo*. II: humeral bilateral asymmetry and bone plasticity. *Am. J. Phys. Anthropol.* 93:1-34.

Trinkaus, E., Ruff, C.B., Churchill, S.E., and Vandermeersch, B. (1998). Locomotion and body proportions of the Saint-Césaire 1 Châtelperronian Neandertal. *Proc. Natl. Acad. Sci. U.S.A.* 95:5836-5840.

Trinkaus, E., Stringer, C.B., Ruff, C.B., Hennessy, R.J., Roberts, M.B., and Parfitt, S.A. (1999). Diaphyseal cross-sectional geometry of the Boxgrove 1 Middle Pleistocene human tibia. *J. Hum. Evol.* 37:1-25.

Trinkaus, E., Ruff, C.B., Esteves, F., Santos Coelho, J.M., Silva, M., and Mendença, M. (2002). The lower limb remains. In *Portrait of the Artist as a Young Child* (eds. J. Zilhão and E. Trinkaus), pp. 435-465. Lisbon: Instituto Português de Arqueología.

Turner, CH., and Burr, D.B. (1993). Basic biomechanical measurements of bone: a tutorial. *Bone* 14:595-608.

Turner, C.H., and Pavalko, F.M. (1998). Mechanotransduction and functional response of the skeleton to physical stress: the mechanisms and mechanics of bone adaptation. *J. Orthop. Sci.* 3:346-355.

Turner, C.H., Takano, Y., and Owan, I. (1995). Aging changes mechanical loading thresholds for bone formation in rats. *J. Bone Miner. Res.* 10:1544-1549.

Turner, C.H., Takano, Y., Owan, I., and Murrell, G.A. (1996). Nitric oxide inhibitor L-NAME suppresses mechanically induced bone formation in rats. *Am. J. Physiol.* 270:E634-E639.

Umemura, Y., Baylink, D.J., Wergedal, J.E., Mohan, S., and Srivastava, A.K. (2002). A time course of bone response to jump exercise in C57BL/6J mice. *J. Bone Miner. Metab.* 20:209-215.

Vaanholt, L.M., Meerlo, P., Garland, T. Jr., Visser, G.H., and van Dijk, G. (2007). Plasma adiponectin is increased in mice selectively bred for high wheel-running activity, but not by wheel running *per se*. *Horm. Metab. Res.* 39:377-383.

Vaanholt, L.M., Jonas, I., Doornbos, M., Schubert, K.A., Nyakas, C., Garland, T. Jr., Visser, G.H., and van Dijk, G. (2008). Metabolic and behavioral responses to high-fat feeding in mice selectively bred for high wheel-running activity. *Int. J. Obes.* 32:1566-1575.

Vicente, W.S., dos Reis, L.M., Graciolli, R.G., Graciolli, F.G., Dominguez, W.V., Wang, C.C., Fonseca, T.L., Velosa, A.P., Roschel, H., Teodoro, W.R., Gualano, B., and Jorgetti, V. (2013). Bone plasticity in response to exercise is sex-dependent in rats. *PLoS ONE* 8:e64725.

Vico, L., Collet, P., Guignandon, A., Lafage-Proust, M.H., Thomas, T., Rehailia, M., and Alexandre, C. (2000). Effects of long-term microgravity exposure on cancellous and cortical weight-bearing bones of cosmonauts. *Lancet* 355:1607-1611.

Villotte, S., Churchill, S.E., Dutour, O., and Henry-Gambier, D. (2010). Subsistence activities and the sexual division of labor in the European Upper Paleolithic and Mesolithic: evidence from upper limb enthesopathies. *J. Hum. Evol.* 59:35-43.

Vinyard, C.J., and Payseur, B.A. (2008). Of "mice" and mammals: utilizing classical inbred mice to study the genetic architecture of function and performance in mammals. *Integr. Comp. Biol.* 48:324-337.

Waddington, C.H. (1961). Genetic assimilation. *Adv. Genet.* 10:257-290.

Wagner, H., Melhus, H., Pedersen, N.L., and Michaëlsson, K. (2013). Genetic influence on bone phenotypes and body composition: a Swedish twin study. *J. Bone Miner. Metab.* 31:681-689.

Wallace, I.J., and Shea, J.J. (2006). Mobility patterns and core technologies in the Middle Paleolithic of the Levant. *J. Archaeol. Sci.* 33:1293-1309.

Wallace, I.J., and Demes, B. (2008). Symmetrical gaits of *Cebus apella*: implications for the functional significance of diagonal sequence gait in primates. *J. Hum. Evol.* 54:783-794.

Wallace, I.J., Middleton, K.M., Lublinsky, S., Kelly, S.A., Judex, S., Garland, T. Jr., and Demes, B. (2010). Functional significance of genetic variation underlying limb bone diaphyseal structure. *Am. J. Phys. Anthropol.* 143:21-31.

Wallace, I.J., Garland, T. Jr., Wallace, S.A., Middleton, K.M., Kelly, S.A., Judex, S., and Demes, B. (2011). Genetic and epigenetic effects on diaphyseal morphology in selectively bred mice with the mini-muscle allele. *Integr. Comp. Biol.* 51(Suppl 1):e263.

Wallace, I.J., Tommasini, S.M., Judex, S., Garland, T. Jr., and Demes, B. (2012). Genetic variations and physical activity as determinants of limb bone morphology: an experimental approach using a mouse model. *Am. J. Phys. Anthropol.* 148:24-35.

Wallace, I.J., Kwaczala, A.T., Judex, S., Demes, B., and Carlson, K.J. (2013). Physical activity engendering loads from diverse directions augments the growing skeleton. *J. Musculoskelet. Neuronal Interact.* 13:245-250.

Wallace, J.M., Rajachar, R.M., Allen, M.R., Bloomfield, S.A., Robey, P.G., Young, M.F., and Kohn, D.H. (2007). Exercise-induced changes in the cortical bone of growing mice are bone- and gender-specific. *Bone* 40:1120-1127.

Wang, N., Butler, J.P., and Ingber, D.E. (1993). Mechanotransduction across the cell surface and through the cytoskeleton. *Science* 260:1124-1127.

Wang, Y.L., McNamara, L.M., Schaffler, M.B., and Weinbaum, S. (2007). A model for the role of integrins in flow induced mechanotransduction in osteocytes. *Proc. Natl. Acad. Sci. U.S.A.* 104:15941-15946.

Ward, K., Alsop, C., Brown, S., Caulton, J., Rubin, C., Adams, J., and Mughal, M. (2004). Low magnitude mechanical loading is osteogenic in children with disabling conditions. *J. Bone Miner. Res.* 19:360-369.

Washburn, S.L. (1983). Evolution of a teacher. *Annu. Rev. Anthropol.* 12:1-24.

Weeks, B.K., Young, C.M., and Beck, B.R. (2008). Eight months of regular in-school jumping improves indices of bone strength in adolescent boys and girls: the POWER PE study. *J. Bone Miner. Res.* 23:1002-1011.

Wesselius, A., Bours, M.J., Agrawal, A., Gartland, A., Dagnelie, P.C., Schwarz, P., and Jørgensen, N.R. (2011). Role of purinergic receptor polymorphisms in human bone. *Front. Biosci.* 16:2572-2585.

West-Eberhard, M.J. (2003). *Developmental Plasticity and Evolution.* Oxford: Oxford University Press.

Wetzsteon, R.J., Zemel, B.S., Shults, J., Howard, K.M., Kibe, L.W., and Leonard, M.B. (2011). Mechanical loads and cortical bone geometry in healthy children and young adults. *Bone* 48:1103-1108.

Wickler, S.J., Hoyt, D.F., Clayton, H.M., Mullineaux, D.R., Cogger, E.A., Sandoval, E., McGuire, R., and Lopez, C. (2004). Energetic and kinematic consequences of weighting the distal limb. *Equine Vet. J.* 8:772-777.

Williams, E., and Scott, J.P. (1954). The development of social behavior patterns in the mouse, in relation to natural periods. *Behaviour* 6:35-64**.**

Willie, B.M., Birkhold, A.I., Razi, H., Thiele, T., Aido, M., Kruck, B., Schill, A., Checa, S., Main, R.P., and Duda, G.N. (2013). Diminished response to in vivo mechanical loading in trabecular and not cortical bone in adulthood of female C57Bl/6 mice coincides with a reduction in deformation to load. *Bone* 55:335-346.

Winters-Stone, K.M., and Snow, C.M. (2003). Musculoskeletal response to exercise is greatest in women with low initial values. *Med. Sci. Sports Exerc.* 35:1691-1696.

Wolff, J. (1892). *Das Gesetz der Transformation der Knochen*. Berlin: A. Hirschwald.

Woo, S.L.Y., Kuei, S.C., Amiel, D., Gomez, M.A., Hayes, W.C., White, F.C., and Akeson, W.H. (1981). The effect of prolonged physical training on the properties of long bone: a study of Wolff's Law. *J. Bone Jt. Surg.* 63A:780-787.

Wrangham, R. (2009). *Catching Fire: How Cooking Made Us Human.* New York: Basic Books.

Wren, T.A.L., Lee, D.C., Hara, R., Rethlefsen, S.A., Kay, R.M., Dorey, F.J., and Gilsanz, V. (2010). Effect of high frequency, low magnitude vibration on bone and muscle in children with cerebral palsy. *J. Pediatr. Orthop.* 30:732-738.

Wu, J., Wang, X.X., Takasaki, M., Ohta, A., Higuchi, M., and Ishimi, Y. (2001). Cooperative effects of exercise training and genistein administration on bone mass in ovariectomized mice. *J. Bone Miner. Res.* 16:1829-1836.

Wu, J., Wang, X.X., Higuchi, M., Yamada, K., and Ishimi, Y. (2004). High bone mass gained by exercise in growing male mice is increased by subsequent reduced exercise. *J. Appl. Physiol.* 97:806-810.

Xie, L., Jacobson, J.M., Choi, E.S., Busa, B., Donahue, L.R., Miller, L.M., Rubin, C.T., and Judex, S. (2006). Low-level mechanical vibrations can influence bone resorption and bone formation in the growing skeleton. *Bone* 39:1059-1066.

Yalcin, B., and Flint, J. (2012). Association studies in outbred mice in a new era of full-genome sequencing. *Mamm. Genome* 23:719-726.

Yalcin B, Nicod J, Bhomra A, Davidson S, Cleak J, Farinelli L, Østerås M, Whitley A, Yuan W, Gan X, Goodson M, Klenerman P, Satpathy A, Mathis D, Benoist C, Adams DJ, Mott R, Flint J. (2010). Commercially available outbred mice for genome-wide association studies. *PLoS Genet.* 6:e1001085.

Yamada, H. (1970). *Strength of Biological Materials.* Baltimore: Williams and Wilkins.

Yellowley, C.E., Li, Z., Zhou, Z., Jacobs, C.R., and Donahue, H.J. (2000). Functional gap junctions between osteocytic and osteoblastic cells. *J. Bone Miner. Res.* 15:209-217.

Yingling, V.R., Davies, S., and Silva, M.J. (2001). The effects of repetitive physiologic loading on bone turnover and mechanical properties in adult female and male rats. *Calcif. Tissue Int.* 68:235-239.

Young, N.M., Hallgrímsson, B., and Garland, T. Jr. (2009). Epigenetic effects on integration of limb lengths in a mouse model: selective breeding for high voluntary locomotor activity. *Evol. Biol.* 36:88-99.

Zhong, N., Garman, R.A., Squire, M.E., Donahue, L.R., Rubin, C.T., Hadjiargyrou, M., and Judex, S. (2005). Gene expression patterns in bone after 4 days of hind-limb unloading in two inbred strains of mice. *Aviat. Space Environ. Med.* 76:530-535.

Zumwalt, A.C., Hamrick, M., and Schmitt, D. (2006). Force plate for measuring the ground reaction forces in small animal locomotion. *J. Biomech.* 39:2877-2881.

Appendix

Table A.1. Means and standard deviations for bone traits across the entire sample in Chapter 2.

| | Control lines | | | | High-Runner lines | | | | Mini-Muscle | | | |
| | Sedentary | | Active | | Sedentary | | Active | | Normal | | Mini | |
Trait	Mean	SD	Mean	SD	Mean	SD	Mean	SD	Mean	SD	Mean	SD
Diaphyseal cortical												
Ps.Ar	1.88	0.15	1.92	0.15	1.94	0.20	1.94	0.20	1.94	0.16	1.75	0.24
Ec.Ar	0.71	0.11	0.80	0.08	0.86	0.13	0.94	0.15	0.82	0.14	0.87	0.20
Ct.Ar	1.17	0.10	1.12	0.13	1.08	0.16	1.00	0.12	1.12	0.13	0.88	0.09
Ct.Th	0.308	0.027	0.284	0.035	0.272	0.043	0.242	0.028	0.283	0.037	0.224	0.027
J	0.496	0.078	0.501	0.087	0.498	0.108	0.466	0.092	0.505	0.081	0.375	0.083
TMD	1128	23	1122	28	1114	22	1108	18	1119	23	1110	26
Metaphyseal cortical												
Ps.Ar	2.67	0.26	2.75	0.23	2.74	0.31	2.75	0.33	2.75	0.28	2.58	0.22
Ec.Ar	1.67	0.23	1.82	0.20	1.85	0.26	1.90	0.28	1.81	0.26	1.78	0.21
Ct.Ar	1.00	0.07	0.93	0.08	0.89	0.07	0.85	0.07	0.93	0.08	0.79	0.03
Ct.Th	0.150	0.013	0.133	0.011	0.126	0.012	0.115	0.010	0.133	0.016	0.113	0.008
J	0.799	0.117	0.753	0.113	0.695	0.126	0.652	0.121	0.746	0.121	0.560	0.052
TMD	1050	21	1034	21	1022	22	1016	25	1033	25	1013	20
Metaphyseal trabecular												
BV/TV	10.7	3.8	9.3	3.9	8.8	2.6	10.2	4.1	10.0	3.6	8.0	4.2
Tb.N	4.4	0.9	4.1	0.7	4.3	0.8	4.4	1.0	4.3	0.8	4.3	1.1
Tb.Th	45.8	3.0	43.7	3.2	41.5	3.3	41.7	2.3	43.6	3.3	39.2	1.5
Tb.Sp	236	61	248	44	244	55	238	63	240	53	250	76
TMD	853	20	857	21	839	20	843	19	851	19	827	22

Ps.Ar = periosteal area (mm^2); Ec.Ar = endocortical area (mm^2); Ct.Ar = cortical area (mm^2); Ct.Th = cortical thickness (mm); J = polar moment of area (mm^4);

TMD = tissue mineral density (mg HA/cm^3); BV/TV = bone volume fraction (%); Tb.N = trabecular number (1/mm); Tb.Th = trabecular thickness (μm); Tb.Sp

= trabecular separation (μm).

Table A.2. Means and standard deviations for bone traits across the High Runner lines in Chapter 2.

	Line 3				Line 6				Line 7				Line 8			
	Sedentary		Active		Sedentary		Active		Sedentary		Active		Sedentary		Active	
Trait	Mean	SD	Mean	SD	Mean	SD	Mean	SD	Mean	SD	Mean	SD	Mean	SD	Mean	SD
Diaphyseal cortical																
Ps.Ar	1.85	0.30	1.77	0.24	1.81	0.07	1.93	0.20	2.07	0.15	2.01	0.16	2.03	0.14	2.04	0.14
Ec.Ar	0.76	0.15	0.84	0.17	0.91	0.05	1.01	0.16	0.85	0.09	0.93	0.13	0.92	0.18	0.99	0.10
Ct.Ar	1.10	0.19	0.93	0.09	0.90	0.09	0.92	0.09	1.22	0.07	1.08	0.07	1.12	0.07	1.05	0.15
Ct.Th	0.280	0.045	0.234	0.019	0.223	0.028	0.223	0.023	0.304	0.013	0.266	0.018	0.279	0.040	0.246	0.034
J	0.480	0.144	0.397	0.094	0.403	0.051	0.444	0.082	0.579	0.084	0.507	0.072	0.531	0.058	0.517	0.088
TMD	1118	9	1110	19	1109	28	1105	30	1116	18	1112	12	1114	33	1104	13
Metaphyseal cortical																
Ps.Ar	2.69	0.42	2.52	0.14	2.57	0.12	2.66	0.16	2.66	0.18	2.63	0.22	3.04	0.26	3.17	0.31
Ec.Ar	1.76	0.33	1.69	0.06	1.75	0.16	1.86	0.14	1.76	0.13	1.79	0.20	2.11	0.24	2.26	0.27
Ct.Ar	0.93	0.10	0.83	0.09	0.82	0.04	0.81	0.03	0.90	0.07	0.84	0.04	0.93	0.03	0.91	0.05
Ct.Th	0.137	0.006	0.122	0.008	0.121	0.013	0.108	0.009	0.128	0.008	0.120	0.008	0.119	0.011	0.109	0.010
J	0.730	0.181	0.599	0.106	0.589	0.035	0.586	0.070	0.682	0.108	0.624	0.075	0.779	0.070	0.801	0.102
TMD	1018	27	1005	24	1030	26	1031	26	1028	15	1029	18	1015	21	999	16
Metaphyseal trabecular																
BV/TV	7.6	3.1	7.5	5.3	8.2	1.2	12.4	2.6	11.0	1.7	10.4	4.0	8.4	3.2	10.2	3.5
Tb.N	3.6	0.7	3.7	1.0	4.5	0.4	5.2	0.7	5.1	0.3	4.6	0.7	3.9	0.8	4.1	0.8
Tb.Th	45.0	4.4	42.2	3.0	39.2	0.8	40.6	1.8	41.2	2.5	41.6	2.7	40.4	1.5	42.4	1.5
Tb.Sp	291	54	290	77	223	21	191	27	197	13	219	35	267	62	253	62
TMD	837	25	837	29	834	18	850	18	849	16	850	16	838	24	836	10

Ps.Ar = periosteal area (mm^2); Ec.Ar = endocortical area (mm^2); Ct.Ar = cortical area (mm^2); Ct.Th = cortical thickness (mm); J = polar moment of area (mm^4); TMD = tissue mineral density ($mg\ HA/cm^3$); BV/TV = bone volume fraction (%); Tb.N = trabecular number (1/mm); Tb.Th = trabecular thickness (μm); Tb.Sp = trabecular separation (μm).

Table A.3. Means and standard deviations for bone traits across the control lines in Chapter 2.

| | Line 1 | | | | Line 2 | | | | Line 4 | | | | Line 5 | | | |
| | Sedentary | | Active | | Sedentary | | Active | | Sedentary | | Active | | Sedentary | | Active | |
Trait	Mean	SD	Mean	SD	Mean	SD	Mean	SD	Mean	SD	Mean	SD	Mean	SD	Mean	SD
Diaphyseal cortical																
Ps.Ar	1.91	0.12	1.87	0.09	1.95	0.13	1.95	0.20	1.85	0.22	2.00	0.18	1.80	0.10	1.86	0.11
Ec.Ar	0.74	0.09	0.83	0.05	0.83	0.08	0.82	0.11	0.63	0.10	0.74	0.07	0.64	0.06	0.80	0.08
Ct.Ar	1.17	0.10	1.04	0.09	1.12	0.08	1.13	0.11	1.22	0.14	1.26	0.16	1.16	0.05	1.05	0.05
Ct.Th	0.307	0.026	0.262	0.024	0.280	0.017	0.281	0.016	0.331	0.022	0.324	0.039	0.315	0.018	0.268	0.018
J	0.506	0.066	0.464	0.052	0.516	0.069	0.512	0.096	0.504	0.121	0.570	0.108	0.458	0.051	0.457	0.046
TMD	1130	18	1123	22	1120	21	1124	28	1125	34	1134	23	1136	19	1111	38
Metaphyseal cortical																
Ps.Ar	2.65	0.28	2.80	0.13	2.78	0.20	2.76	0.32	2.66	0.38	2.79	0.21	2.60	0.18	2.65	0.26
Ec.Ar	1.68	0.26	1.92	0.09	1.77	0.18	1.84	0.26	1.63	0.31	1.78	0.19	1.58	0.18	1.74	0.22
Ct.Ar	0.96	0.07	0.88	0.04	1.01	0.06	0.91	0.06	1.03	0.09	1.01	0.10	1.02	0.03	0.91	0.06
Ct.Th	0.148	0.016	0.123	0.007	0.149	0.012	0.136	0.005	0.155	0.010	0.143	0.013	0.146	0.016	0.130	0.009
J	0.767	0.114	0.718	0.079	0.839	0.118	0.749	0.129	0.822	0.173	0.841	0.127	0.769	0.052	0.703	0.085
TMD	1065	25	1029	19	1047	16	1047	14	1046	20	1045	22	1041	22	1018	18
Metaphyseal trabecular																
BV/TV	9.9	1.3	7.0	1.84	6.3	1.1	6.8	1.60	13.8	3.9	13.5	5.1	12.8	3.3	9.9	2.1
Tb.N	4.6	0.4	3.6	0.22	3.3	0.6	3.6	0.40	4.8	0.6	4.9	0.8	4.9	0.7	4.4	0.5
Tb.Th	42.8	1.5	42.4	5.13	47.0	3.7	44.2	1.30	46.8	2.9	44.8	2.9	46.6	1.9	43.2	3.1
Tb.Sp	217	20	277	19	316	65	285	33	205	30	202	31	205	38	231	30
TMD	863	10	859	25	842	16	862	12	854	22	863	17	851	26	845	27

Ps.Ar = periosteal area (mm^2); Ec.Ar = endocortical area (mm^2); Ct.Ar = cortical area (mm^2); Ct.Th = cortical thickness (mm); J = polar moment of area (mm^4); TMD = tissue mineral density (mg HA/cm^3); BV/TV = bone volume fraction (%); Tb.N = trabecular number (1/mm); Tb.Th = trabecular thickness (μm); Tb.Sp = trabecular separation (μm).